NUREG/CR-6185
ANL-94/5
TMIV(93)AL01

TMI-2 Instrument Nozzle Examinations at Argonne National Laboratory

February 1991 – June 1993

Manuscript Completed: February 1994
Date Published: March 1994

Prepared by L. A. Neimark, T. L. Shearer, A. Purohit, A. G. Hins

Argonne National Laboratory
9700 South Cass Avenue
Argonne, IL 60439

Prepared for
Division of Systems Research
Office of Nuclear Regulatory Research
U.S. Nuclear Regulatory Commission
Washington, DC 20555-0001
NRC FIN A2220

MASTER

DISTRIBUTION OF THIS DOCUMENT IS UNLIMITED

Abstract

Six of the fourteen instrument tube nozzles extracted from the TMI-2 lower head were examined at Argonne National Laboratory to provide information on their metallurgical state, on interactions with core debris that made its way to the lower head, and on penetration of the core debris into the nozzles. The objectives of the examinations were to determine the temperatures near the lower head, the mechanisms, modes, and extent of nozzle degradation to evaluate the challenge to the lower head containment boundary, and contribute to the generation of a scenario for fuel movement on the lower head. The examination techniques were visual examination, gamma scanning, metallography, microhardness measurements, and scanning electron microscopy-energy dispersive X-ray (SEM-EDX) analysis.

The results of the examinations indicate that some nozzles were melted off by interaction with molten core debris, whereas others were only thermally affected by contact with core debris, some of which attached itself to nozzle surfaces. The elevations at which the nozzles were melted off suggest that the liquid core debris was atop a crust of solidified material that apparently generally insulated the reactor vessel from the hottest debris. The pattern of nozzle degradation was consistent with the location of a hot spot in the vessel at the E7-8/F7-8 location as determined by metallurgical examination of the vessel steel samples by others. Based on the severe damage to some nozzles and not to others in relatively close proximity, it can be concluded that the flow of material across the lower head was multi-directional and not unified. It is believed that a significant portion of the core debris moved across the lower head, from the east and southeast toward the hot spot, in a lava-like flow, the basal crust insulating the vessel and the lower portions of the nozzles. The finding of significant quantities of control assembly materials (Ag, Cd, In, Zr, Fe, and Cr without U) in the nozzle material and on nozzle surfaces indicates their presence on the lower head prior to the massive relocation of core debris 226 minutes into the accident.

Contents

I. INTRODUCTION 1

II. OBJECTIVES 1

III. SCOPE 3

IV. GENERAL PROCEDURES 3

V. EXAMINATION RESULTS 5

A. Nozzle M9 7
B. Nozzle L6 10
C. Nozzle H5 12
D. Nozzle H8 15
E. Nozzle D10 17
F. Nozzle E11 22

VI. DISCUSSION 25

A. Defining "Debris" 25
B. Nature of Nozzle Damage 26
C. Postulated Fuel Relocation Scenario 28
D. Presence of Control Assembly Materials 31
E. Temperature Indicators 33
F. Penetration of Materials into Nozzles 35

VII. CONCLUSIONS 37

VIII. REFERENCES 101

IX. APPENDIX A-1

Figures

1. Grid map of TMI core showing locations of nozzles examined at ANL.. 43

2. Typical in-core nozzle with seal and retaining weld..... 44

3. Lower head area and incore instrument guide tubes..... 45

4. Elevation view of nozzle segment M9, as received..... 46

5. Top and bottom views of M9 nozzle segment, as received 47

6. Gamma activity profile and sectioning scheme for Nozzle M9..... 48

7. Longitudinal sections through top of Nozzle M9 near the center (left) and at the center (right)..... 49

8. Longitudinal section through top of Nozzle M9..... 50

9. SEM-BSE image of multiphase fuel in Nozzle M9..... 51

10. As-cut transverse section at 241-mm elevation of M9, showing metallic and possibly ceramic debris between 5 and 8 o'clock in the annulus..... 51

11. Elevation view of nozzle segment L6..... 52

12. Top and bottom views of L6 nozzle segment..... 53

13. Gamma activity profile and sectioning scheme for Nozzle L6..... 54

14. As-cut transverse section at 283-mm elevation of L6, showing a porous material in the annulus..... 55

15. Instrument string and fuel debris at 283-mm elevation of L6..... 56

16. Partially transformed fuel mass at 283-mm elevation of L6..... 57

17. As-cut transverse section at 77-mm elevation of L6..... 57

18. Partially transformed zirconium instrument lead at 77-mm elevation in L6..... 58

19. Etched microstructure of Inconel 600 nozzle at 77-mm elevation in L6..... 58

20. Elevation view of nozzle segment H5..... 59

21. Top and bottom views of H5 nozzle segment..... 60

22. As-polished bottom end of H5 segment, revealing only a solidified metallic mass..... 61

23. Gamma activity profile and sectioning scheme for Nozzle H5..... 62

24. As-cut transverse section through H5 at the 114-mm elevation..... 63

25. As-cut longitudinal section through top of H5 segment..... 63

26. Metallic and ceramic debris at top of Nozzle H5..... 64

27. Microstructure of debris at top of H5, showing intimate mixture of U-rich phases (light), Zr-rich phases (medium), and Cr-rich matrix (darkest)..... 65

28. Chromium-rich platelets precipitated in Cr-depleted Inconel..... 65

29. Instrument string and solidified Inconel mass at the bottom of the H5 segment..... 66

30. Shards of Inconel 600 (a) and fuel debris (b) within instrument string at bottom of H5..... 67

31. Bottom weldment of the H5 nozzle..... 68

32. Top, elevation, and bottom views of H8 nozzle segment..... 69

33. Gamma activity profile and sectioning scheme for Nozzle H8..... 70

34. As-cut longitudinal section through the top of H8..... 71

35. As-cut transverse section at the 64-mm elevation in H8..... 72

36. Metallographic section of instrument string and metallic debris at the 64-mm elevation of H8..... 73

37. Eutectic structures, containing Zr, U, In, Ni, Cr, and Fe at the 64-mm elevation in H8..... 74

38. Ablated surface of H8 nozzle at the 64-mm elevation..... 75

39. SEM-BSE image of Ag-Cd particle, and Zr-rich material penetrating surface of H8 nozzle at 64-mm elevation..... 75

40. Elevation views of D10 nozzle segment..... 76

41. Top and bottom views of the D10 nozzle segment..... 77

42. Gamma activity profile and sectioning scheme for D10 nozzle segment 78

43. Two sides of the longitudinal section through the top of the D10 nozzle..... 79

44. Typical area of fuel shards found at top of D10 nozzle..... 80

45. As-cut transverse section through D10 at the 266-mm elevation, showing metallic and ceramic debris inside..... 80

46. Surface deposits at 266 mm on Nozzle D10..... 81

47. As-cut transverse section through D10 at the 177-mm elevation..... 81

48. As-cut transverse section through D10 at the 158-mm elevation..... 82

49. Area of grain boundary separations in D10 at the 158-mm elevation.. 83

50. Examples of Ag-Cd deposits in D10 at the 158-mm elevation, showing Ag-Cd penetration as (a) stringers and (b) discrete particles..... 84

51. Examples of particulate fuel debris trapped in grain boundary separations at 158 mm in D10..... 85

52. Area of grain boundary separations in D10 at the 158-mm elevation, etched to show possible second phase and internal grain structure.. 86

53. Portion of thick exterior deposit on D10 at the 158-mm elevation... 87

54. Examples of Ag-Cd in Inconel at 158 mm in Nozzle D10..... 88

55. Segregated U-rich (light) and Zr-rich (dark) phases in fuel particle in a deposit at 158 mm on D10..... 89

56. Instrument string at 158 mm in D10..... 90

57. Melted Zr lead wire at 158 mm in D10..... 91

58. Layer of debris on outer surface of D10 at the 82-mm elevation..... 92

59. Elevation view of nozzle segment E11..... 93

60. Top and bottom views of nozzle segment E11..... 94

61. Gamma activity profile and sectioning scheme for Nozzle E11..... 95

62. As-cut transverse section at 274 mm and longitudinal section through top of Nozzle E11..... 96

63. Fuel debris in the top of Nozzle E11..... 97

64. "Micro-folds" with trapped fuel debris in the outer surface at the top of Nozzle E11..... 98

65. SEM image of fuel debris attached to the inner surface of E11 at the 274-mm elevation..... 98

66. SEM image of surface reaction at 274 mm on E11..... 99

67. As-cut transverse section through E11 at 220 mm..... 99

68. Flaking surface debris-bearing scale and surface-adherent scale beneath it at 90-mm elevation on Nozzle E11..... 100

69. SEM-BSE image of scales shown in Fig. 68..... 100

Tables

1. ANL Nozzle Segment Lengths, Elevations, and Fuel Penetration Depths 39

2. Composition of Debris Areas/Particles Containing U-Zr..... 40

3. Summary of Hardness Determinations..... 42

Foreword

The contents of this report were developed as part of the Three Mile Island Unit 2 Vessel Investigation Project. This project is jointly sponsored by eleven countries under the auspices of the Nuclear Energy Agency of the Organisation for Economic Cooperation and Development. The eleven sponsoring organizations are:

* The Centre d'Etuces d'Energie Nucléaires of Belgium,
* The Säteilyturvakeskus of Finland,
* The commissariat à l'Energie Atomique of France,
* The Gesellschaft für Reaktorsicherheit mbH of Germany,
* The Comitato Nazionale per La Ricerca e per Lo Sviluppo Dell' Energia Nucleare e Delle Energie Alternative of Italy,
* The Japan Atomic Energy Research Institute,
* The Consejo de Seguridad Nuclear of Spain,
* The Statens Kärnkraftinspektion of Sweden,
* The Office Fédéral de l'Energie of Switzerland,
* AEA Technology of the United Kingdom and
* The United States Nuclear Regulatory Commission.

The primary objectives of the Nuclear Energy Agency (NEA) are to promote cooperation between its Member governments on the safety and regulatory aspects of nuclear development, and on assessing the future role of nuclear energy as a contributor to economic progress.

This is achieved by:

- encouraging harmonisation of governments' regulatory policies and practices in the nuclear field, with particular reference to the safety of nuclear installations, protection of man against ionising radiation and preservation of the environment, radioactive waste management, and nuclear third party liability and insurance;

- keeping under review the technical and economic characteristics of nuclear power growth and of the nuclear fuel cycle, and assessing demand and supply for the different phases of the nuclear fuel cycle and the potential future contribution of nuclear power to overall energy demand;

- developing exchanges of scientific and technical information on nuclear energy, particularly through participation in common services;

- setting up international research and development programmes and undertakings jointly organized and operated by OECD countries.

In these and related tasks, NEA works in close collaboration with the International Atomic Energy Agency in Vienna, with which it has concluded a Cooperation Agreement, as well as with other international organisations in the nuclear field.

Acknowledgments

The authors acknowledge the unstinting support and patience of A. Rubin, C. Serpan, and E. Hackett during the course of this work. The endeavors of J. Sanecki for his consultations on analytical results; D. Pushis, W. Kettman, F. Pausche, D. Evans, and L. Essenmacher for photography, specimen preparation, and metallography; and E. Hartig for manuscript preparation are gratefully acknowledged. The authors sincerely thank D. Diercks and T. Kassner for their consultations and being the sounding boards for many of the concepts documented here.

I. Introduction

The accident at the Three Mile Island Unit 2 (TMI-2) reactor in March 1979 resulted in the relocation of approximately 19,000 kg of molten core material to the lower head of the reactor vessel.[1] This material caused extensive damage to the instrument guide tubes and nozzles and was suspected of having caused significant metallurgical changes in the condition of the lower head itself. These changes and their effect on the margin-to-failure of the lower head became the focal point of an investigation co-sponsored by the United States Nuclear Regulatory Commission (NRC) and the Organisation for Economic Co-operation and Development (OECD). The TMI-2 Vessel Investigation Project (VIP) was formed to determine the metallurgical state of the vessel at the lower head and to assess the margin-to-failure of the vessel under the conditions existing during the accident. This report was prepared under the auspices of the OECD/NEA Three Mile Island Vessel Investigation Project.

Under the auspices of the VIP, specimens of the reactor vessel were removed in February 1990 by MPR Associates, Inc.[2] In addition to these specimens, fourteen instrument nozzle segments and two segments of instrument guide tubes were retrieved for metallurgical evaluation. The purpose of this evaluation was to provide additional information on the thermal conditions on the lower head that would influence the margin-to-failure, and to provide insight into the progression of the accident scenario, specifically the movement of the molten fuel across the lower head.

II. Objectives

The VIP has as its principal goal the determination of the margin-to-failure of the reactor's lower head. Concomitant with this goal is the development of a lower-head-damage scenario and input data needs for the margin-to-failure analysis. To this end, the Idaho National Engineering Laboratory (INEL) developed a VIP Coordination Plan that identifies the scope of the lower-head-damage-scenario needs and the data required for the margin-to-failure analysis.

Thus, the overall objectives of the nozzle examination effort at Argonne National Laboratory (ANL) were to

(1) Provide information on the temporal and locational movement of fuel onto and across the lower head;

(2) Estimate peak temperatures of the nozzles from their metallurgical end-state; and

(3) Determine the mechanisms, modes, and extent of nozzle degradation to evaluate the imperilment of the lower-head containment boundary.

Data requirements provided in the Coordination Plan established the following specific objectives for the nozzle examinations:

(1) Determine the nature and extent (axial and radial) of fuel/debris ingress into a nozzle;

(2) Determine the nature and degree of chemical and thermal interaction between fuel, debris, and nozzles;

(3) Determine thermal-related metallurgical changes in the nozzle as a function of axial position to evaluate the axial temperature distribution and attempt to quantify temperatures near the vessel; and

(4) Determine the position and composition of debris adhering to nozzle surfaces to establish a "debris bed depth".

In addition to satisfying the contribution of ANL to the data needs, an evaluation of the data obtained would be a good basis for contributing to an accident scenario that describes the fuel movement across the lower head.

III. Scope

Fourteen nozzles were removed from the TMI-2 lower head. Six of these were examined at ANL and eight were to be examined at INEL.

The scope of the examinations at ANL consisted of visual examination and macrophotography, axial gamma scanning (^{137}Cs), sectioning followed by macrophotography of the as-cut surfaces, metallography with selected microphotography (some in the etched condition), microhardness measurements on selected samples, and scanning electron microscopy-energy dispersive X-ray (SEM-EDX) analysis on selected samples. In all, 43 samples were prepared metallographically. This seemingly large number was required because the metallograph stage limited the mount size to a diameter of 32 mm. Of these, 33 samples were examined by SEM-EDX, the microhardness was measured on 21, and three were etched to observe the microstructure.

IV. General Procedures

The nozzles were received in individual sealed containers. Each was visually examined immediately after removal from its container to identify any especially notable areas. Macrophotography was done at 1X magnification through a hot-cell window with a long-bellows camera. Photos were taken of the entire external surface at 120° intervals, of the bottom surface, as cut at TMI, and of the top surface, sometimes in stereo because of the complex, three-dimensional nature of the surface.

For gamma-scanning, each nozzle was placed in an aluminum container to prevent loss of material that might slough off. Scanning along the height of the nozzle was performed as the container was slowly moved across the face of a collimated germanium detector. Only ^{137}Cs activity was scanned because this would be representative of the UO_2 fuel.

The locations on each nozzle to be sectioned for further investigation were established based on a combination of the following criteria:

(1) Top and bottom locations to obtain information on the hottest (sometimes molten) and coldest (nearest the vessel) temperature extremes in a nozzle;

(2) Fuel/nozzle interaction areas (nozzle degradation mechanism);

(3) Indications from gamma scans of fuel penetration into the nozzle;

(4) Obvious locations of surface layers on a nozzle; and

(5) Locations of surface cracking (nozzle degradation mechanism).

Before sectioning, each nozzle was placed in a copper tube, 6.35 mm in diameter, which was then vacuum-impregnated with cold-setting epoxy resin. This was done to stabilize loose surface debris, fragile solidified masses, and internal components. Additional vacuum-impregnation was done during sectioning if significant voids were found in the epoxy and there was a possibility of material fall-out.

Transverse sectioning was done with a dry SiC cut-off wheel while the canned nozzle was rotated in a chuck. The cutting, therefore, was actually circumferential to eliminate localized heating. Longitudinal sections were made with a reciprocating motion of the blade. The location of the longitudinal cuts in the sectioning diagrams in this report are not shown in the actual plane of cutting because it is not possible to do this in an elevation view. The locations provided are intended to indicate only the degree of segmentation of each nozzle.

Metallographic specimens were placed in hollowed-out, preformed Bakelite mounts, vacuum-impregnated with epoxy resin, and polished with diamond paste down to 1 μ using a kerosene-based lubricant.

Microhardness was measured with a diamond pyramid indentor in a Leitz MM5-RT metallograph and a 200-g load. Usually, five to ten measurements were made, from the nozzle surface (inner or outer) inward. Values affected by the surface or internal voids were rejected. Although a surface hardening, or a

subsequent softening attributed to accident-induced annealing, could be discerned in some measurement profiles, for purposes of this determination, the population was averaged and a standard deviation reported. This data treatment appears to be adequate to identify qualitative trends in the axial temperature distributions of the nozzles and provide some insight into quantitative temperatures when compared to limited data from Korth.[3] Some very low measured values proved to be from areas that were either once-molten, had been involved in liquid-metal attack, or were depleted in Cr and thus no longer Inconel 600. These low values are not representative of a metallurgical state of the Inconel 600 that could be used as a temperature indicator. Because the Project has not been able to determine a correlation between microhardness and the metallurgical state of true archival Inconel 600 nozzle material, the microhardness data are, at best, qualitative.

A number of etchants for Inconel 600 were tried, but 3 pts glycerine-3 pts HCl-1 pt HNO_3 gave the best results. However, because of the lack of comparative microstructures of archival material that could be used in a time/temperature effect correlation, the effort to etch more samples was abandoned.

V. Examination Results

This section will describe the examination results on a nozzle-by-nozzle basis, moving essentially from east to west along the lower head. It is believed that this was the direction of the principal fuel flow across the lower head some 226 minutes into the accident.

The six nozzles examined at ANL were from core locations M9, L6, H5, H8, D10, and E11; their locations on the reactor grid are shown in Fig. 1. The damage to these nozzles provides a representative sample of the damage that occurred to all 14 nozzles that were removed from the vessel and, together with information from the eight nozzles being examined at INEL, provides good information from which to construct a scenario for the temporal and locational movement of molten fuel onto and across the lower head. The typical nozzle configuration is shown in Fig. 2.

In the course of analyzing the results for the preparation of this report, it was discovered that four of the six ANL nozzles had been mis-identified during the handling process before the nozzles arrived at ANL. The basis for subsequently making the true identification of these nozzles was a comparison of the records generated by MPR Associates[4] and the visual observations made when the nozzles arrived at ANL. The mis-identified nozzles were H5 (nee D10), D10 (nee H5), E11 (nee L6), and L6 (nee E11). All nozzle identities in this report are the true identities, except any references, as above, to the former identity. It must be recognized that these identities differ from those in all previous presentations of ANL's nozzle examination results. The true nozzle identities now provide a more consistent story of the conditions on the lower head than previously conceived.

To provide the reader with a perspective of the observed damage to individual nozzles with respect to a global lower-head-damage scenario, two sample elevations are used in this report where appropriate. The primary sample elevation is the distance from the base of the nozzle, which was not usually the cut-off surface during removal from the vessel. The second elevation is the vertical distance from the lowest vessel location, at H8 (Fig. 1), to the nozzle surface in question. Figure 3 shows the relationship of these reference elevations. The severing of the nozzles from the vessel usually left a stub attached to the vessel. The height of this stub for the ANL nozzles was determined either from the nozzle's companion boat sample that was processed at ANL, or from knowledge of the nozzle's dimensions, as shown in Fig. 2. For Nozzles M9 and L6, there were no companion boat samples, and the latter method was used. Thus, the reported sample elevation for a given nozzle is the height of the residual stub plus the distance on the nozzle from the cut-off end to the particular elevation. The secondary elevation is the primary elevation plus the elevation from the low-point reference (location H8) to the base of the particular nozzle. (NOTE: In previous ANL reporting and presentations, the "elevation" has been only the distance on the nozzle from the cut-off end to the particular elevation. The changes have been made to better reflect the elevation of a location for debris penetration and axial temperature considerations and for accident scenario considerations.) Table 1 provides a summary of nozzle segment lengths and relevant elevations.

Also tabulated in Table 1 are the fuel penetration distances into each nozzle, as determined by the ^{137}Cs axial activity profile. The data are provided as the elevation of fuel material above the base of the nozzle. Maximum and minimum values are given for nozzles for which it could not be absolutely concluded that the ^{137}Cs activity was inside and not on the surface of the nozzle. The use of the gamma-activity profiles rather than visual observation of "ceramic" material in the nozzle cavity was deemed more appropriate because of the possibility that the "ceramic" material could be a nozzle oxidation product and not actually a fuel mass.

A. Nozzle M9

The M9 nozzle segment received at ANL was 254 mm long. Based on a nominal as-fabricated nozzle length of 305 mm (centerline; slope of base not considered), a 26-mm stub remained on the vessel after severance. Figure 4 shows one view of Nozzle M9 as it was received. The top 25 mm of the nozzle had been melted off and the next 25 mm show signs of melting, including the initiation of candling. The 25-50 mm below the melted area appeared to be lightly scaled, whereas the remainder of the nozzle was bright and shiny. As-fabricated vibra-tooled lettering was apparent just below the midplane.

Figure 5 shows the top and bottom views of the as-received nozzle. The top appeared to be totally sealed with molten material, whereas the bottom showed no material in the annulus between the instrument string and the nozzle; however, there appeared to be material in the central tube of the instrument string.

The axial gamma scan and the locations of major cutting of the nozzle with the resulting breakoff identifications [Alpha/Gamma (A/G) hot-cell numbers] are shown in Fig. 6. The A/G numbers correspond to the specimen identifications found in the Appendix. This sectioning provided an overall view of the damage to the top of the nozzle where the gamma scan indicated the presence of fuel, and an area from the bottom of the nozzle where core debris may have been in intimate contact with the outer surface.[1] Figure 7 shows two as-cut longitudinal surfaces through the top of the nozzle. Melting of the noz-

zle was restricted to the top 25 mm, but the instrument tube showed signs of melting below that elevation. Vertically-oriented voids in the molten nozzle were also found in other once-molten nozzles. The voids are believed to be the result of a solidification phenomena in which spherical voids interlink in a vertical array and surface tension causes the horizontal ligaments to contract and disappear, and thus form a continuous longitudinal void. Such spherical voids, or bubbles, are shown in the molten material in Fig. 8. The spherical bubbles, which were closer to the nozzle centerline, would be indicative of rapid cooling, whereas the longitudinal bubbles outward from the center would be indicative of a somewhat slower cooling rate. In Fig. 8, the metallic debris in the center (bright phases) is the remnant of the outer tube of the instrument string (Inconel 600), whereas the gray phases are, apparently, oxides of the metal and fuel (the SEM-EDX system cannot analyze for oxygen).

What remains of the instrument leads (generally Zr wires in Al_2O_3 insulation with Inconel sheathing) is on the right in Fig. 8. The gray mass on the left, adjacent to the molten nozzle, is Cr-rich, apparently an oxide. The adjacent molten Inconel was almost devoid of Cr. The lighter ceramic phases surrounding the metallic phases in the center consisted of discrete areas of fuel of different macro-compositions and void morphologies. The macro-compositions of these areas are given in Table 2, which summarizes the compositions and locations of selected fuel-bearing species that were identified during examination of the nozzles. The general matrix in which these discrete fuel islands exist is essentially a solidified Cr-oxide which contains fine bits of solidified fuel as a "second phase." On a microscopic scale, some of these areas, shown in Fig. 9, consisted of Zr-rich phases with significant U content, U-rich phases with significant Zr content, and Cr-rich areas with traces of Fe, Ni, Ti, Mn, Zr, and U. The segregation into U-rich and Zr-rich fuel phases is indicative of a sufficiently slow cooling rate for segregation to occur. The spherical bubbles contained apparently condensed phases of Al, Si, and Ca while other bubbles contained Ag and Cd deposits. The presence of Ag-Cd in the molten Inconel indicates that these materials were either in or on the nozzle at this location before melting occurred.

A transverse section 38 mm below the top of the melted-off nozzle in the scaled area (241 mm from the base) is shown in Fig. 10. This section shows a metallic mass that is similar in appearance to a mass in the H8 nozzle that analysis showed to be molten Inconel 600, but deficient in Cr. On the basis of that similarity, no metallography or SEM work was undertaken for this section. A possible ceramic mass, which could be fuel, is also visible in Fig. 10. Fuel is a distinct possibility because this area is at the lower end of the ^{137}Cs activity profile shown in Fig. 6.

A segment of the nozzle surface 38 mm above the base (183 mm above the lowest point in the vessel), from the very clean area in Fig. 4, was examined by SEM-EDX to search for evidence of debris deposits. A 0.5-1.0-μ-thick layer of enhanced Cr material, apparently Cr-oxide, was found on the surface, along with occasional deposits of Al, probably Al_2O_3. There were traces of control rod materials in the Cr-oxide layer, but no fuel. Also, there was no Fe-matrix layer that contained core debris.

The principal gamma activity peak at the top of the nozzle (Fig. 6) corresponds to the fuel that was found at this location. The secondary peaks are adjacent to the scaled surface area, which was not found to contain measurable quantities of fuel in the area examined. These peaks likely reflect fuel in the outside candling piece and/or fuel in the inside candling material. For purposes of a debris penetration distance, the 241-mm elevation is suggested as at least a minimum, as indicated in Fig. 10.

Microhardness measurements were made on a specimen from the top longitudinal section and on the bottom nozzle specimen. The measurements at the top averaged 124 ± 5 diamond-point hardness (DPH), while the average of measurements from the bottom specimen was 202 ± 28 DPH. A summary of all hardness measurements on all nozzles is given in Table 3. The low values from the top reflect the significant Cr depletion in this area, with the result that the matrix was no longer Inconel 600.

B. Nozzle L6

The L6 nozzle segment (nee E11) was ≈241 mm long, and a stub ≈64 mm high would have been left on the vessel. Figure 11 shows one view of the nozzle as it was received. This nozzle was essentially untouched externally by the accident. Vibra-tooled identification markings are clearly visible on the non-scaled surface. The four notches in the side of the nozzle were put there by MPR Associates for identification purposes. The top and bottom views, Fig. 12, show that the instrument string was either snipped off or bent off, but not melted off. Debris inside the nozzle, external to the instrument string, can be seen in both the top and bottom views. The ^{137}Cs axial gamma scan, Fig. 13, indicates that the contained material is apparently fuel-bearing.

The nozzle was sectioned transversely at five locations as shown in Fig. 13. These elevations were selected principally to attempt to determine the nature of the material that was creating the ^{137}Cs activity inside the nozzle. Figure 14 shows an as-cut section 22 mm below the top of the nozzle (283-mm elevation), and a gray, porous ceramic-appearing material. Some of the fuel in the top of the nozzle can be seen in Fig. 15; the rest was apparently lost in the cutting operations. Analysis of the fueled areas showed a potpourri of materials and compositions. The triangular particle in Fig. 15 was pure UO_2, apparently unmelted and a true pellet fragment. The porous mass at 3 o'clock in this figure contained U, Zr, Fe, Cr, and Al. The microstructure of this particle, Fig. 16, shows that the fuel had been only partially transformed into U-rich (light) and Zr-rich (medium) phases, indicating rapid cooling. The Fe, Cr, and Al are the dark phase in the grain boundaries. This is a fuel structure identical to that found in debris retrieved from the lower plenum in 1985 and that was postulated to be capable of flowing, in a viscous fashion, at temperatures as low as 1350°C.[5] Also found were non-porous particles of Ag, Fe, and Al; Ag, Zr, U, Fe, and Ni; Fe, Zr, Ag, Cd, and Ni; and Cr, Fe, Al, and Ni in a U-Zr phase. Many, if not most, of the fuel particles appeared to have the darker grain boundary phase typical of the low-melting oxides of Fe, Cr, and Al.

There was a very thin, 0.6-1 μ, complex deposition layer on the outer nozzle surface at the 283-mm elevation (top). There appeared to be no interaction with the Inconel 600 as the composition of the Inconel was unchanged 50 μ from the surface. This inhomogeneous layer contained areas rich in Fe and Al, with Ag-Cd-In particles also present. The top-most part of the layer occasionally contained very small U-Zr fuel shards.

The as-cut transverse sections at the 250-mm elevation exhibited some extraneous material attached to the instrument conduit and a thin deposit on the nozzle ID; neither material was obviously similar to the fuel at 283 mm, and no further examination was made of this material. The as-cut transverse sections at the 120-mm and 145-mm elevations indicated some form of material between the instrument string and the inside surface of the nozzle, but the material had the same texture as the epoxy potting outside of the nozzle and no metallography was performed on these areas.

There were no obvious fuel masses at the 77-mm elevation (Fig. 17), but a piece of metallic Al with Ti as a second phase was between the instrument string and the inside surface of the nozzle. This piece was coated with fuel particles. The inner nozzle surface was covered with a 15-μ layer of non-Zr-bearing UO_2 fuel particles. The Zr instrument leads at this elevation may be indicative of the temperature reached here. Figure 18 shows one of the leads. The microstructure is that of transformed β phase with, apparently, a transformation to α phase occurring at the surface. Other leads were also in varying stages of transformation. Assuming the material was initially α phase, the transformation to β would have occurred at 862°C if there was little oxygen present; the transformation temperature rises rapidly with increasing oxygen in the α phase. The transformation back to α on the surface, the white areas in Fig. 18, either could have occurred rapidly (minutes) if oxygen was present, or more slowly (hours) if oxygen was low. A low-oxygen level apparently existed because the Zr did not oxidize. Because there was no redox reaction with the Al_2O_3, the temperature was <1200°C.

Another qualitative indicator of temperature at this elevation is the microstructure of the Inconel 600 nozzle, shown in Fig. 19. The structure exhibits large grains, 0.1-0.3 mm, in dynamic movement. Annealing twins are present. The black spots are probably a TiN impurity, as seen by Korth,[3] and are the likely source of Ti that was found in many surface interactions on these nozzles. Unfortunately, without knowing the as-fabricated metallurgical state of the nozzle, it is not possible to make even a semi-quantitative estimate of the temperature reached.

The fact that neither the nozzle nor the guide tube that overlapped it were damaged[6] is indicative that the material in the nozzle probably came down the guide tube and not from a flow of fuel across the lower head.

Microhardness measurements were made on the transverse top and bottom nozzle sections. The hardness was 167 ± 7 DPH at the top and 169 ± 13 DPH at the bottom. This relative axial uniformity over ≈200 mm is attributed to the apparent presence of fuel essentially along the inside length of the nozzle.

C. Nozzle H5

The H5 nozzle segment (nee D10) was 146 mm long, and the segment was cut off flush with the vessel, leaving no residual stub. An elevation view of the nozzle segment is shown in Fig. 20. Close inspection of the uneven lower right side of the nozzle suggests that this is part of the nozzle/vessel weldment. (This was subsequently confirmed by metallography of this area.) The nozzle appears to have been melted off, with candling occurring down one side. At least some of the candled material (the lowest exterior nodule was analyzed by SEM-EDX) is Type 304 stainless steel, possibly from the conduit that surrounds the instrument string, but also possibly core debris from elsewhere. The top and bottom views of the as-received segment are shown in Fig. 21. The top view shows obliteration of the instrument string and filling of the nozzle cross section with molten material. The bottom view indicates a material in the annulus, but the nature of the white, smeared-appearing material filling the annulus and covering the instrument string was not established. After

polishing, the only significant mass of material in the annulus at this elevation was a once-molten Inconel mass, shown in Fig. 22.

The sectioning diagram for H5 is shown in Fig. 23. Figure 24 shows the as-cut transverse surface just below the molten top of the nozzle segment at the 114-mm elevation. Figure 25 shows the as-cut longitudinal surface through the top of the segment. This section shows filling of the nozzle with both metallic (shiny) and ceramic material (shades of gray). Just below the top (Fig. 24), however, the predominant material filling the center is metallic. Figure 26 shows the mix of metallic and ceramic materials at the top of the segment. The metal is essentially Cr-depleted Inconel 600. The ceramic, typical of similar analyzed areas across the top of this nozzle, is a Cr-rich oxide that contains U and Zr, probably as oxides, intimately mixed as U-rich and Zr-rich areas in what was apparently a molten ceramic (see Fig. 27); the melting point of Cr_2O_3 is 1990°C. In Fig. 27, note the porosity in the Cr-rich (darkest) phase. This is an indicator of the volatility of Cr oxides, as will be discussed later. The compositions of some debris areas can be found in Table 2. It is this "fuel" material that apparently gave rise to the fission-product peak in this region of the gamma scan. There were also local concentrations of Al and Ti in this ceramic material. The source of the Al would be the Al_2O_3 insulating material in the instrument leads. The Ti apparently was an impurity in the Inconel 600 and came out with the Cr, both being strong oxide formers. A Cr-rich phase also precipitated as plates within the Cr-depleted Inconel areas, as shown in Fig. 28. This molten metal, from the right side in Fig. 25, was also found to contain dissolved fuel constituents (≈9 wt.% U, ≈3 wt.% Zr).

Areas of Ag, Cd, and In were found in the surface oxide on some of the former Inconel 600 masses shown in Fig. 26. Deposits of Ag-Cd and Si, Mn, Ti, and Zr were also found within the spherical bubbles in the once-molten Inconel, similar to those in Fig. 28.

A metallographic specimen was made at the 25-mm elevation to examine any surface deposits, examine the Inconel microstructure, and to perform hardness measurements. There was a 50-μ-thick oxide on the surface, topped with fine

particles of debris. Although neither the particulate nor the layer were analyzed, the backscatter electron (BSE) image of the particles indicated them to be a mixture of high- and low-atomic number materials, apparently fuel and other core debris. The oxide layer had the physical appearance of Fe-oxide layers analyzed on Nozzles D10 and E11. Nodules of Pb were found ≈650 μ beneath the surface of the nozzle. The source of the Pb is unknown, but its morphology in the Inconel (centered in a dimple) indicates that it is not an artifact. The etched nozzle microstructure was similar to that from Nozzle L6 (Fig. 19) in that the grain boundaries were not at equilibrium and annealing twins were present. However, the grain size was larger with grains up to 0.5 mm in diameter.

The bottom surface (0-mm elevation) of the H5 segment is shown at higher magnification in Fig. 29. The Type 304 stainless steel conduit is not oxidized. It should be noted the Inconel 600 sheathing on six of the leads is cracked in a brittle mode. The metal shards between the leads, shown in Fig. 30, are Inconel 600 plus Mn (≈6 wt.%) and they are apparently the result of brittle failure of this sheathing somewhere above. The Mn source is not obvious, but it was also present in the sheathing only next to a fracture. Also shown in Fig. 30 are fuel particles and particles of Ag-Cd that also collected between the leads. The Zr leads, shown in Fig. 29, were in various stages of phase transformation, from β- to α-phase Zr, similar to what was found in Nozzle L6 (see Fig. 18).

Metallography of a section from the bottom surface, Fig. 31, showed a dendritic structure that is typical of a weldment. This would be expected as this nozzle was cut off flush with the vessel wall, through the weld.

Microhardness measurements were made on specimens from the three elevations: 135 mm, 25 mm, and 0 mm. The average of measurements at the top (135 mm) was 105 ± 2 DPH in a region that was Cr-depleted. The bottom surface, however, which was the weldment, measured an average of 217 ± 13 DPH. The values from the bottom were the highest measured on any nozzle. The hardness at the 25-mm elevation in nozzle material was 198 ± 8 DPH.

D. Nozzle H8

The H8 nozzle segment was 70 mm long and a 51-mm stub remained on the vessel. It was reported by MPR[4] that ≈50 mm of the top of what remained of this nozzle after the accident was broken off during defueling of the lower head. Inspection of the photos of the as-received condition of the segment, Fig. 32, indeed, shows evidence (fractured leads and bent conduit) that the instrument string was broken off, not melted, even though the nozzle around it obviously had been ablated and severely necked down. It is likely that only the instrument string was holding the two segments of the nozzle together. If that was the case, the full remaining segment of this nozzle was hour-glassed shaped, similar to K11. The ^{137}Cs gamma scan for the segment is shown in Fig. 33. The activity profile indicates that fuel is contained throughout. A likely fuel mass within the nozzle can be seen at the bottom face in Fig. 31.

The sectioning diagram for the nozzle is shown in Fig. 33. The as-cut longitudinal section, shown in Fig. 34, shows that the instrument string, including its stainless steel conduit, is fairly well intact, but bent. Solidified fuel and metallic debris can be seen to the left of the string. The "goose-neck" bend of the ablated upper left corner may have occurred when the upper mating segment was broken off during the defueling operation. Analyses of the surfaces at the top of this segment identified Zr, with very little U, as the principal reactant with the nozzle. Uranium, in combination with Zr, was found in grain boundaries in the reaction areas, but Zr without U was layered on the reacted surfaces. Cadmium was also present intergranularly with the U and Zr, whereas In was found on the surface with Zr. Unlike the fuel in the tops of Nozzles M9 and H5, some of the fuel areas in the one sample examined at the top of H8 were more agglomerated particulates rather than a heterogeneous solidified mass.

The as-cut transverse section at the 64-mm elevation is shown in Fig. 35. At this elevation, there was a combination of some ceramic and predominantly metallic debris in the nozzle annulus. The metallic debris, shown in greater detail in Fig. 36, was essentially solidified Inconel 600 with ≈20 wt.% Zr and 1 wt.% U that apparently had come down in several rivulets.

Trapped in this debris were solidified inclusions of Ag-Cd. The surfaces of some rivulets were eutectic structures (Fig. 37) that contain Zr, U, and In, in addition to Ni, Cr, and Fe. Similar microstructures of primary solidification grains and eutectic structures were found in the material higher in the annulus between the nozzle and the conduit. The quantity of Ag-In-Cd material in this debris is significant in that it indicates an appreciable amount of control materials in the vicinity of the nozzle breach, either at the 120-mm elevation or higher up at the ≈170-mm elevation, where the top of the nozzle had apparently melted away. It is also significant that there appears to be no obvious Cr depletion from the Inconel with subsequent oxidation, as was found at the top of Nozzle M9. It can also be seen in Fig. 36 that the outer Inconel tube of the instrument string had been under sufficient external pressure to collapse onto the instrument leads. The Type 304 instrument conduit was barely oxidized at this elevation. Slightly higher up, the conduit was oxidized on its inside, whereas its outside was "protected" by molten material that had run down into the annulus. But at the very top it was entirely oxidized.

To summarize, there were three types of fuel-bearing "debris" found in the H8 Nozzle. Unique to this nozzle was Zr and U in solidified metallic structures of essentially Inconel. In these, the Zr:U atomic ratios were ≈35:1. Second, there was agglomerated particulate (<50 μ), in which the Zr:U atomic ratios were ≈1.2:1. Last, there were what appeared to be solidified, porous masses; unfortunately, these were not captured in the samples analyzed by SEM-EDX. Such masses are evident in the as-cut surface shown in Figs. 32 and 34.

The nozzle outer surface at this 64-mm elevation, Fig. 38, was ablated and reacted with liquid Zr that also contained a large quantity of Ni and smaller quantities of U, Fe, and Cr (Zr:U ≈8.5:1). The SEM secondary electron image of this area, Fig. 39, shows that a Zr-rich liquid phase has penetrated the grain boundaries of the Inconel 600. Also shown in the figure are second phases that contain higher concentrations of Zr, Fe, and Cr than the matrix phase. The significance of the nature of this surface material is twofold. First, it contains all of the elements of a control rod assembly: Ag-In-Cd;

Zr from the Zircaloy guide tubes; and Fe-Ni-Cr from the stainless steel cladding. Second, the Zr:U atomic ratio of the surface and sub-surface reactant, ≈8.5:1, is significantly different from that of the particulate fuel found in this nozzle and in the fuel debris in most other nozzles where the content of U is generally greater than that of Zr (see Table 2). These two points strongly suggest that this nozzle was in contact with material from the control rod assemblies before the major fuel flow arrived on the vessel.

Microhardness measurements on the nozzle averaged 133 ± 4 DPH at the 64-mm elevation and 148 ± 7 DPH at 108 mm. These values were among the lowest values measured on Inconel that did not exhibit Cr-depletion and reflect a high nozzle temperature 64 mm from the vessel.

E. Nozzle D10

The D10 nozzle segment (nee H5) was 235 mm long, leaving an ≈57-mm-long stub on the vessel. An elevation view of the nozzle segment is shown in Fig. 40. Close inspection of the beveled top of the nozzle indicates that ≈13 mm of the top had melted off.

There were a number of noteworthy features on this nozzle. The top 75 mm appear to have a crust with wide, shallow depressions. The middle 75 mm are covered with a crust that is thicker and quite porous, and only on one side of the nozzle, indicating its deposition was unidirectional. The ^{137}Cs activity profile (Fig. 42) indicates that there is a small amount of fuel at the very top of the nozzle and that the porous debris contains fuel as well. (Subsequent sectioning through the debris, described below, indicates that there was more fuel mass attached to one side of the nozzle than inside the nozzle at the elevation of the section. The gamma activity, therefore, was principally from surface debris.)

Just above the midplane bevel is a crack, ≈20 mm long, that penetrates the nozzle body. The surface debris and scale terminate just above the cut-off elevation, ≈75 mm from the bottom of the nozzle. The top and bottom views of the nozzle segment are shown in Fig. 41. The top view shows that the instrument string has been generally melted, with melted material, probably the

missing top 13 mm, filling the nozzle's annulus. Candling down one side can be seen. The bottom view shows the instrument conduit to be intact with what might be fuel fragments on one side of the nozzle's annulus.

The sectioning diagram for the D10 nozzle is shown in Fig. 42 together with the gamma activity profile. The segment was cut into nine major pieces, from which 13 smaller specimens were generated for detailed examination. The longitudinal section through the top of the nozzle, Fig. 43, shows melting of the instrument string, severe damage to the stainless steel conduit, and the melted Cr-depleted Inconel that filled the annulus around the conduit. The ceramic-appearing material on the other side appears to be, based on the M9 analytical results, a fuel-bearing oxide of Cr. (The sample from this ceramic region was lost during metallographic preparation.) Only fuel in the form of shards was found in a metallographic section from the instrument-tube side of this section (Fig. 44). The compositions of such particulate areas are given in Table 2. The significance here is the particulate and inhomogeneous nature of the debris within the melted metallic structure of this nozzle, unlike the tops of M9 and H5. The surface of the nozzle at the top was ablated with evidence of U-Zr imbedded in the Cr/Ti-rich surface. Aluminum had advanced ≈200 μ into the nozzle, beyond the Cr/Ti oxidation areas, and was usually associated with Mg, the source of which is unknown. Cadmium was sporadically located on the surface. Silver and Cd nodules that also contained U-Zr were located in seemingly unaffected Inconel at least 300 μ from the surface.

The transverse section at the 266-mm elevation, Fig. 45, showed extensive damage to the instrument string and conduit and possibly some fuel debris in the annulus but none on the exterior. The exterior surface at this elevation exhibited an alternating pattern of interacted/ablated areas and areas showing little evidence of attack. The interacted areas, which would be the shallow depressions shown in Fig. 40, were up to 2 mm deep and consisted of both sub-surface-affected zones and layered deposits of debris and reaction products on the surface, as shown in Fig. 46. Aluminum was aggressive in interacting beneath the Inconel surface. On the ablated surface, Cr and Ti, likely as oxides, formed a thick layer, with an additional Cr-rich layer containing control assembly fragments on top of it. The outermost layer was

almost pure Fe (oxide). In some areas this layer contained fragments of a mixture of U-Zr and Ag-Cd. On surface areas where there was no ablation, the surface layer was ≈1 μ thick and contained Al, Zr, Ag, Cd, In, Ti, Cr, Fe, and Ni, but no fuel.

The transverse section at the 177-mm elevation, Fig. 47, shows an area of fuel debris on the exterior surface, solidified metal in the annulus, oxidation of the conduit, collapse of the central Inconel 600 tube, and large bubble formation in the Inconel on the surface of the nozzle. Almost all of the surface damage was limited to one side, an arc of ≈180°.

At the 158-mm elevation, Fig. 48, the surface damage extended farther around the nozzle. A solidified ingot of what proved to be Inconel was inside the annulus. This ingot contained imbedded particles of solidified Ag-Cd, generally at a ratio of 10:1, as did the adjacent nozzle body. There was no evidence of foreign elements on the apparently ablated surface, only layers rich in Cr, Ti, or Ni. There was an extensive area of intergranular separation on one side of the nozzle body, adjacent to the surface crack that was visible in Fig. 40. This area, shown in more detail in Fig. 49, was extensively penetrated by Ag-Cd, both as stringers, Fig. 50(a), and discrete particles, Fig. 50(b). Many of the larger cavities appear to be grain-boundary separations, or grain boundaries that have been dissolved by a penetrating liquid, such as Ag-Cd. In some cases, the protuberances on the surfaces of the cavity were sufficiently rounded to have the appearance of having been molten. Some of the larger cavities were filled with shards of fuel in a matrix of Cr-oxide, as shown in Fig. 51. The compositions of some of these shards are given in Table 2. Aluminum, Cr, and Fe, all strong oxide formers, were found in the grain boundaries of one such fuel particle. The etched microstructure of this area, Fig. 52, indicates a very large grain structure with a possible second phase in the grain boundaries. The nature of this grain-boundary phase was not actually determined; only Ag-Cd, as in Fig. 50(a), was determined in the SEM-EDX analyses. The average microhardness of this area was only 124 ± 2 DPH, indicating that a very-high temperature was achieved. The area was not depleted in Cr, however, as was the case in other low-hardness areas.

Although a cast, dendritic microstructure was not brought out metallographically, it is not inconceivable that at least one side of the upper part of this nozzle was essentially molten, or very close to it, the apparently undisturbed exterior shape notwithstanding. Measurements on the nozzle cross section in Fig. 48 indicate that not only is the center hole eccentric but the outer surface is as well. The outer surface has moved outward by ≈3.5 mm opposite the eccentricity of the ID. The fact that the inner instrument tube is collapsed at this elevation is evidence that there was a high internal pressure in the nozzle that would have been the driving force to move the weak side of the nozzle outward. The large surface bubble at 177 mm is another indication of melting of at least the surface. Assuming the fuel flow enveloped the nozzle from the bottom up, a fuel crust could have rapidly solidified against the nozzle forming a mold in which areas of the nozzle rapidly melted, at ≈1400°C, and then solidified, trapping some fuel debris and control rod material inside. The rough nature of the surface of this nozzle can be contrasted to the smooth surface of the ablated areas on the surface of Nozzle H8.

The massive surface deposit diametrally opposite to the intergranular separations is shown in Fig. 53. It is assumed that this type of deposit is typical of the thick deposit on this side of the nozzle between the 120- and 180-mm elevations. This complex structure is a combination of solidified Cr-depleted Inconel (white areas) and physical mixtures of oxides of Cr, Zr, U, Fe, and Ni (gray areas). Part of the original nozzle surface is assumed to be the thin gray line of Cr and Ti (oxide) at 5 o'clock in the figure and extending upward through the wide band of voids to 12 o'clock. The gray phases to the right of this line are principally Cr, Al, and Ti rich, with some U and Zr. The Inconel matrix to the right of these oxides contains inclusions of Ag-Cd, as does the large Cr-depleted Inconel masses between 6 and 8 o'clock. These inclusions are shown in Fig. 54. Their nominal compositions were in the range of 70-80 wt.% Ag - 20-30 wt.% Cd. A fuel-containing area is a triangular-shaped particle at the outer edge of the deposit shown in Fig. 53. The microstructure of this area, Fig. 55, shows segregation of the fuel into a U-rich phase (89 wt.% U-3 wt.% Zr-8 wt.% Fe) and a Zr-rich phase (25 wt.% U-57 wt.% Zr-18 wt.% Fe). Such fuel concentrations were the exception. Generally,

fuel constituents were more randomly dispersed in other phases of Cr and Fe oxides. The areas containing the larger amounts of U and Zr were in the outer areas of the deposit.

Figure 56 shows the instrument string at the 158-mm elevation. The Type 304 stainless steel conduit was almost completely oxidized but the Inconel 600 inner and outer instrument tubes were not; there was only a small amount of oxidation on the outer tube. The inner tube had collapsed from external pressure and was filled with solidified Inconel, slightly deficient in Cr. The Zr instrument wires had reacted to varying degrees with Al_2O_3 insulation, resulting in oxidation of the Zr and reduction of the Al_2O_3. The relative free energies of formation of these oxides suggest that a temperature of at least 1200°C was reached for this redox reaction to occur. One instrument wire, at 5 o'clock in Fig. 56 and shown enlarged in Fig. 57, apparently had melted and sent six stringers outward toward the cladding. An analysis of one such stringer indicated only Zr, but, because the melting point of Zr is high at 1850°C, it is more likely that the stringers are the eutectic of Al and Zr at a melting point of 1350°C. This is more in keeping with the ≈1200°C minimum temperature for the redox reaction. One stringer reached the sheath and caused local melting in the wall. Although the melting point of Inconel is ≈1400°C, the localized melting could have occurred at a lower temperature because the Zr-Ni eutectic occurs at 960°C. In any event, the temperature of the instrument string at this elevation was at least 1200°C.

There was a 0.25-mm-thick layer of debris on the surface of this nozzle at the 82-mm elevation. The debris, a section of which is shown in Fig. 58, was multilayered immediately adjacent to the nozzle. The innermost reaction zone was somewhat depleted in Cr and Fe and contained 9.5 wt.% In. Moving outward, the zones contained an increasing amount of In, combined principally with Ni, with up to 95 wt.% In (balance Fe) in the outermost of the inner reaction zones. An intermetallic, Ni_3In_7, was one such zone. The blocky gray mass that was the principal constituent of the 0.25-mm-thick layer was Fe (oxide). Small particles near the reaction zones contained Cd and In. Large fuel shards of various compositions were trapped in the Fe (oxide) matrix.

The compositions of these various particles, or specific phases within these particles (denoted by a number), are summarized in Table 2.

Microhardness measurements made on the nozzle body at the 82-mm elevation gave an average hardness of 161 ± 4 DPH for four values.

The surface layer at the 69-mm elevation was only 1-10 μ thick. In the thinnest areas of the layer, random particles of fuel (82 wt.% U-12 wt.% Zr) were imbedded in the surface. As the surface layer became thicker, the underlying reaction zones into the nozzle surface, ≈5 μ wide, contained Al, Si, Ag, Cd, In, and Sn in addition to Ni, Zr, and Fe. The thickest outer layers consisted of partial bands containing U, Zr, Ag, Cd, In, Sn, Mo, and Al in addition to Fe, Ni, and Cr, in various combinations. Where Zr and U were found together, the Zr:U atomic ratio was very high, i.e., >10:1.

The microhardness of the nozzle at the 69-mm elevation was an average 168 ± 10 DPH, essentially the same as it was 13 mm above.

F. Nozzle E11

The E11 nozzle segment (nee L6), shown in Fig. 59, was 225 mm long. The base of the nozzle was 221 mm above the lowest point of the vessel. After severance from the vessel, an ≈77-mm stub of the nozzle remained with the vessel. The nozzle surface was bright and apparently unaffected by the accident over about half of its length. There was a loosely adherent scale over the upper 145 mm and part of the bottom 38 mm. The tapered top of the nozzle was wrinkled and ≈3 mm of the top was missing, but as will be seen, this material melted and ran down into the nozzle. Figure 60 shows the top and bottom views of the nozzle segment. The top view indicates that nozzle material had entered the annulus between the instrument string and the nozzle ID, and the string is visible in the top view. The bottom view shows the string partially withdrawn and it subsequently fell out on handling. From subsequent sectioning, it was apparent that the string had separated ≈25 mm from the top of the nozzle. The cause of the separation was not determined. The ^{137}Cs activity profile for the segment, Fig. 61, indicates that there was fuel in the top ≈15 mm of the segment and in an area between the 210- and 250-mm elevations.

The segment was sectioned transversely and the upper end was sectioned longitudinally to investigate, principally, the possible fueled area indicated in the gamma scan. The basic sectioning diagram is shown in Fig. 61. Figure 62 shows the transverse section through the 274-mm elevation and the longitudinal section through the top piece just above it. The instrument conduit is visible in the longitudinal section but not in the transverse section, indicating that the instrument string had been severed at this elevation.

An enlarged view of the material in the top of the nozzle is shown in Fig. 63. The principal components of this debris were fine (<100-μ) particles of fuel and nozzle debris that formed a matrix in which large fuel shards and oxidized pieces of the conduit were trapped. Some fuel particles in this region showed segregation into U-rich and Zr-rich phases, which is indicative of relatively slow cooling from the solidus temperature. The large shards, however, showed no such segregation and appeared to have solidified very rapidly. There were Ag-Cd particles trapped in some of these fuel areas. The compositions of some fuel areas and particles are given in Table 2. The principal non-fuel constituent in this matrix of debris material was Fe, not Cr as in other nozzles.

The inner and outer nozzle surfaces at the top were severely attacked by Al, presumably from the Al_2O_3 insulation in the instrument string. Titanium and Cr were also strongly evident in surface interactions. It is assumed that the Ti was an impurity in this Inconel 600 and came to the surface, as did Cr, under the strongly oxidizing environment. The outer surface apparently was sufficiently hot and plastic to form "micro-folds" that trapped particulate matter (see Fig. 64). The particulate consisted of fuel (see Table 2 for composition) and Zr-, Cd-containing particles, among others. The ablated surface was covered with an apparent oxide layer of principally Cr and Ti.

Examination of the transverse section at the 274-mm elevation showed that the solidified metallic material on the inside surface was contiguous with the nozzle with a composition essentially that of Inconel. Areas of the surface of this material had undergone post-movement reaction with Al. The ceramic material attached to the inner surface was a loose agglomeration of

particulate shards (Fig. 65) that included fuel, fine fuel particles in an Fe-oxide matrix, calcium-silicate, Fe-Ni alloy, and an Ag-Cd/fuel-Fe agglomerate. Apparently insufficient fuel/fission products were present in this material to cause an indication in the gamma activity profile at this elevation.

The outer surface at this elevation contained areas of surface scale, about 10-20 μ thick, and other areas of surface attack. The outermost part of the scale contained Ag (11-45 wt.%) and Cd (4-15 wt.%), the balance being Al, Fe, Si, Ni, and Cr in descending order of content. The inner part of the scale consisted more of the latter constituents. A reaction area, shown in Fig. 66, contained Ag, Cd, In, and Zr in addition to Fe, Ni, Cr, Al, and Si. Silver-cadmium nodules were found up to at least 1 mm into the nozzle.

Hardness measurements taken near the inner and outer surfaces all indicated a hardness in the range of 136-141 DPH (average of 137 ± 4 DPH). This is significantly lower than the hardness closer to the nozzle top only 15 mm above.

The transverse section made at the 220-mm elevation to intercept the gamma peak there is shown in Fig 67. Except for a small, ceramic-appearing mass on one side of the inner surface, there was no obvious cause of the gamma peak and no metallographic section was made at this location. It can be assumed that the ceramic-appearing mass is similar to the material found at the 274-mm elevation.

The outer surface at the ≈90-mm elevation exhibited a flaking, 0.13-mm-thick scale (Fig. 68). The scale consisted essentially of fuel particles in a matrix of Fe-oxide, similar to the scales found on the outside of the other nozzles. More significantly, however, immediately on the nozzle surface beneath the thick scale was a 10-μ scale that contained imbedded particles of Ag-Cd, as shown in Fig. 69. This thin scale is strong evidence that a Ag-Cd-containing debris layer existed on the vessel before the massive fuel flow occurred. The hardness of the nozzle at this elevation was ≈190 DPH, about that of unaffected Inconel 600, indicating that the nozzle did not get exceptionally hot at this elevation.

VI. Discussion

A. Defining "Debris"

It is appropriate at this point to define "debris" as it will be used in this discussion. Fuel "debris" is defined here as the material that flowed to the lower head 226 minutes into the accident. Temporally and positionally this debris could have been liquid, liquid plus solid ("wet sand"), or solid (a crust against the vessel, nozzles, guide tubes, or anywhere on the surface of the solid/liquid material that is below the solidus temperature for that heterogeneous mass of material). From these examinations or others that have been performed, it is not possible to distinguish between the debris as defined here from other fuel that may have arrived on the lower head earlier than the 226-minute demarcation. Therefore, all fuel debris, with exceptions to be noted, is considered to be from the same source, whether the material is "companion material," from the "lower debris bed," or on the surface of nozzles as a thick crust or a thin scale. A debris "bed," or crust, of this material would only be that portion of the "fuel debris" that had solidified, i.e., no liquid phase, either upon initial contact with the vessel or subsequently after all of the liquid had solidified wherever it came to rest. Thus, "the" debris bed, or crust, on the lower head would have a changing character with respect to time and location as the fuel solidified, depending upon local temperatures and geometry of the lower head. This distinction is made in this report when discussing the damage to individual nozzles.

In addition to "fuel debris," this report will discuss "control rod assembly debris," consisting of all the major constituents of a control rod assembly: Ag, In, Cd, Zr, Sn, Fe, Ni, and Cr. Fuel rod materials would be minor constituents in this debris, and it is difficult to distinguish whether their involvement was early in the accident or later after the "fuel debris" reached the lower head. It will be shown later in this discussion that there is substantial evidence to conclude that there was a bed of "control assembly debris" on the lower head before the fuel debris arrived.

B. Nature of Nozzle Damage

The six nozzle segments examined at ANL fall into essentially two categories: (1) nozzles destructively affected by molten fuel: H8, H5, and M9; and (2) nozzles thermally affected by fuel debris but outwardly exhibiting little damage: L6 and E11. Nozzle D10 falls into a middle category that, depending upon interpretation, encompasses both categories.

The tops of Nozzles H5 and M9 were destroyed directly by molten fuel. The intimate mixing of molten fuel-bearing particles with molten nozzle and instrument string materials is evidence for this conclusion. Because only the lower part of the remaining H8 nozzle was received at ANL, it is not possible to say positively what the mechanism for severance was at the ≈170-mm elevation. However, with a total remaining height of only 170 mm, it may be assumed that the nozzle was melted off in a manner similar to that which occurred with Nozzles M9 and H5, and apparently G5. The finding of what appears to be porous fuel in the bottom of the H5 segment supports this conclusion. Although Nozzles D10 and E11 did not melt-off as dramatically as M9, H5, and H8, their tops did melt, as evidenced by the metallic debris within the nozzles.

Nozzles L6, H5, D10, and E11 were found to be covered, to varying degrees with an Fe-(oxide) surface scale that ranged in thickness from a few microns (L6) to 0.25 mm (D10). The thick crust patches on one side of D10 are similar in nature, i.e., Fe-based, but these patches also contain an abundance of molten Inconel and Cr-oxide, which makes them different in nature but not in source. What is probably a similar scale near the top of M9 just beneath the melted portion was not examined. These Fe-based scales are different from the porous Cr-based ceramic that was prevalent in the top of the nozzles that melted, M9 and H5 (and probably H8). The Fe-based scales are barely adherent to the nozzles and do not appear to have grown from the base metal.* Because of its apparently non-nozzle nature, it is believed that the source of the Fe-based exterior scales and the Fe-based matrix in the top of E11 was the fuel

---

*T. F. Kassner, ANL-MCT Corrosion Section, Private Communication.

flow that melted its way through stainless steel structure on the way to the lower head, regardless of its exact path. These Fe-based materials are generally located in temperature regimes that are between that of molten Inconel and that of the very clean nozzle surfaces at the cooler lower elevations. It is not obvious why these Fe-based scales contain only adventitious pieces of core debris and not material more akin to the "companion" samples.[1] Chromium apparently is not present in these scales because Cr-oxides are very volatile above 1000°C and would have migrated out of the debris during the movement to the lower head. In contrast, the Cr-oxide that formed at the tops of the nozzles when they were melted by molten fuel stayed in place, indicating very rapid cooling. (Rapid cooling of the molten nozzle tops is also evidenced by a general lack of rundown of fuel-bearing debris in most nozzles, with the noted exception of the exceptionally hot H8). The bubbles formed in the remains of Cr-depleted Inconel were likely caused by Cr-oxide vapor, which apparently precipitated into the platelets found in the H5 microstructure when the vapor could not vent to a free surface.

The assumed hour-glass shape of the "whole" remaining H8 nozzle, of which ANL received only the bottom part, may possibly be explained by the finding of extensive surface interaction between a Zr-rich phase and the nozzle. There is sufficient evidence (see next section) to conclude that there was a debris bed of control assembly materials on the lower head before the major fuel flow occurred at 226 minutes. The depth and nature of that bed cannot be determined because any direct evidence of it was obliterated by subsequent fuel flow. However, it is clear that liquid Zr, from this bed, was a primary ablating agent on the surface of the H8 nozzle and that the source of that Zr, without significant quantities of U but with Ag-Cd, was control assembly components. The appearance of the D10 nozzle surface (rough, craggy, and crusty) may be contrasted to the comparatively smoother surface of the necked-down region of H8. Nozzle D10 was in contact principally with hot fuel at temperatures sufficient to possibly have caused melting on one side. Nozzle H8, on the other hand, was in contact with Zr, which has a eutectic with Ni at 961°C. This lower temperature for liquefaction of H8 likely caused the severe necking down and smoothing of the surface compared to D10. An estimate of the minimum depth of the Zr-containing debris on the surface before

the fuel flow re-melted it would be ≈120 mm, the height of the bottom portion of the nozzle segment. A maximum height might be an additional 50 mm, if the ablation was truly hour-glass shaped.

C. Postulated Fuel Relocation Scenario

The differentiation of Fe-matrix debris from Cr-matrix debris makes possible postulation of a fuel movement scenario and estimations of initial "debris bed" depths at the nozzle locations; the final "debris bed" depths would be those measured by MPR Associates during the defueling operations. The postulated fuel movement scenario and estimation of the initial debris-bed depths are described below.

The external scales combined with known nozzle melting provide a qualitative assessment of the axial temperature profiles of the nozzles. The scales were adherent in obviously hot areas (e.g., beneath the melt zones of M9 and H5) and less adherent in the lower, colder region near the vessel. The finding of even thin scales near the bottom of some of the nozzles (not all nozzles were extensively examined for scale formation at every elevation) indicates that all the nozzles were likely surrounded by a debris bed that was colder against the vessel and hotter above. This is consistent with a fuel flow that moved down and across the lower head in a lava-like movement, generating a solid crust against the vessel and the cold nozzles it contacted. This crust apparently cooled sufficiently fast to result in no surface interaction with the lower portions of, perhaps, the first nozzles it contacted. In effect, this cold crust protected the lower portions of the nozzles from the hotter fuel debris above. Above this crust would have been a liquid-solid mixture ("wet sand") of high-solidus-temperature material (U-Zr oxide phases) and lower melting materials (Al, Fe, Cr oxide eutectics). Above the "wet sand" would have been the liquid "core" of the flow, and above that some sort of thin crust that formed in contact with steam. In such a lava-like flow, the initial basal crust would have been thick because the cold vessel acted as an excellent heat sink. As the flow moved, the vessel would have heated up and the ensuing crust would have been thinner. At some point in the movement, apparently in the E7-8/F7-8 area, the basal crust could have become suffi-

ciently thin to diminish its insulating properties and a hot spot in the vessel developed. Continued movement of the flow would have brought sufficiently hot fuel to one side of the D10 nozzle to form the thick crust and then envelop the entire nozzle at some temperature higher than the solidus temperature of Inconel 600. As described previously, it is postulated that an effectively simultaneous cooling of the fuel debris and surface melting of the nozzle resulted in entrapment of fuel particles beneath the surface of the nozzle and the cratered appearance of the surface. The bulging of the weak side of the nozzle would have occurred at this time. The adjacent and slightly elevated E11 nozzle was affected only to the extent of fairly extensive scale formation, surface melting ("pruning") of its tapered top, and melting and collapse of its top 3 mm. The finding of the Fe-based debris in the top of the nozzle indicates that some of the fuel flow came straight down as it passed over the nozzle, but it was too cold to cause more than superficial surface melting of the nozzle tip.

(It must be pointed out that there is no direct evidence for such a lava-like flow moving in contact with the vessel. An alternative scenario would have the same layered lava-like flow, but elevated, by perhaps a steam vapor, as it moved through the water in the lower head. As it lost momentum, it could have dropped to the lower head at E7-8/F7-8, causing the vessel hot spot. The explanation of the elevated melt-offs of Nozzles M9, H5, and H8 would be the same, as would the effects on the other nozzles.)

In the lava-like surface movement scenario, a "debris bed depth" can be estimated for five of the six nozzles. If one applies the definition that the debris bed is the solid crust that is formed beneath the liquid fuel, then the elevation of melting on a given nozzle, i.e., the elevation at which liquid fuel melted the nozzle and interacted with it, would be the effective thickness of the debris bed at the time the nozzle melted. However, what was believed to be candling of metallic debris down the side of the H5 nozzle could not have occurred if there had been solid debris at a level just beneath the melted area. However, two points should be considered. First, the candled material had a composition closer to Type 304 stainless steel than to Inconel 600 and its source may not have been the H5 nozzle, but rather the moving

debris itself. Second, the failure of individual nozzles may have been caused by fuel coming directly from above before debris built up along the sides. In that case, the instrument string conduit would be the likely source of the stainless steel.

An alternative fuel-flow direction is appropriate for H5, and perhaps other nozzles, for another reason. Considering that the nearby H8 nozzle apparently melted off at ≈170 mm, the relative elevations of the nozzles (see Column 1 in Table 1) would mean that H5 melted off ≈83 mm above the melt-off of H8. This would mean that these two nozzles could not have been melted off by the same liquid level in a stagnant or moving pool. The same argument can be used for the M9 nozzle, which melted off some 230 mm above where H8 apparently did. In the case of M9, however, it could be argued that the flow at that point was moving downhill and the basal crust was very thick because the vessel was still relatively cold. (Please note that the G5 nozzle segment, now at INEL, is similar in height to the adjacent H5 segment and could have been melted off by the same height of liquid as H5.) The implication here is that H5 and G5 were melted by a downward-moving pool and that they were melted before the pool reached H8. Both the H5 and G5 guide tubes were melted off significantly above their respective nozzles, indicating that such a moving pool was deep as well as elevated. Directionally, this flow would not be inconsistent with the location of the vessel hot spot; Nozzle G6, just beyond H5, was apparently melted down to a small stub on the periphery of the hot spot.

Given the lava-like flow scenario and its attendant debris bed height/nozzle melt-off characteristics, the significant differences between Nozzles L6 and M9 suggest that multiple fuel flow paths existed and that the flow across the lower head was not one massive unified flow. Nozzle M9 suggests a deep basal crust and a high liquid level, consistent with a fresh fuel flow contacting the vessel, with a direction toward H8 and the eventual hot spot. The cleanliness of Nozzle L6 indicates that there was no large liquid flow coming from the southeast between H5 and M9; although the bottom of the adjacent K5 guide tube was damaged, the K5 nozzle apparently was not. The surface debris found on L6 would have been material from the periphery of the

flow, or simply adherent material when the fuel debris eventually settled to form the "companion material."

The fuel material inside Nozzle L6 is believed to have come straight down the guide tube and not from a lava-like fuel flow for the following reasons. First, both the L6 nozzle and its overlapping guide tube were virtually unscathed, and it would have been difficult, albeit not impossible, for a relatively rigid lateral flow to have made its way up into the guide tube and then down into the nozzle. Second, there was an unreacted fuel pellet segment inside the nozzle. Such a piece would not have survived in that form in a hot fuel flow. Third, the L6 nozzle was beneath a control rod, and appreciable numbers of Ag-Cd-bearing particles were found in the annulus. Fourth, fuel that had been melted contained Fe, but the transformation into U-rich and Zr-rich phases was incomplete, indicating relatively rapid cooling. This was not typical of transformed fuel found in the hotter nozzles. Even though the matrix binding the particulate was Fe-based, this material would have had a similar history to that in the lava-like flow, except its movement would have been only downward. In the overall scenario, the source of this potpourri of material is almost irrelevant. The significance of its presence is that it apparently generated sufficient internal heat to anneal the Inconel 600, as evidenced by the relatively low and axially uniform microhardness values for this nozzle.

D. Presence of Control Assembly Materials

Four of the six nozzle segments examined at ANL were under control rod assemblies: M9, L6, H5, and H8. One, D10, was beneath an axial power shaping rod that contained 914 mm of Ag-In-Cd clad in stainless steel. The last, H5, was beneath a burnable poison rod that contained Al_2O_3-B_4C pellets clad in Zircaloy. There is pervasive evidence from the ANL examinations that the assemblies containing Ag-In-Cd failed relatively early during the accident and that the debris from these assemblies deposited in some form, probably as solid particulates, on the lower head before the principal fuel flow occurred at 226 minutes. In this section will be summarized the evidence to support

this conclusion. This material being on the lower head when it was may be a factor in determining the margin-to-failure of the lower head.

There is no direct, unequivocal evidence that the postulated control rod debris bed existed on the lower head. Examination of companion material[1] found no such evidence, either because the sampling of the "hard pan" was random and not site-specific, or because the analytical techniques were too gross to identify what would be a small percentage of the fuel debris. Most, if not all, of such a control rod debris bed would have re-melted when it came in contact with even the basal crust of the fuel flow; possibly it would have been consumed into it. Therefore, evidence for such a bed would now be, at best, on a microscopic scale and fortuitously derived.

The first evidence that the control materials were on the lower head before the fuel flow arrived was the finding of Ag-Cd nodules and In-Fe-Ni-Zr phases solidified in situ in the vessel cladding cracks in the E6 and G8 boat samples. The only fuel present in the cracks was apparently adventitious shards that likely fell in during defueling. Had there not been a control rod debris layer present when the fuel flow occurred, there would be no reasonable explanation for this finding. These materials would not have segregated in that manner from the partially solidified fuel flow.

The overwhelmingly Zr-rich liquid that contained Ag-Cd masses and ablated the H8 nozzle is further evidence for the presence of the control rod debris bed. The Zr:U ratio of ≈8.5:1 was far in excess of the Zr/U ratios found in fuel masses that were analyzed. This excess of Zr would be from the Zircaloy shroud tubes in the control assemblies. The minimum depth of this Zr-containing debris bed was ≈120 mm.

The findings of Ag and Ag-Cd inclusions deep beneath the surfaces in most of the nozzles in a form of liquid metal penetration indicates that there was a layer of control materials either adhering to the surface ready to be melted when contacted by the hot fuel, or there was a thick debris bed up against the nozzle that would yield the same result. That liquid Ag-Cd had penetrated the Inconel nozzles somewhat before nozzle melting occurred is evi-

denced by the apparently vapor-pressure-derived bubbles in the Inconel that contained Ag-Cd and other core debris constituents.

Perhaps the most striking evidence for the superposition of Ag-Cd beneath fuel debris is shown in Fig. 69, where 10-μ particles of Ag-Cd are beneath a fuel debris scale on Nozzle E11.

Because the ANL nozzles were almost all beneath control rods, the presence of such debris on or in the immediate vicinity of the nozzles could almost be expected. Given the narrow 4-mm annulus between the instrument string and the inside of the guide tube, debris coming from directly above would be fine particulate. Indeed, such fine particulate was found on the top of L6, as well as at the bottom of E11. However, whether this material came down directly from above or was circulated to the lower plenum by the coolant pumps is not the issue. (Such a distinction might be made by examining other nozzles that were not beneath control rods. The ANL findings for H5, which was not beneath a control or axial power shaping rod, showed some Ag-Cd in molten masses but only minimally on exterior surfaces and none in the Inconel.) The material in the cracks in the boat samples and the Zr attack of Nozzle H8 is sufficient evidence to conclude that there was a stagnant control material debris bed of some, unfortunately, undetermined depth and breadth.

E. Temperature Indicators

A principal objective of the nozzle examinations was to provide quantitative data on the temperature of the nozzles in proximity to the vessel. This objective was satisfied only to a limited degree. The principal reason for this was the lack of time-temperature annealing data for archival Inconel 600. Korth's work using Gleeble tests on non-archival Inconel 600[3] provides insight, but quantification using grain size and hardness data cannot be absolute. The following discussion is an attempt to glean some relative, if not quantitative information, from the ANL examinations.

1. Hardness Measurements

The microhardness measurements on the Inconel 600 nozzles, summarized in Table 3, are essentially in qualitative agreement with what was found by observation. The data from Cr-depleted areas should be disregarded because the values do not represent Inconel 600, only a Ni-Fe alloy of varying composition. Likewise, the value for the hardness of the top of E11, which partially melted, is inexplicably high and should also be disregarded as not representative. It appears that the nominal hardness of the as-fabricated material is ≈200 DPH, considerably higher than the 155-160 DPH range for Korth's material. The most significant data is from H8, where the hardness 64 mm from the vessel was 133 DPH, a value that Korth's data indicate is achieved in 10 minutes at ≈1000°C. Following this line of reasoning, none of the other nozzles within 70 mm of the vessel achieved 1000°C. It is interesting to note that the Zr surface ablation of Nozzle H8 would have begun at the 961°C Zr-Ni eutectic, a temperature well in keeping with the 1000°C estimated from the hardness measurement.

2. Microstructure

The microstructures at the 77-mm elevation in L6 and the 25-mm elevation in H5 showed active grain growth, which Korth's data indicate a temperature of at least 950°C was reached. Because the grain size was so large in H5, 0.5 mm, the temperature may have been higher, or the time at elevated temperature longer. Grain size and growth kinetics are highly dependent upon metallurgical history. Because Korth's material was not truly archival, this correlation should be viewed with skepticism, particularly since it does not agree with the hardness correlation.

3. Penetration by Ag-Cd

A Ag-Cd alloy with a nominal composition of 80 wt.% Ag-20 w.t% Cd, typical of the deposits found, melts at ≈860°C; Ag melts at 960°C. Liquid penetration occurred only in the upper elevations of the nozzles where such temperatures would be easily achieved. Lack of such penetration nearer the vessel suggests that either the nozzles did not achieve that temperature, save

H8, or there was insufficient Ag or Ag-Cd to penetrate, or our analytical techniques simply did not see it.

4. Miscellaneous Indicators

Qualitatively, a good indicator of the axial temperature profile in a nozzle was the presence and then the relative adherence of the fuel debris scale on the outside nozzle surfaces. For all nozzles except L6, which has no obvious external scale and apparently was not in a flow path, there is a reasonable correlation between scale location and nozzle hardness. On nozzle D10, the scale was adherent at the 82-mm elevation, which had a hardness of 161 DPH. That hardness is above Korth's breakpoint at ≈1000°C, where Inconel apparently anneals rapidly and the hardness falls to ≈130 DPH, or below. With this correlation, it could be subjectively concluded, again, that only Nozzle H8 had a high temperature near the vessel. The temperature of the other nozzles would have been less than 1000°C below the following elevations:

M9	215 mm
H5	38 mm
D10	82 mm
E11	255 mm

Deriving nozzle temperatures from the condition of the Zr instrument leads is considerably less direct than using any other indicator, because the leads were insulated in Al_2O_3 and the radial heat transfer path to the nozzle is impossible to calculate. The observations on β-to-α transformations only establish a minimum threshold of 860°C, which was likely achieved in most nozzles. The 1200°C threshold temperature for the Zr/Al_2O_3 redox reaction would be a good indicator except for the heat transfer issue. It is significant, however, that the 158-mm elevation in D10, where this reaction was obvious, is also the elevation where the hardness was the lowest for that nozzle, 124 DPH.

F. Penetration of Materials into Nozzles

The penetration of gamma-active materials downward into the nozzles was estimated from the ^{137}Cs gamma activity profiles and the results are summarized

in Table 1. It was assumed that the gamma activity was associated with fission products in fuel and, therefore, the results are reported as "fuel penetration." Metallic debris, essentially molten Inconel from the nozzle, were also found in the nozzles, but not tabulated. Their penetration may be estimated from the as-cut transverse sections of the nozzles. Although some of this debris contained small quantities of fuel, the quantities apparently were insufficient to register in the activity profiles.

Although porous, ceramic-appearing material was seen in the as-cut transverse sections at elevations below the nozzle tops, such as in H8 and L6, there seemed to be difficulty in retaining it during the subsequent sectioning operations to form metallographic mounts. This would attest to the friable nature of the material.

Fuel material that was retained at the lower elevations in most cases had two features. First, it appeared to be in the early stages of transformation to U-rich and Zr-rich phases, indicating relatively rapid cooling. Second, it contained Fe, Al, and Cr in the grain boundaries, indicating likely fluidity significantly below 2000°C. That would aid the fuel's mobility to the elevation where it finally solidified.[5]

In Nozzles M9 and H5, which melted off, the penetration was shallow, indicating a quick melting and relatively rapid cooling, the phase transformations in the fuel areas notwithstanding. It is likely that the melting point of Cr-oxide (Cr_2O_3 melts at 1990°C) dominated the mobility of this material before thermal equilibrium and lower-melting eutectics could form. The phase transformation of the fuel would have occurred below 1990°C while the solidified fuel was trapped in the insulating Cr-oxide.

The fuel in the tops of D10 and E11 differed from that in M9 and H5 in that it was trapped in an Fe- rather than a Cr-based matrix. This reflects two things. First, the Inconel did not readily give up its Cr to oxidation, probably because the temperature was too low. Second, the source of the fuel and the Fe-based matrix was probably the same as that of the Fe-based surface scales. That many of the fuel particles were shards and not solidified in-

situ masses indicates that the fuel flow in this region of the vessel was cooler than the flow that contacted M9, H5, and H8. This is consistent with a scenario that has the fuel flow coming to the vessel hot spot from the east and southeast and piling up on the far side against D10 and E11. (Note that the surface crust and major heating load was only on one side of D10.)

VII. Conclusions

The following are conclusions reached from the nozzle examinations and that bear on the examination objectives.

1. The nature of the degradation of Nozzles M9, H5, and H8 indicate that their melt-off was by liquid fuel coming at the nozzles at an elevation ranging from ≈140 to 270 mm above the lower head. Surface scale on the nozzles below the melt-offs suggests, albeit not conclusively, that the liquid was atop a crust of solidified and partially solidified fuel debris that had been cooled below its solidus by contact with the lower head.

2. The fuel flow on the lower head followed multiple paths. Nozzles M9, H5, and H8 suggest that flows occurred from the east and southeast, but bypassed Nozzle L6.

3. The fuel debris in and on Nozzles D10 and E11 suggest that these nozzles were at the periphery of the fuel flow, likely on the cooler far side.

4. The pattern of nozzle degradation, the assumption of a decreasing-thickness initial debris bed, and the assumed fuel flow directions are consistent with a vessel hot spot at E7-8/F7-8 that was caused by hot liquid fuel atop a progressively thinner crust because of lessening heat transfer to a warming vessel.

5. Significant nozzle temperatures ranged from 1400°C (melting) at 140 mm from the vessel at H5, down to ≈1000°C at 64 mm from the vessel at H8.

6. In addition to melting, nozzle degradation mechanisms were ablation by liquid Zr, intergranular penetration by Zr and Ag-Cd, chemical interaction with Al, Cr-depletion caused by extensive oxidation, and internal pressurization causing hot-tearing and nozzle ballooning.

7. The presence of significant quantities of Zr and Ag-Cd on the vessel to interact with the nozzles is attributed to the prior deposition at that location of control assembly debris. The depth or nature of such a debris bed could not be confirmed, but the depth is estimated to have been a minimum of 120 mm at the H8 location.

8. Fuel debris penetration downward into the nozzles was influenced by the temperature of the fuel at the time of entry; its composition, and hence fluidity; the temperature of the nozzle and its ability to solidify the debris; and the degree of interaction between the fuel and the molten nozzle in entrapping the fuel in Cr-oxide.

Table 1 - ANL Nozzle Segment Lengths, Elevations, and Fuel Penetration Depths

Nozzle	Elevation of Nozzle Base, mm	Segment Length, mm	Stub Length, mm	Missing[a] Top, mm	Elevation of Top of Segment,[b] mm	Fuel Penetration Elevation above Nozzle Base,[c] mm
M9	119	254	26[d]	25	280	241
L6	94	241	64[d]	0	305	75
H5	107	146	0	159	146	89 max 117 min
H8	0	70	51	184	121	<64
O10	244	235	57[d]	13	292	55 max 184 min
E11	221	225	77[d]	3	302	204

[a]Based on measurement from either top taper point or midplane bevel.
[b]Referenced to nozzle base.
[c]Based only on gamma scans.
[d]Calculated as the difference between 305 mm and the sum of the two known values. Measurements of stub lengths for O10 and E11 from photographs were not deemed sufficiently accurate because of angle of photo.

Table 2 - Composition of Debris Areas/Particles Containing U-Zr[a]

Nozzle/Location	Composition, wt.%[b]							
	U	Zr	Fe	Ni	Cr	Ag	Cd	Al
M9/279 mm (inside nozzle)								
Matrix	29	8	6	5	43	-	-	7
Matrix	55	12	5	2	15	-	-	9
Particulate	58	19	8	11	3	-	-	-
Fuel mass	88	9	1	1	1	-	-	-
Fuel mass	83	15	1	-	1	-	-	-
Fuel mass	55	12	5	15	2	-	-	9
L6/283 mm (inside nozzle)								
Shard	100	-	-	-	-	-	-	-
Solidified mass, 1[c]	83-87	11-13	2	-	1	-	-	-
Grain boundary, 1	41	19	17	-	14	-	-	8
Solidified mass, 2	17	54	9	1	11	-	-	9
Solidified mass, 2	74	27	-	-	-	-	-	-
H5/140 mm (inside nozzle)								
Ceramic area, edge	25-30	13-15	1-3	1	51-57	-	-	-
Ceramic area, edge	82	12	1	3	1	-	-	-
Ceramic areas, center[d]	(35-40)	(12-16)	-	-	(40-55)	-	-	-
Ceramic areas, center	13-30	8-12	7-22	2-10	40-77	-	-	-
Ceramic area, edge	28	15	33	11	13	-	-	-
H8/120 mm (inside nozzle)								
Particulate areas	60	30	4	3	1	-	-	-
D10/280 mm (inside nozzle)								
Particulate 1	65	23	4	3	5	-	-	-
Particulate 2	63	12	5	15	6	-	-	-
D10/158 mm (imbedded in nozzle)								
Particle 1	68	23	4	2	2	-	-	-
Particle 2	77	20	1	1	1	-	-	-
Particle 3	91	8	-	1	-	-	-	-
D10/82 mm (outside nozzle)								
Particle 1	14	62	8	6	2	7	-	-
Particle 2	81	16	2	1	-	-	-	-
Particle 2	75	16	6	2	2	-	-	-
Particle 3	10	77	6	5	1	-	-	-
Particle 4	22	78	-	-	-	-	-	-
D10/69 mm (outer surface)								
Imbedded particle	82	12	1	3	1	-	-	-

[a]Normalized to ≈100% metal; oxygen not considered.
[b]Estimated accuracy is ±20%.
[c]Like numbers indicate either more than one analysis on a particular structure, or individual areas in a structure.
[d]Parentheses identify estimated values for portion of analyzed area.

Table 2 (continued)

Nozzle/Location	Composition, wt.%[b]							
	U	Zr	Fe	Ni	Cr	Ag	Cd	Al
E11/280 mm (inside nozzle)								
Large shard	83	14	1	-	1	-	-	-
Small shard	83	14	2	-	1	-	-	-
Matrix	34	53	8	3	3	-	-	-
Matrix	47	44	6	2	1	-	-	-
Matrix	66	27	4	2	1	-	-	-
Matrix	87	10	1	-	1	-	-	-
Surface fold (outside)	74	10	2	6	2	-	-	6
E11/274 mm (inside nozzle)								
Inside nozzle	≈9	≈85	4	2	1	-	-	-
Inside nozzle	27	71	1	1	-	-	-	-
Inside, agglomerates (avg)	62	16	19	3	-	-	-	-
E11/90 mm (outer surface)								
Outer scale	20	20	57	2	1	-	-	-

Table 3 - Summary of Hardness Determinations

Elevation from Vessel, mm	Nozzle					
	D10	E11	H8	H5	L6	M9
290	-	208 ± 29	-	-	-	-
283	-	-	-	-	167 ± 7	-
280	140 ± 4	-	-	-	-	-
274	-	137 ± 4	-	-	-	-
266	136 ± 3	-	-	-	-	-
260	-	-	-	-	-	124 ± 5[a]
158	124 ± 2	-	-	-	-	-
130	-	-	-	105 ± 2[a]	-	-
90	-	190 ± 9	-	-	-	-
82	161 ± 4	-	-	-	-	-
77	-	-	-	-	169 ± 13	-
69	168 ± 10	-	-	-	-	-
64	-	-	133 ± 4	-	-	-
38	-	-	-	-	-	202 ± 28
25	-	-	-	198 ± 8	-	-
0	-	-	-	217 ± 13[b]	-	-

[a]Cr-depleted material.
[b]Weldment.

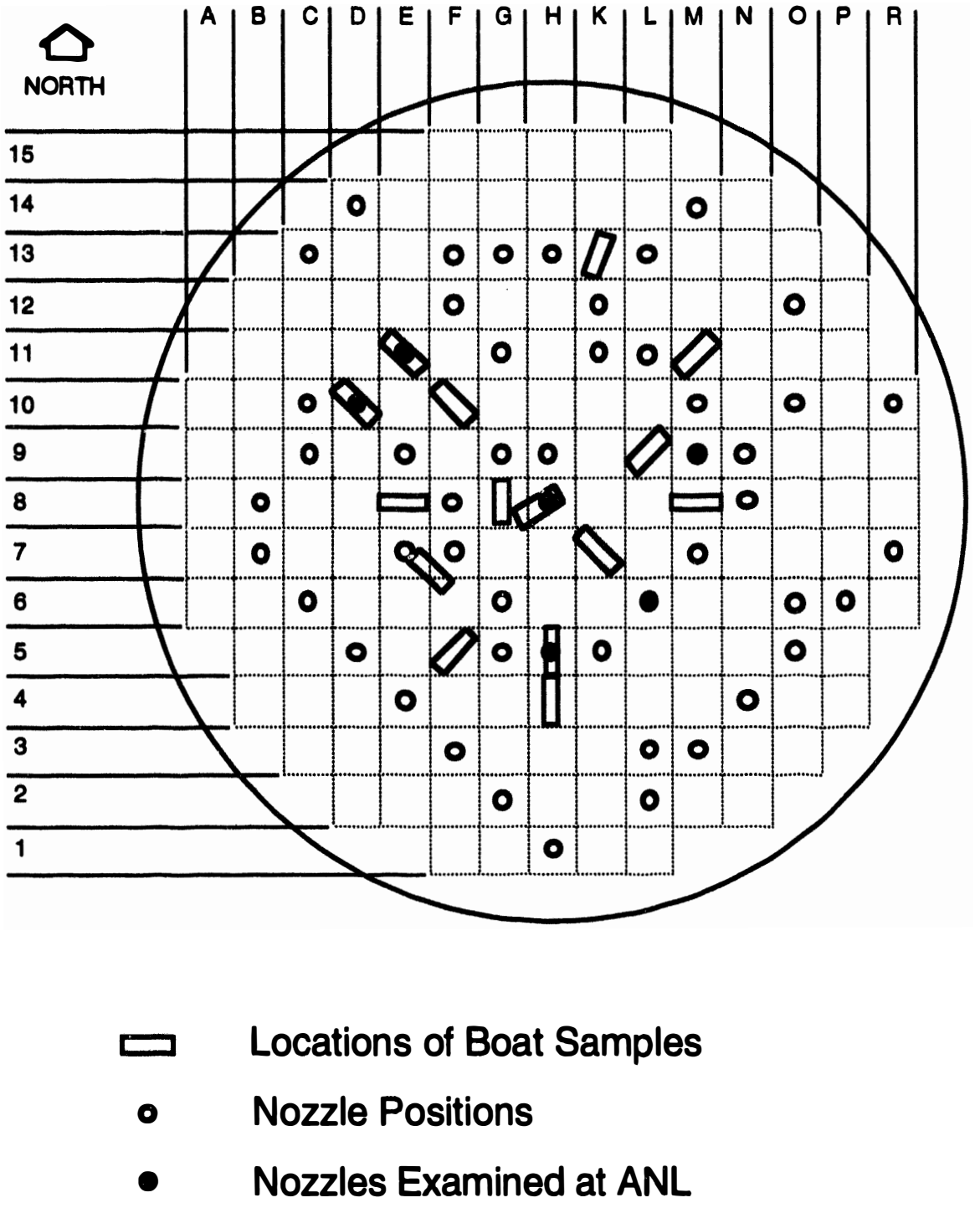

Fig. 1. Grid map of TMI core showing locations of nozzles examined at ANL.

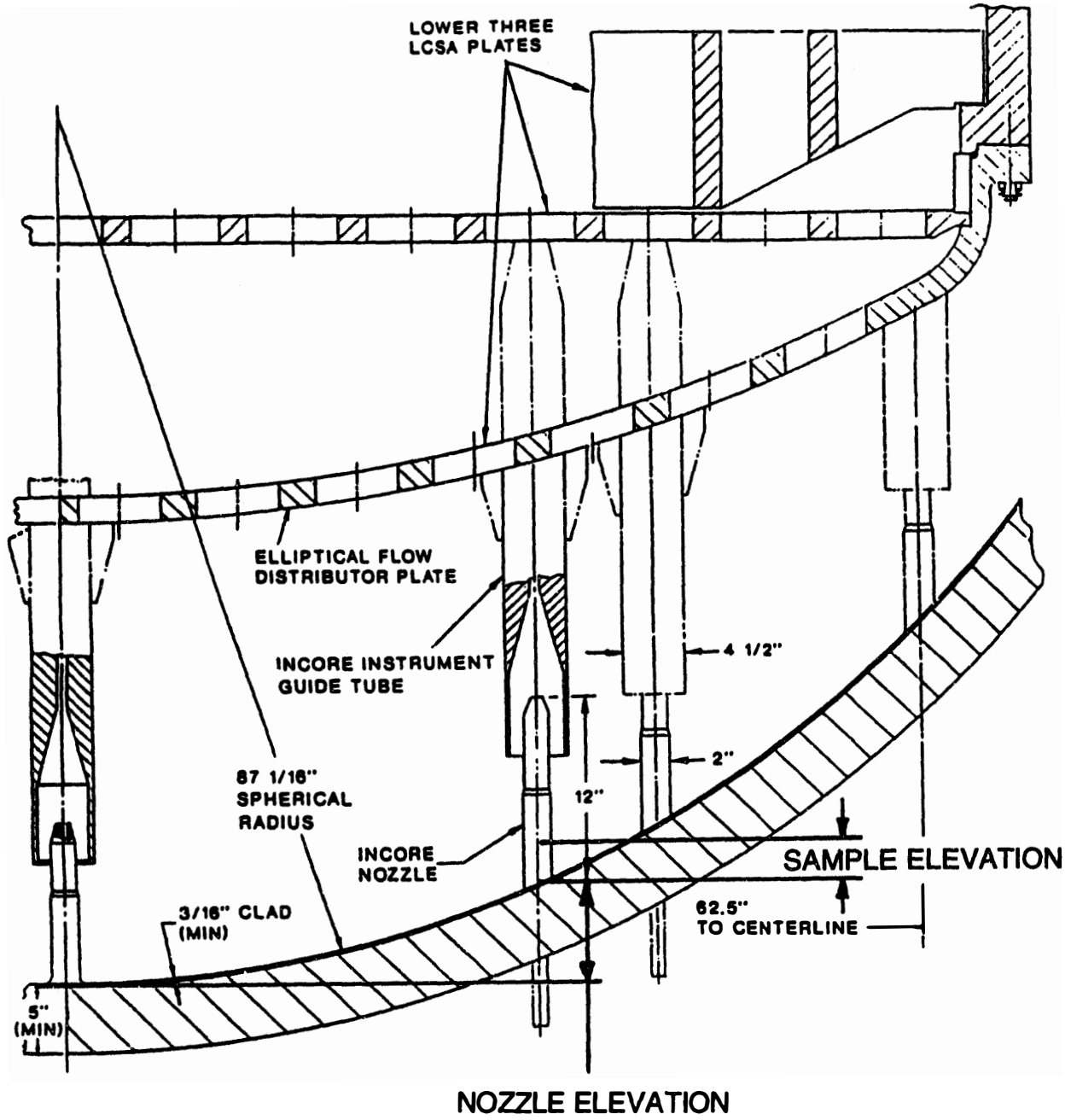

Fig. 2. Typical incore nozzle with seal and retaining weld.

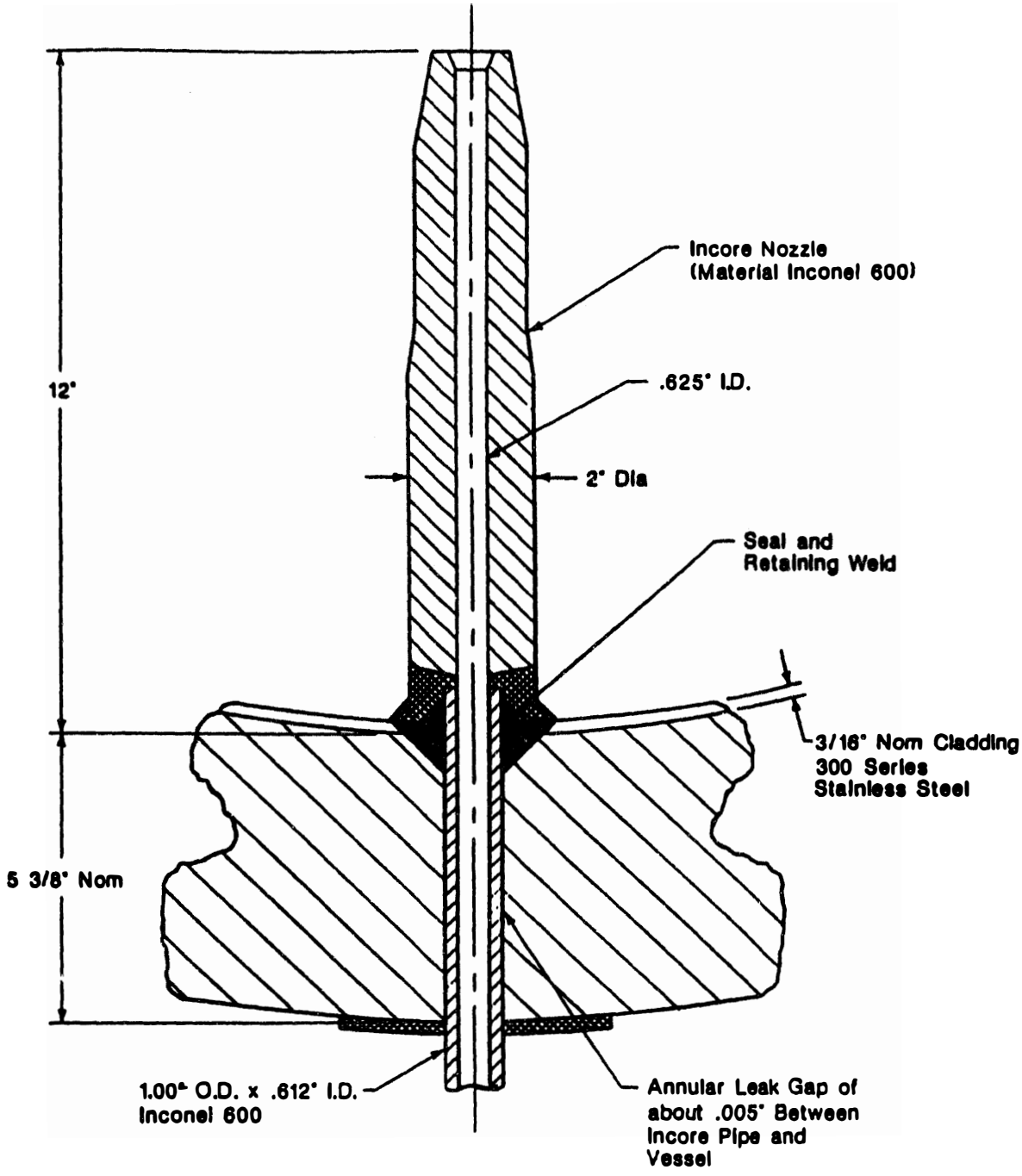

Fig. 3. Lower-head area and incore instrument guide tubes.

Fig. 4. Elevation view of nozzle segment M9, as received. (282582)

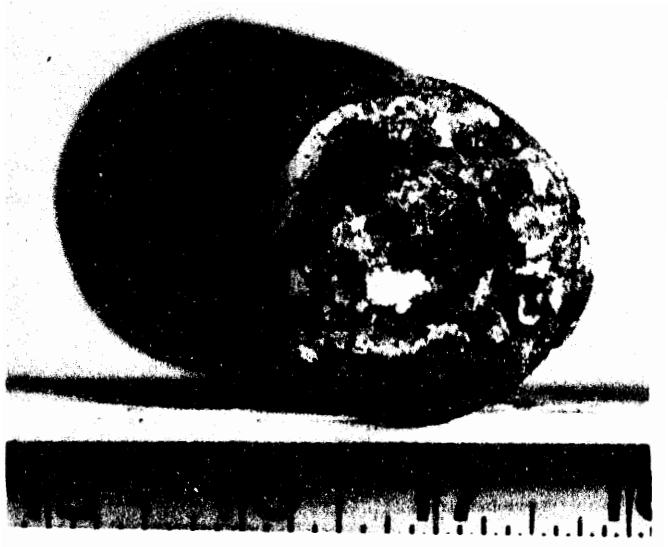

Top

Bottom

Fig. 5. Top and bottom views of M9 nozzle segment, as received. (282558)

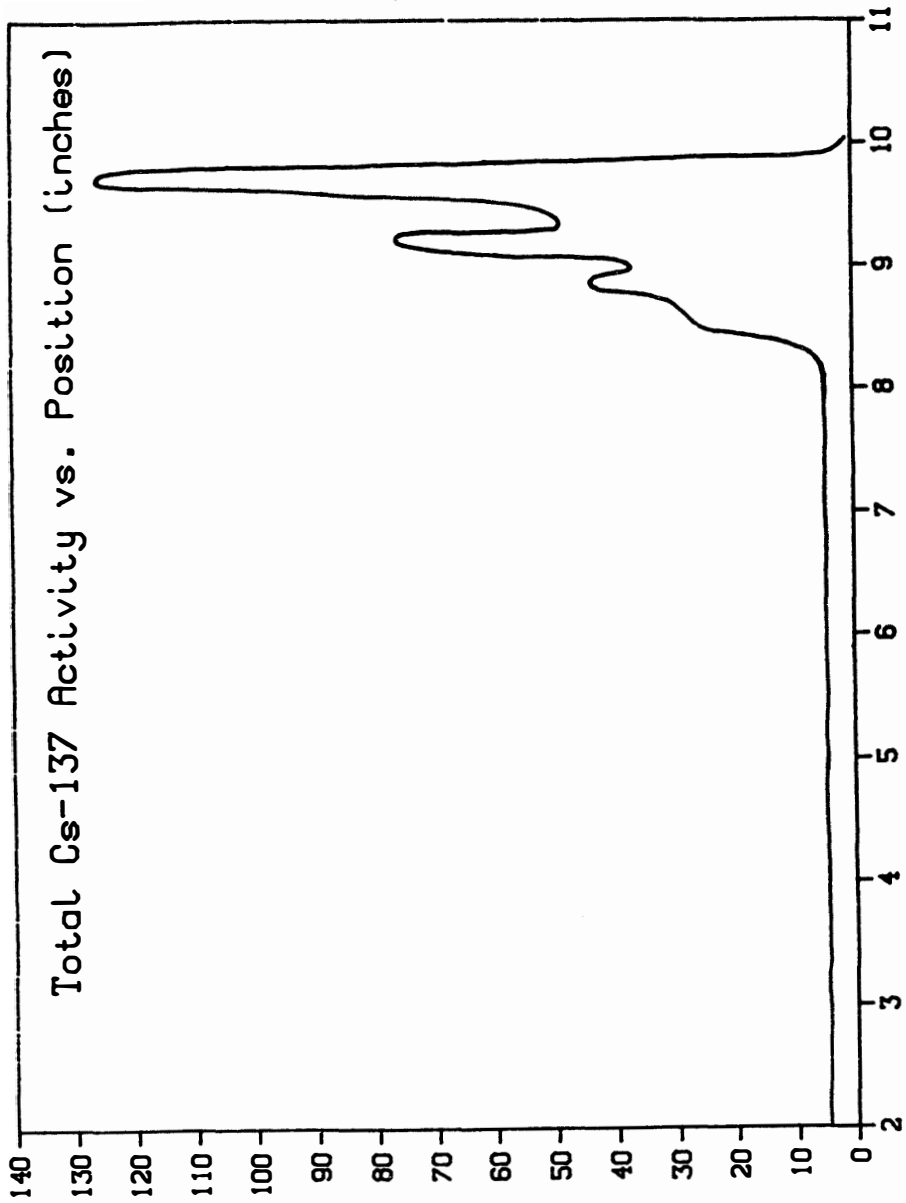

Fig. 6. Gamma activity profile and sectioning scheme for Nozzle M9. Location of longitudinal cuts shown only to identify specimens, not actual cutting planes.

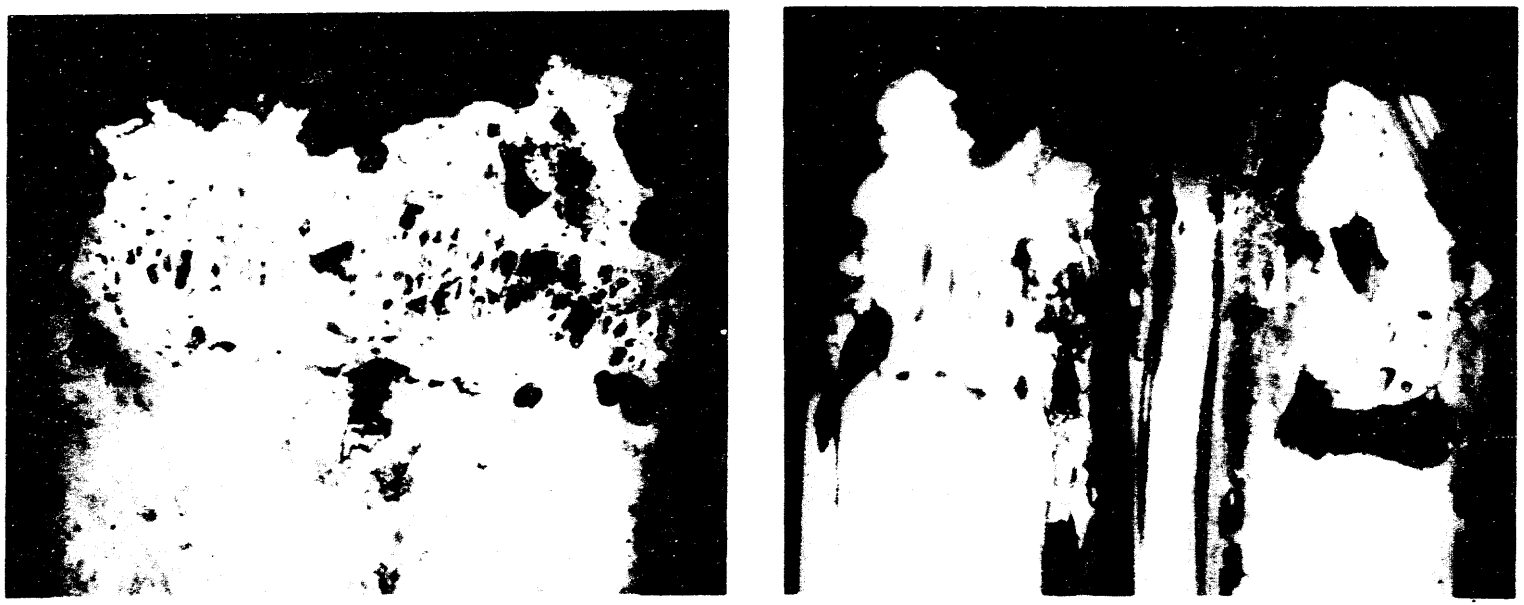

Fig. 7. Longitudinal sections through top of Nozzle M9 near the center (left) and at the center (right). 2X (280683 and 280687)

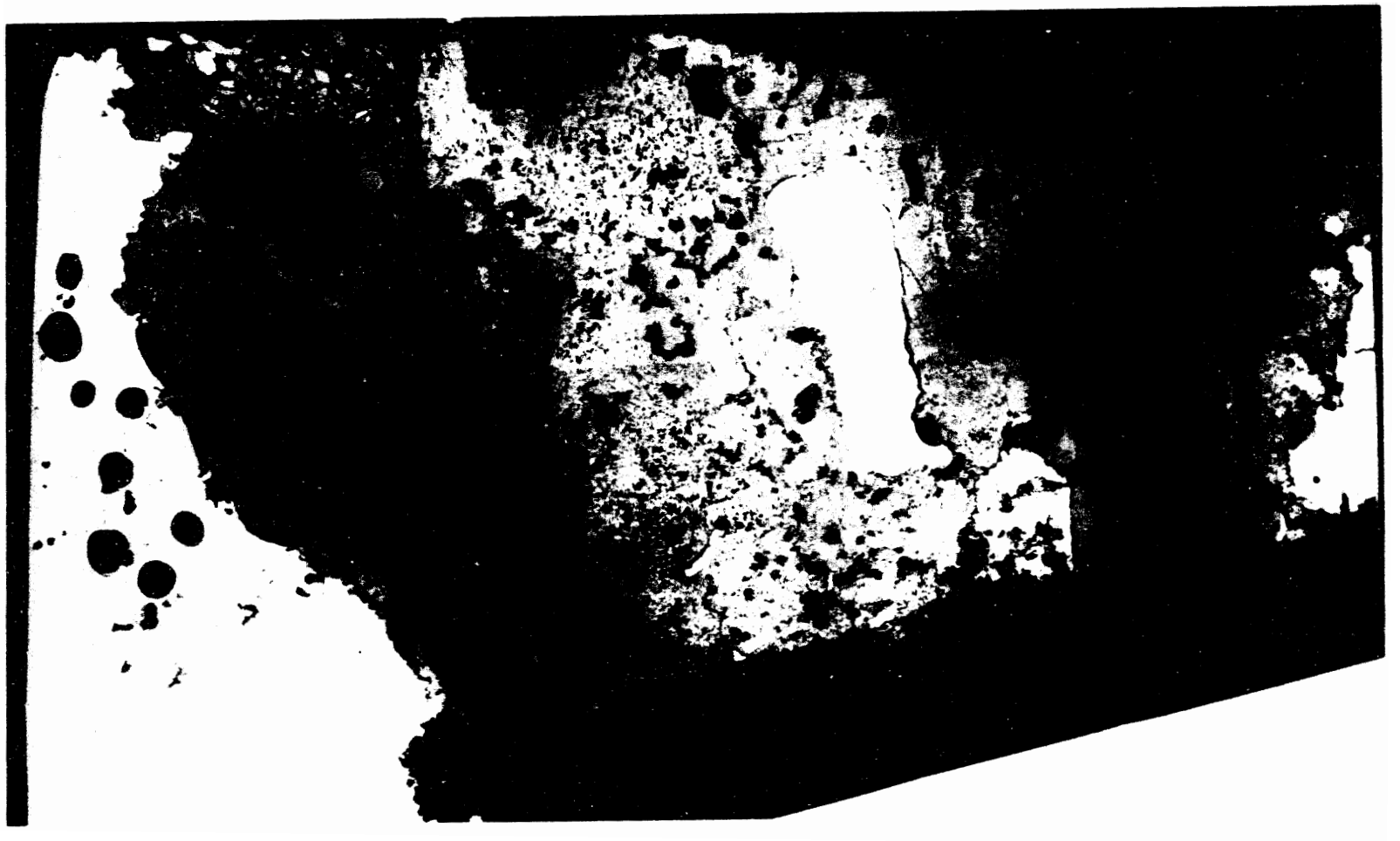

Fig. 8. Longitudinal section through top of Nozzle M9. (Original at 25X, reduced to 14X; 280695)

Fig. 9. SEM-BSE image of multiphase fuel in Nozzle M9. Light material is U-rich, medium is Zr-rich, and darkest is Cr-rich matrix.

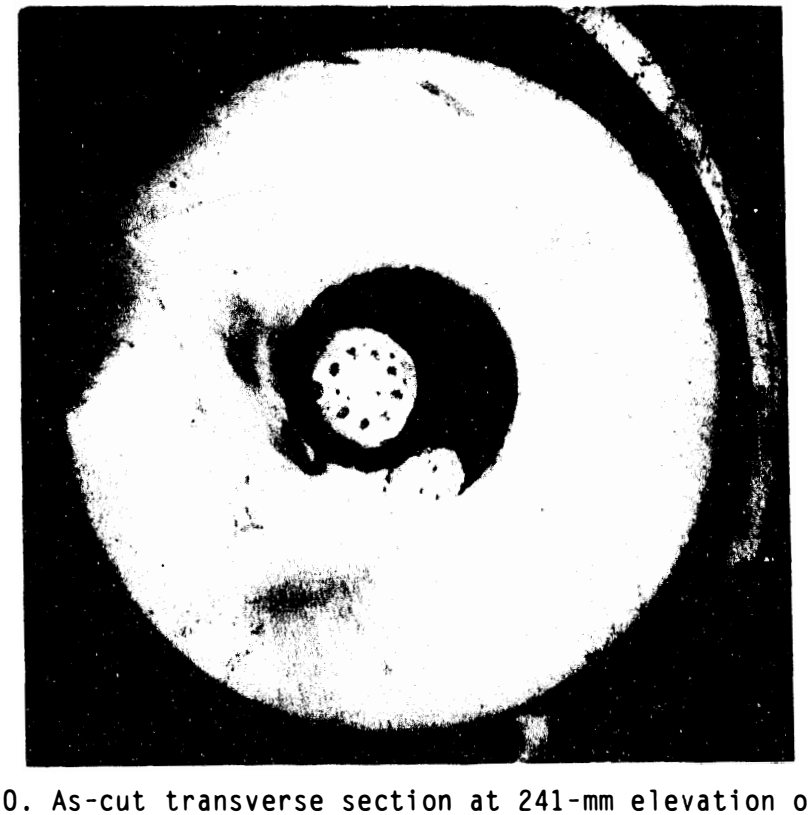

Fig. 10. As-cut transverse section at 241-mm elevation of M9, showing metallic and possibly ceramic debris between 5 and 8 o'clock in the annulus. 2X (280685)

Fig. 11. Elevation view of nozzle segment L6. (282581)

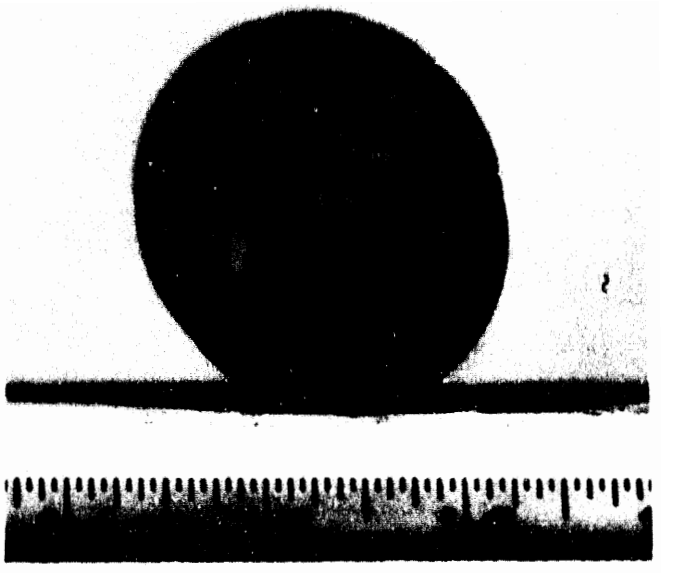

Top

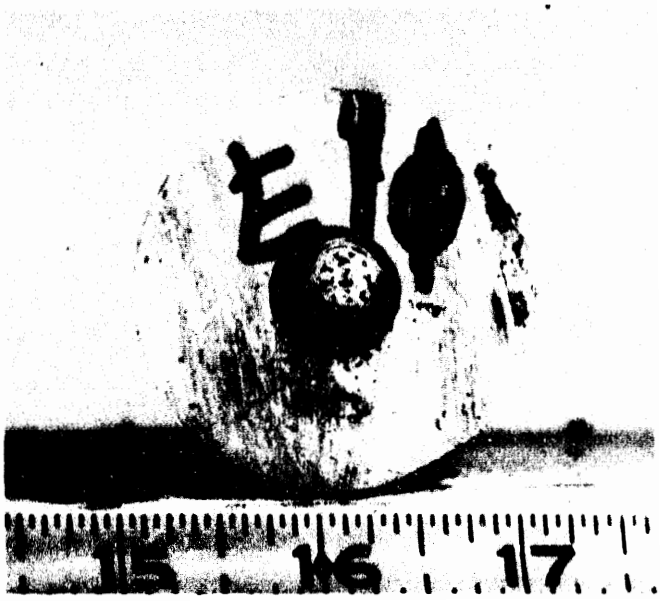

Bottom

Fig. 12. Top and bottom views of L6 nozzle segment. (282587)

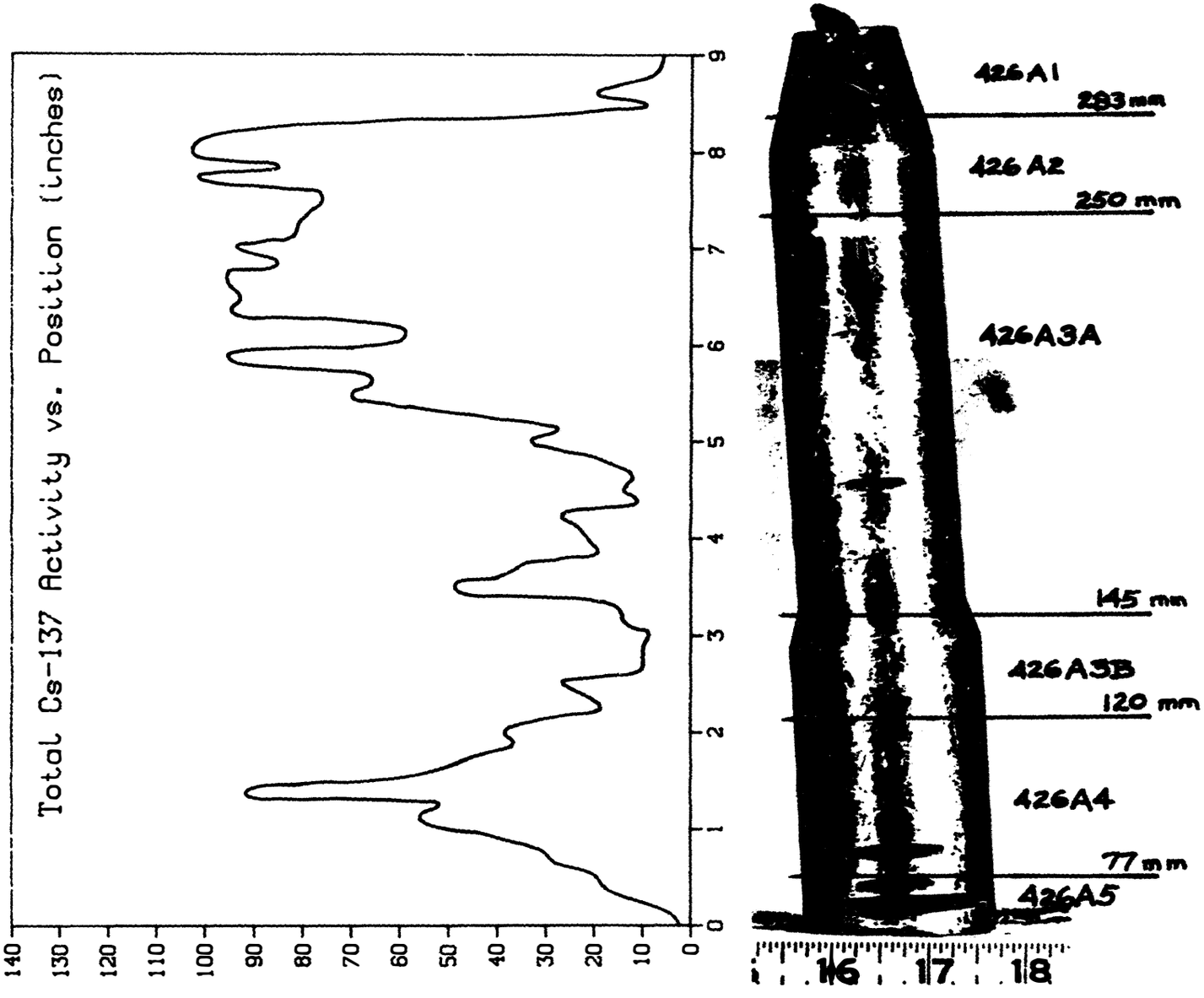

Fig. 13. Gamma activity profile and sectioning scheme for Nozzle L6.

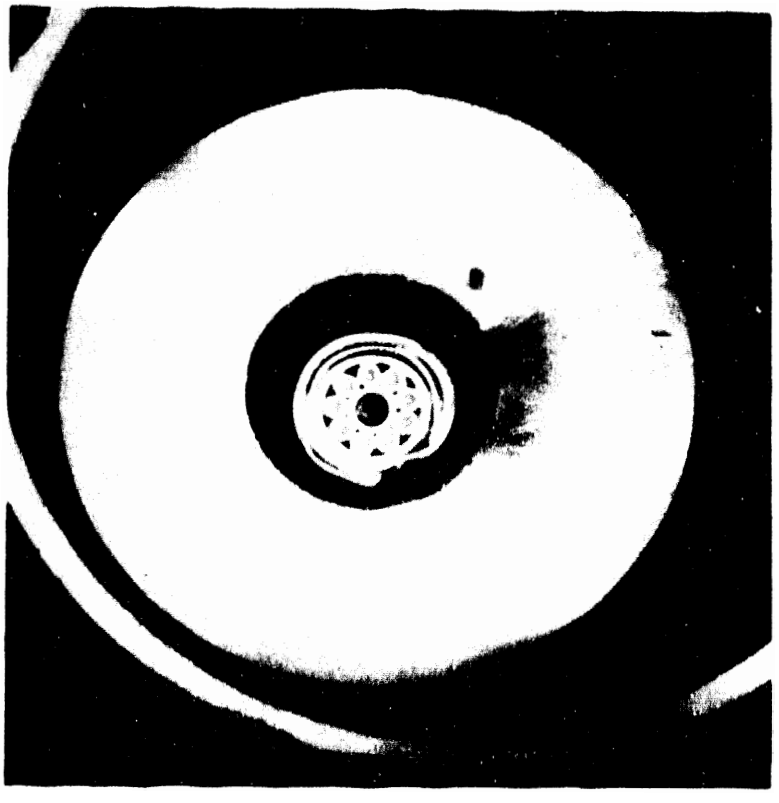

Fig. 14. As-cut transverse section at 283-mm elevation of L6, showing a porous material in the annulus. 2X (280675)

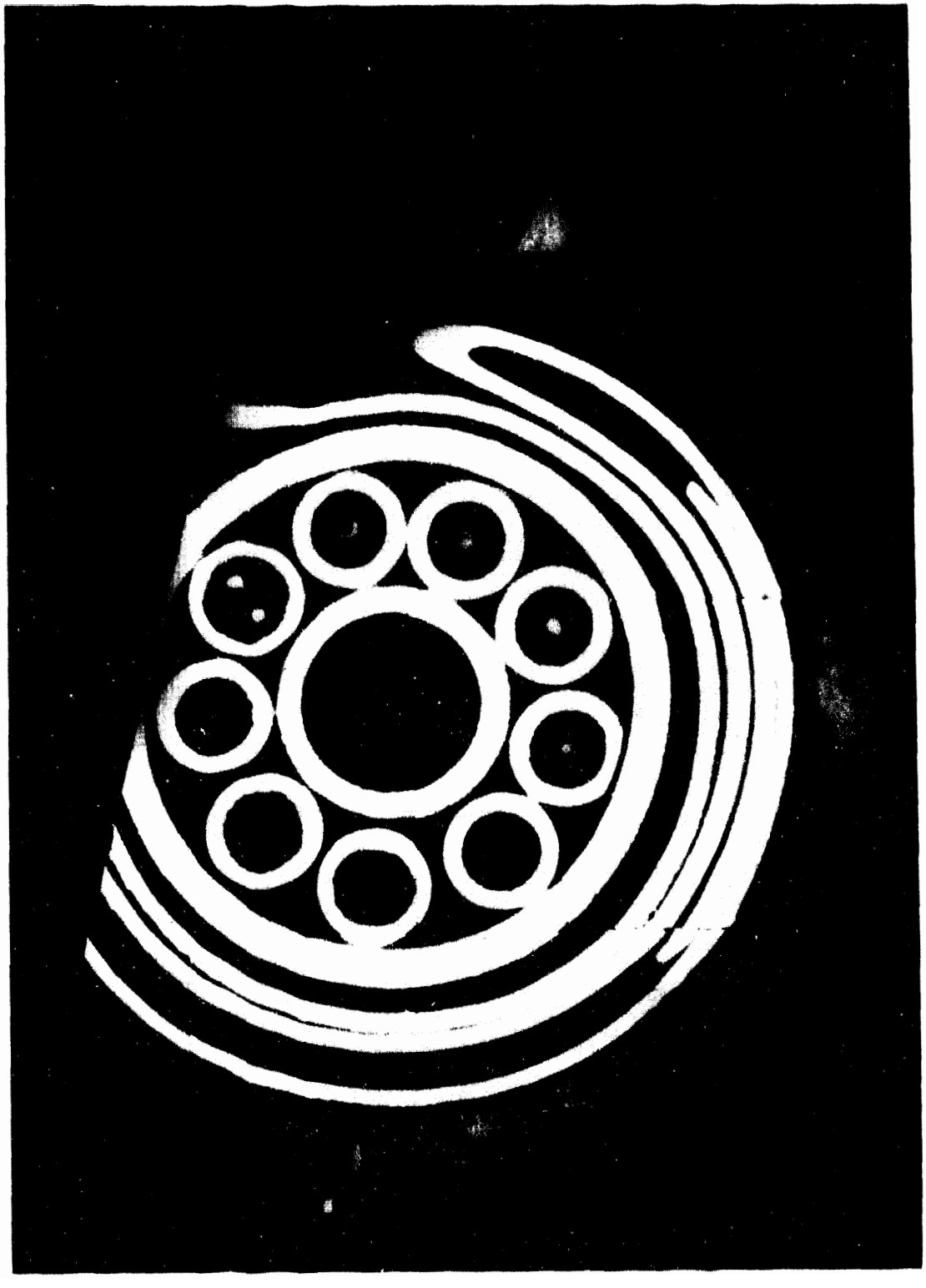

Fig. 15. Instrument string and fuel debris at 283-mm elevation of L6.
(Original at 25X, reduced to 11X, 281570)

Fig. 16. Partially transformed fuel mass at 283-mm elevation of L6.

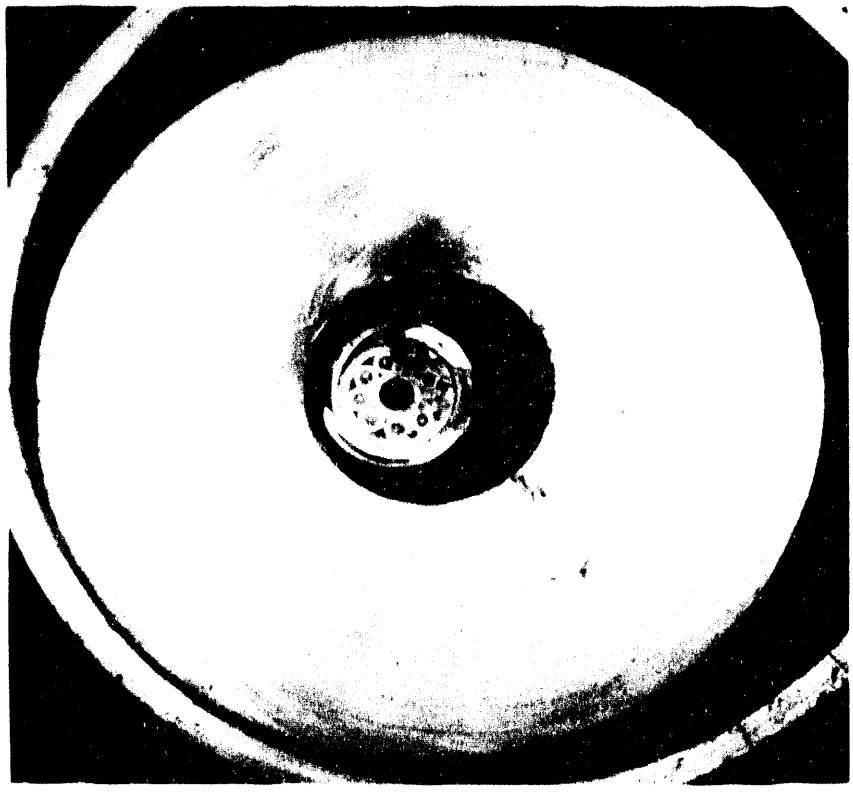

Fig. 17. As-cut transverse section at 77-mm elevation of L6. 2X (280680)

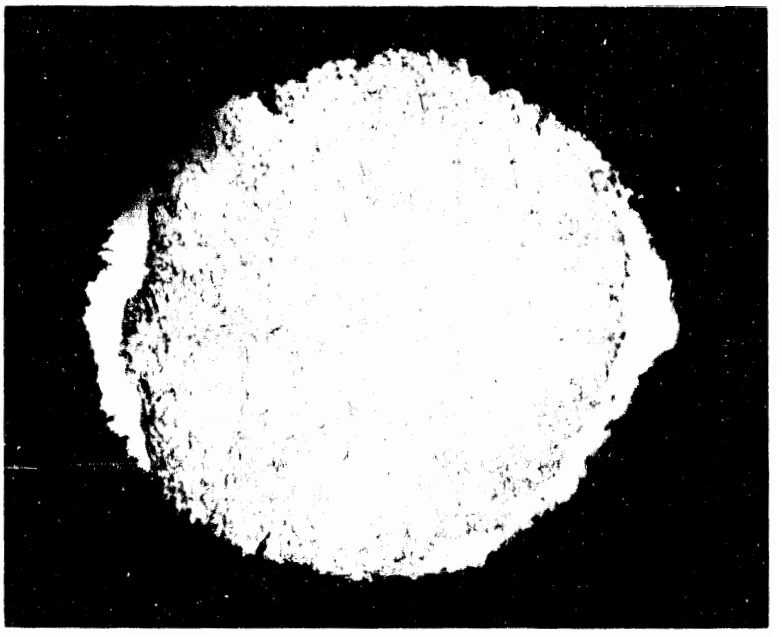

Fig. 18. Partially transformed zirconium instrument lead at 77-mm elevation in L6. 250X (281664)

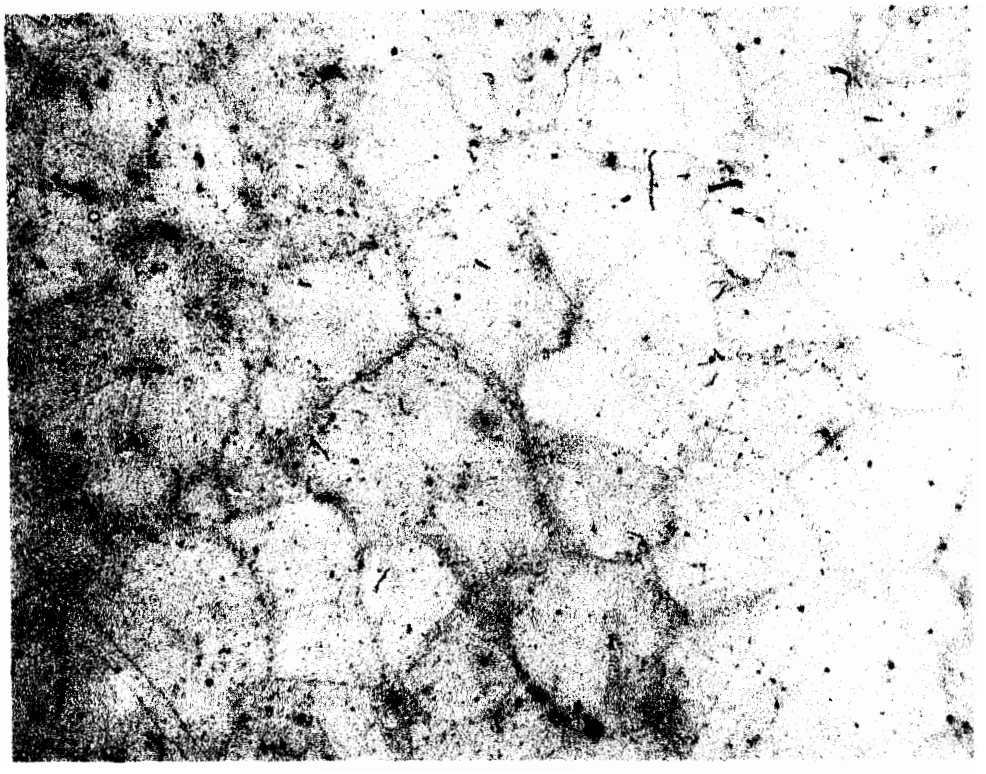

Fig. 19. Etched microstructure of Inconel 600 nozzle at 77-mm elevation in L6. 100X (282531)

Fig. 20. Elevation view of nozzle segment H5. (282580)

Top (stereo pair)

Bottom

Fig. 21. Top and bottom views of H5 nozzle segment. (282585)

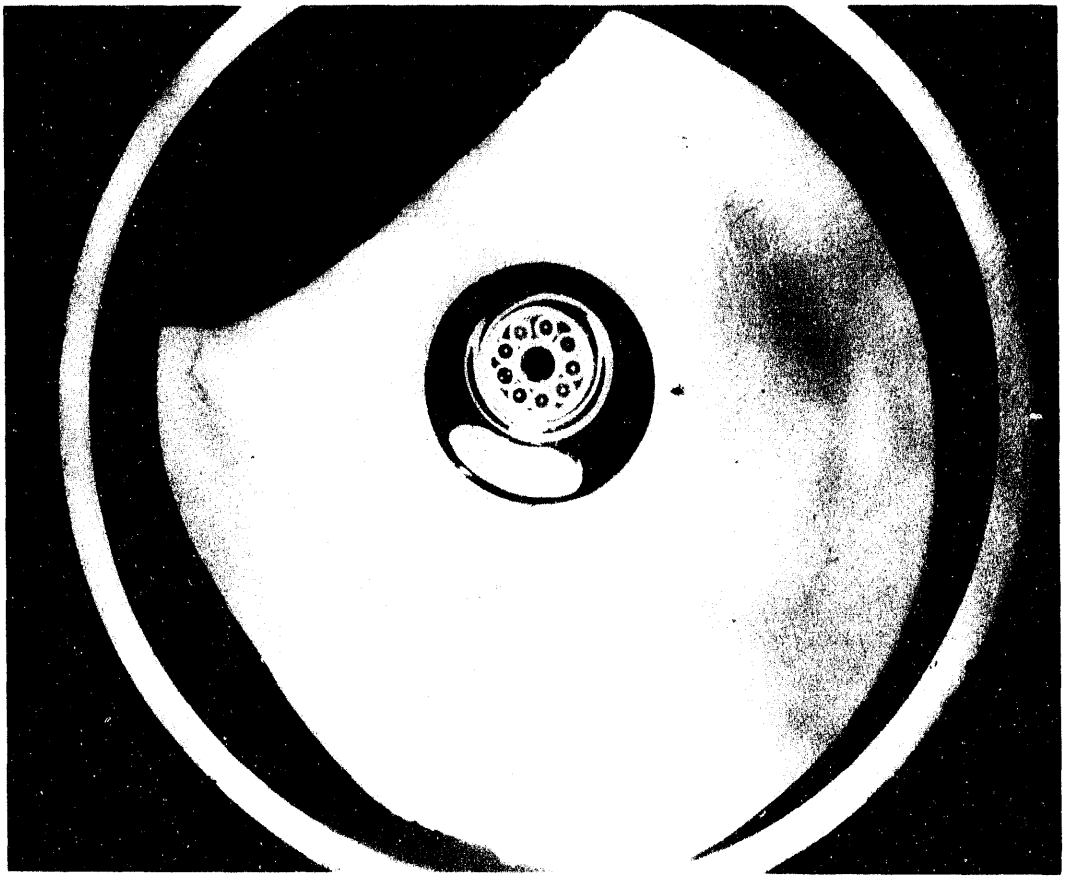

Fig. 22. As-polished bottom end of H5 segment, revealing only a solidified metallic mass. 2X (280533)

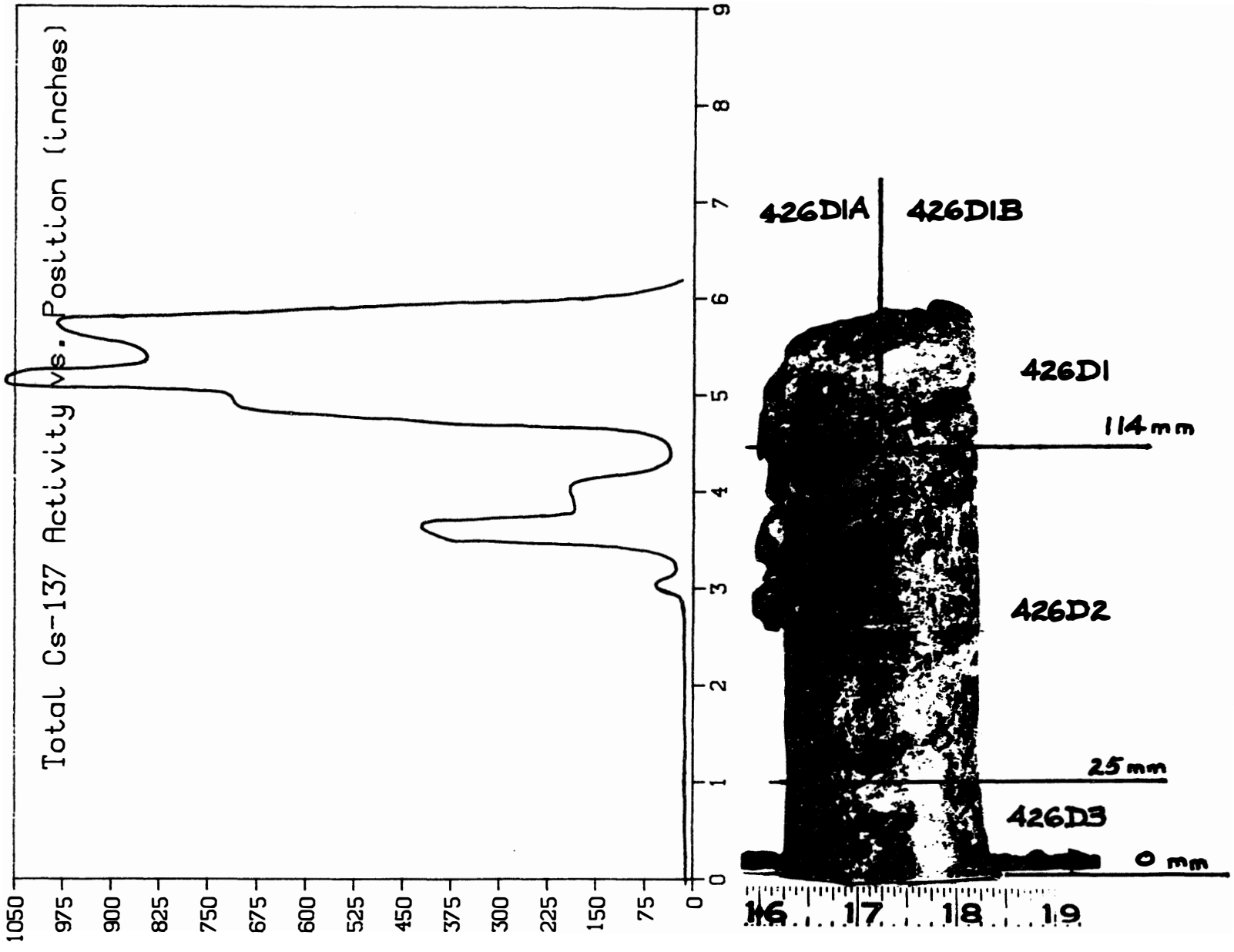

Fig. 23. Gamma activity profile and sectioning scheme for Nozzle H5. Location of longitudinal cut shown only to identify specimens, not actual cutting plane.

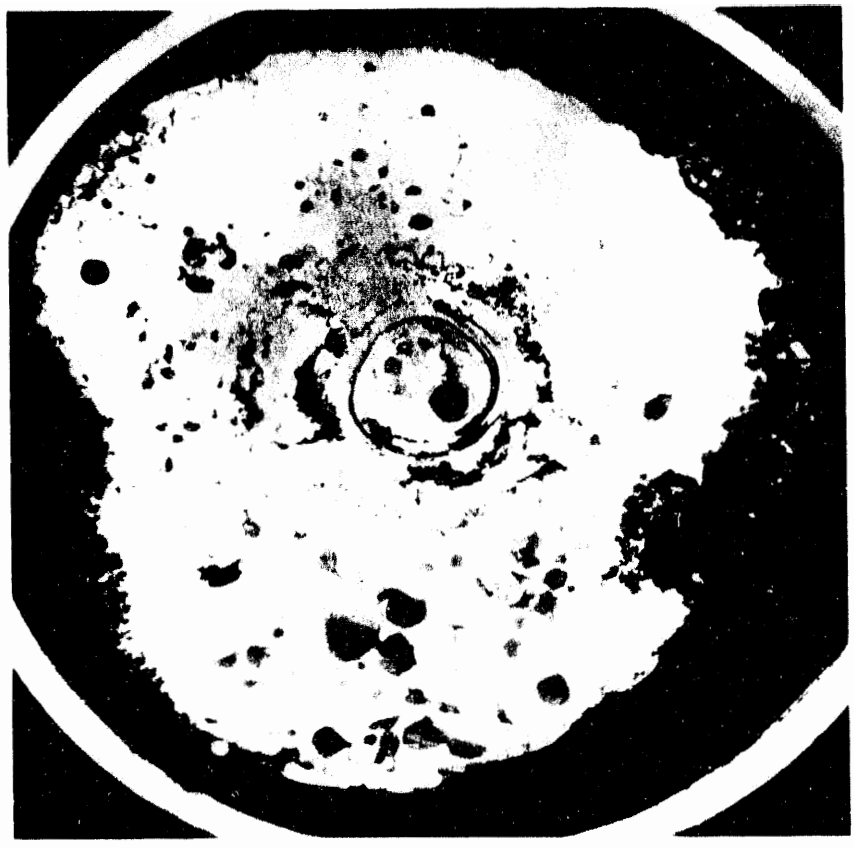

Fig. 24. As-cut transverse section through H5 at the 114-mm elevation. 2X (280530)

Fig. 25. As-cut longitudinal section through top of H5 segment. 2X (280535)

Fig. 26. Metallic and ceramic debris at top of H5. (Original at 25X, reduced to 15X; 280693)

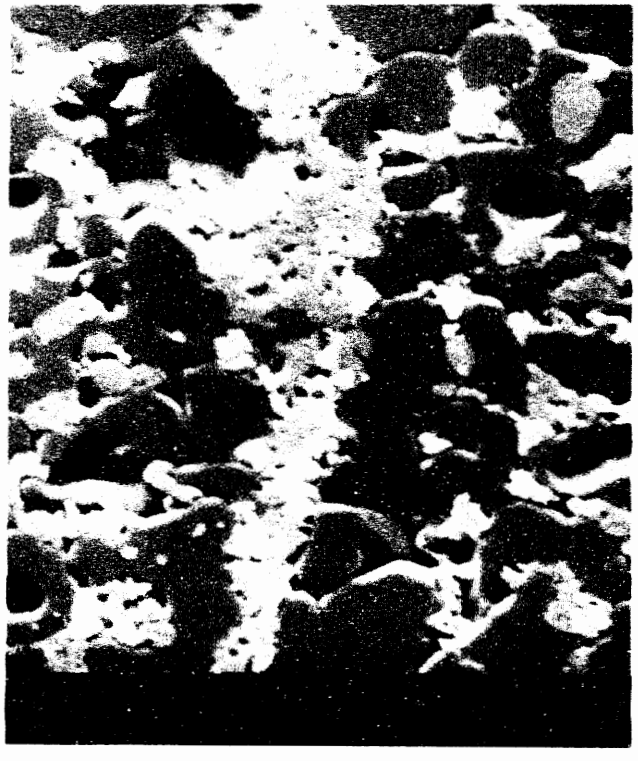

Fig. 27. Microstructure of debris at top of H5, showing intimate mixture of U-rich phases (light), Zr-rich phases (medium), and Cr-rich matrix (darkest).

Fig. 28. Chromium-rich platelets precipitated in Cr-depleted Inconel. Bubble contains deposits of core debris.

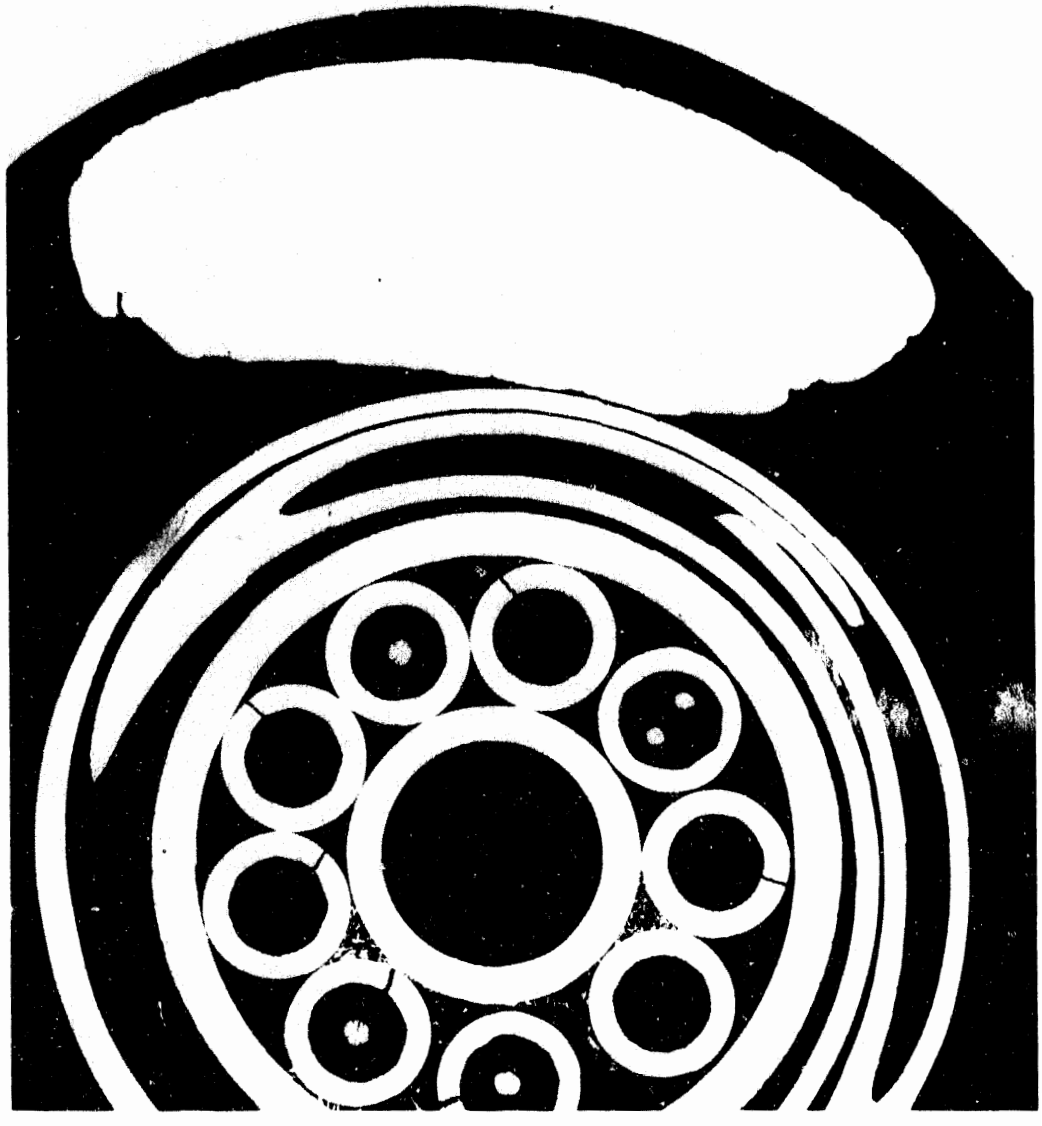

Fig. 29. Instrument string and solidified Inconel mass at the bottom of the H5 segment. (Original at 25X, reduced to 12X, 280635)

(a)

(b)

Fig. 30. Shards of Inconel 600 (a) and fuel debris (b) within instrument string at bottom of H5. 250X (280582 and 280584)

Fig. 31. Bottom weldment of the H5 nozzle. 9X (281587); insert at 260X (281635)

Top

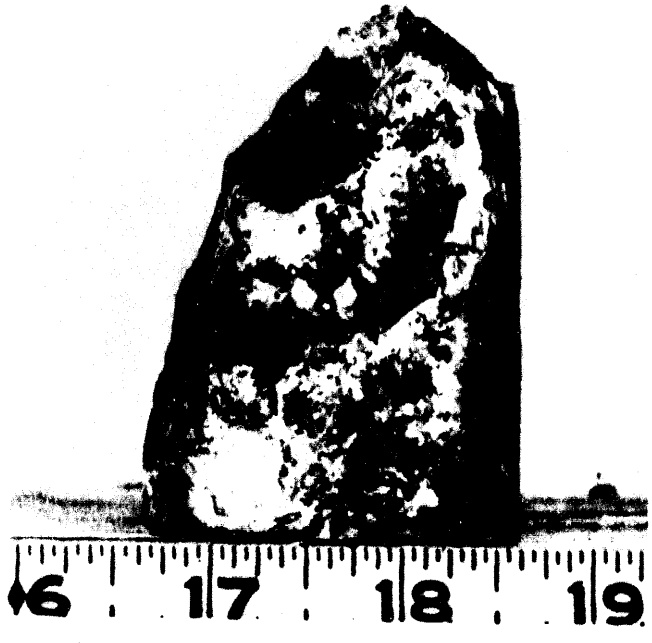

Side

Fig. 32

Top, elevation, and bottom views of H8 nozzle segment. (282586)

Bottom

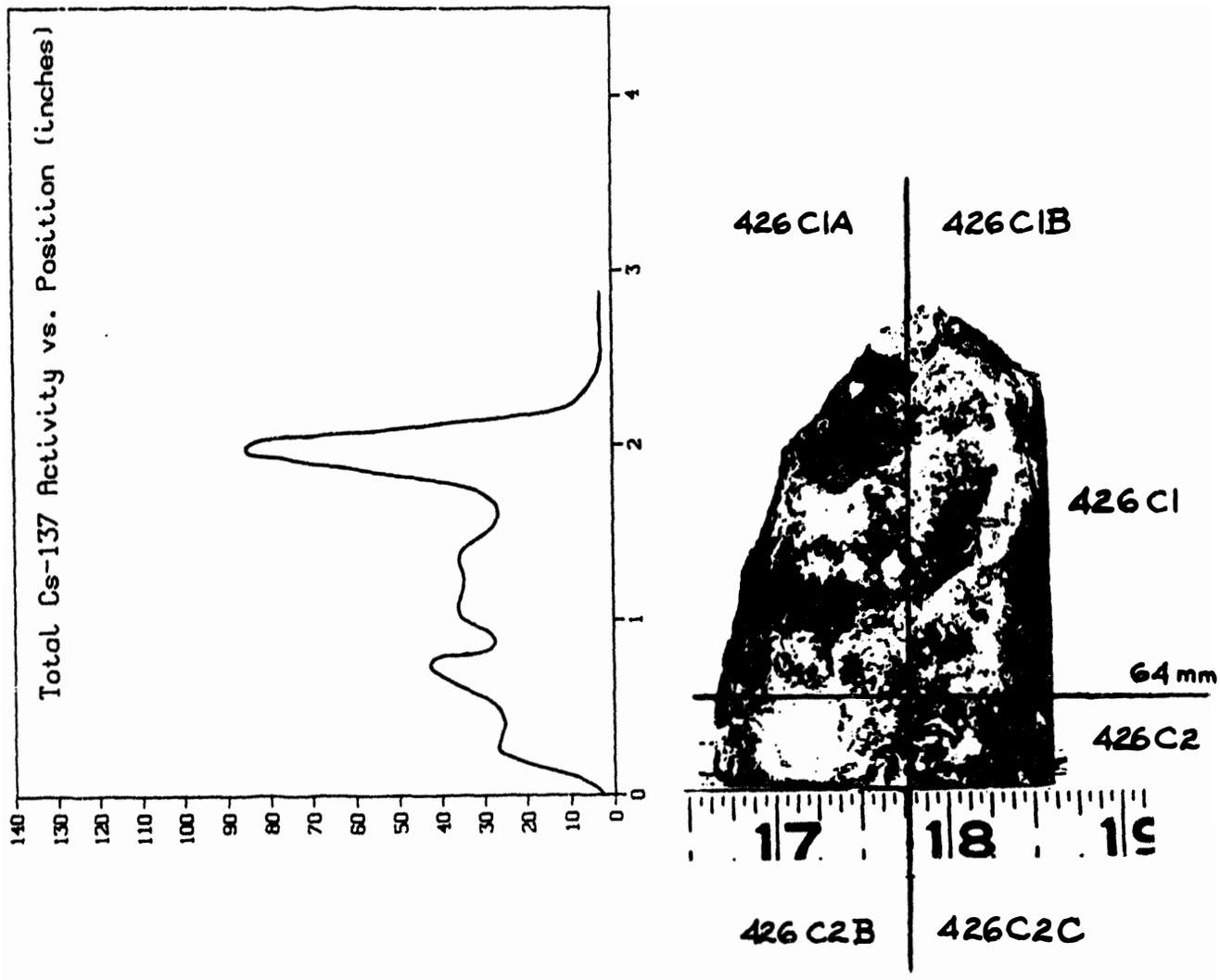

Fig. 33. Gamma activity profile and sectioning scheme for Nozzle H8. Location of longitudinal cut shown only to identify specimens, not actual cutting plane.

Fig. 34. As-cut longitudinal section through the top of H8. 2X (280653)

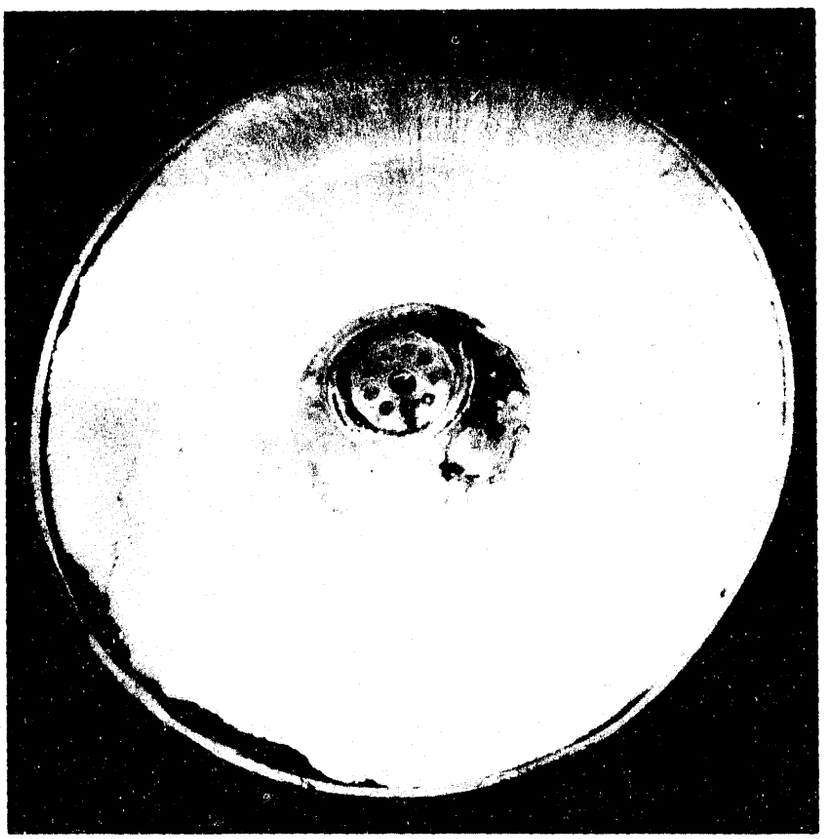

Fig. 35. As-cut transverse section at the 64-mm elevation in H8. 2X (280652)

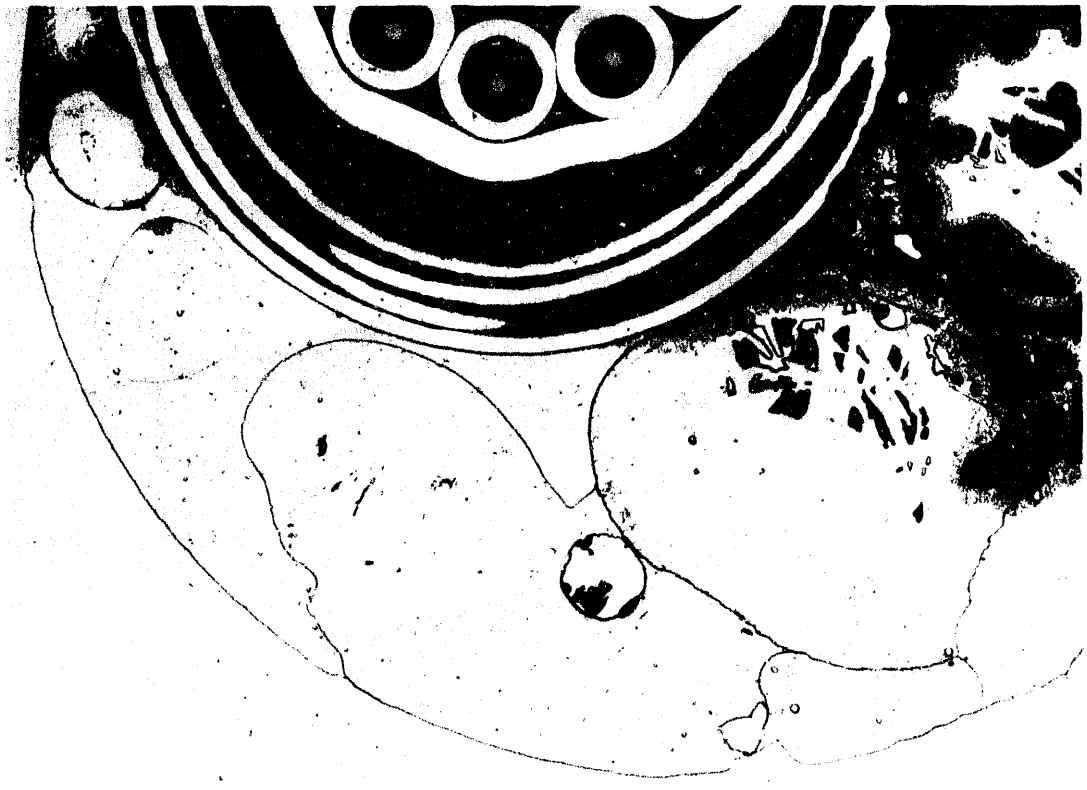

Fig. 36. Metallographic section of instrument string and metallic debris at the 64-mm elevation of H8. (Original at 35X, reduced to 11X, 280453)

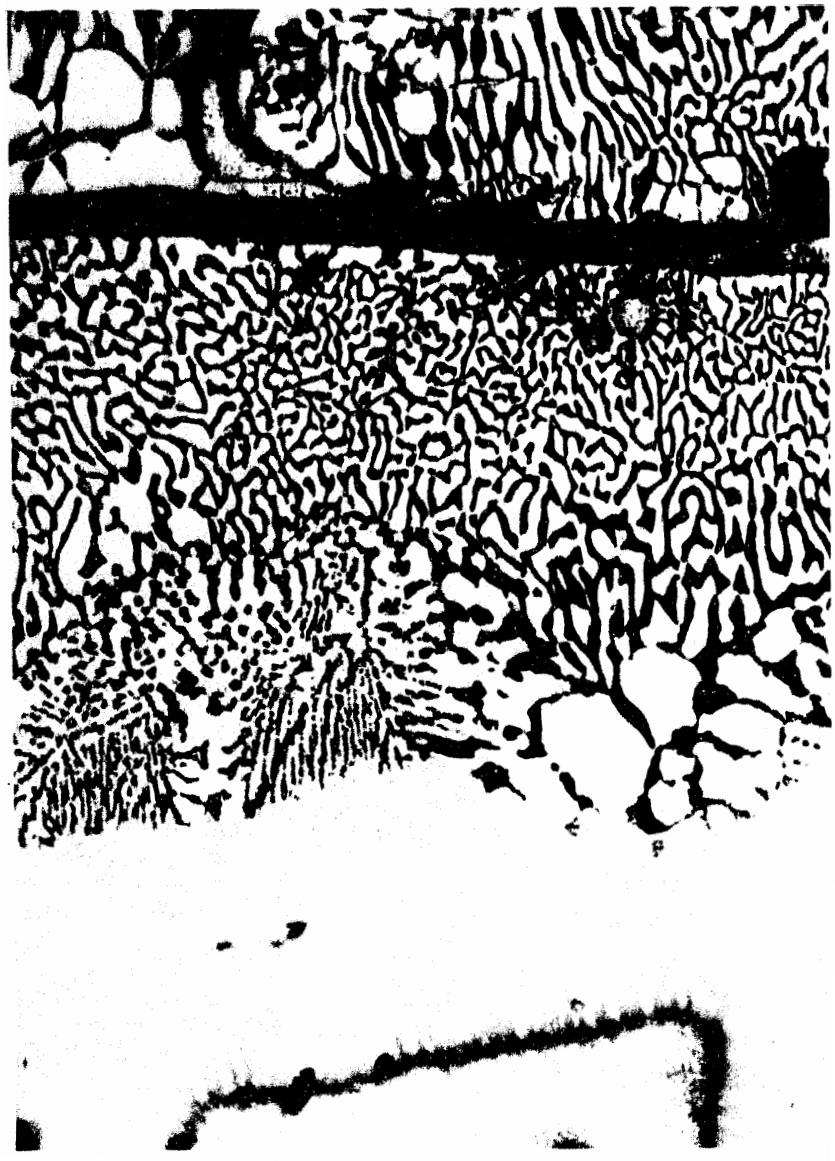

Fig. 37. Eutectic structures, containing Zr, U, In, Ni, Cr, and Fe at the 64-mm elevation in H8. 250X (280462)

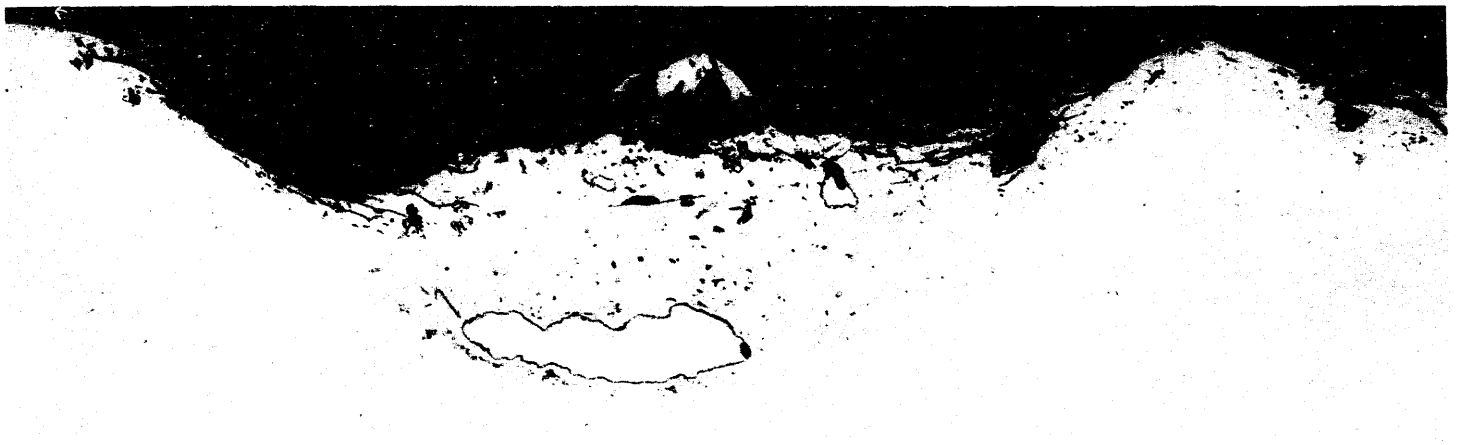

Fig. 38. Ablated surface of H8 nozzle at the 64-mm elevation. (Original at 150X, reduced to 56X, 280733)

Fig. 39. SEM-BSE image of Ag-Cd particle, and Zr-rich material penetrating surface of H8 nozzle at 64-mm elevation.

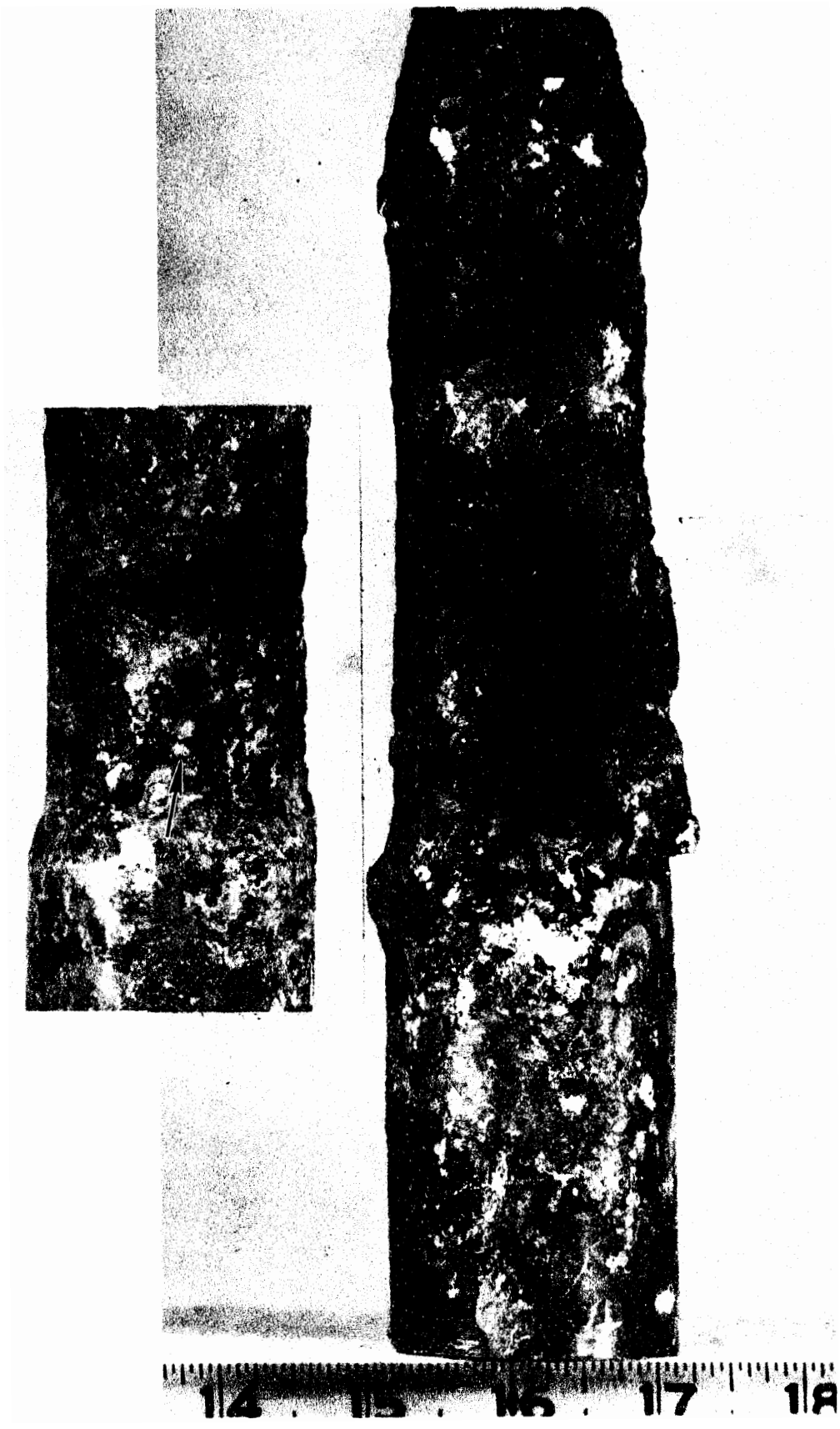

Fig. 40. Elevation views of D10 nozzle segment.
Side view shows crack in nozzle surface. (282578)

Top (stereo pair)

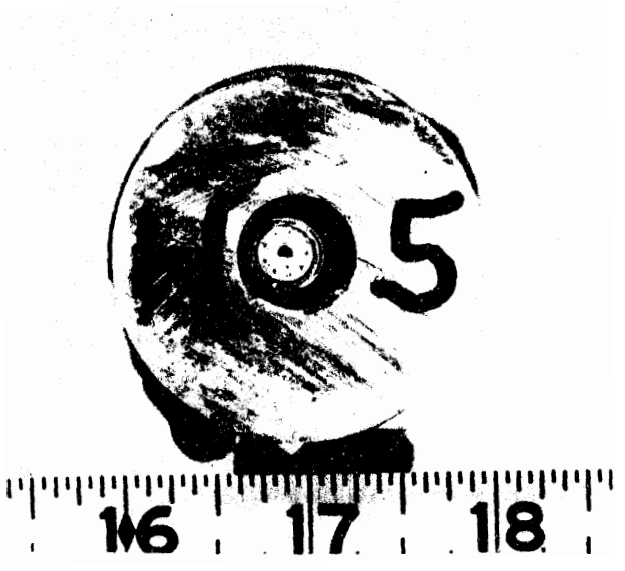

Bottom

Fig. 41. Top and bottom views of the D10 nozzle segment. (282583)

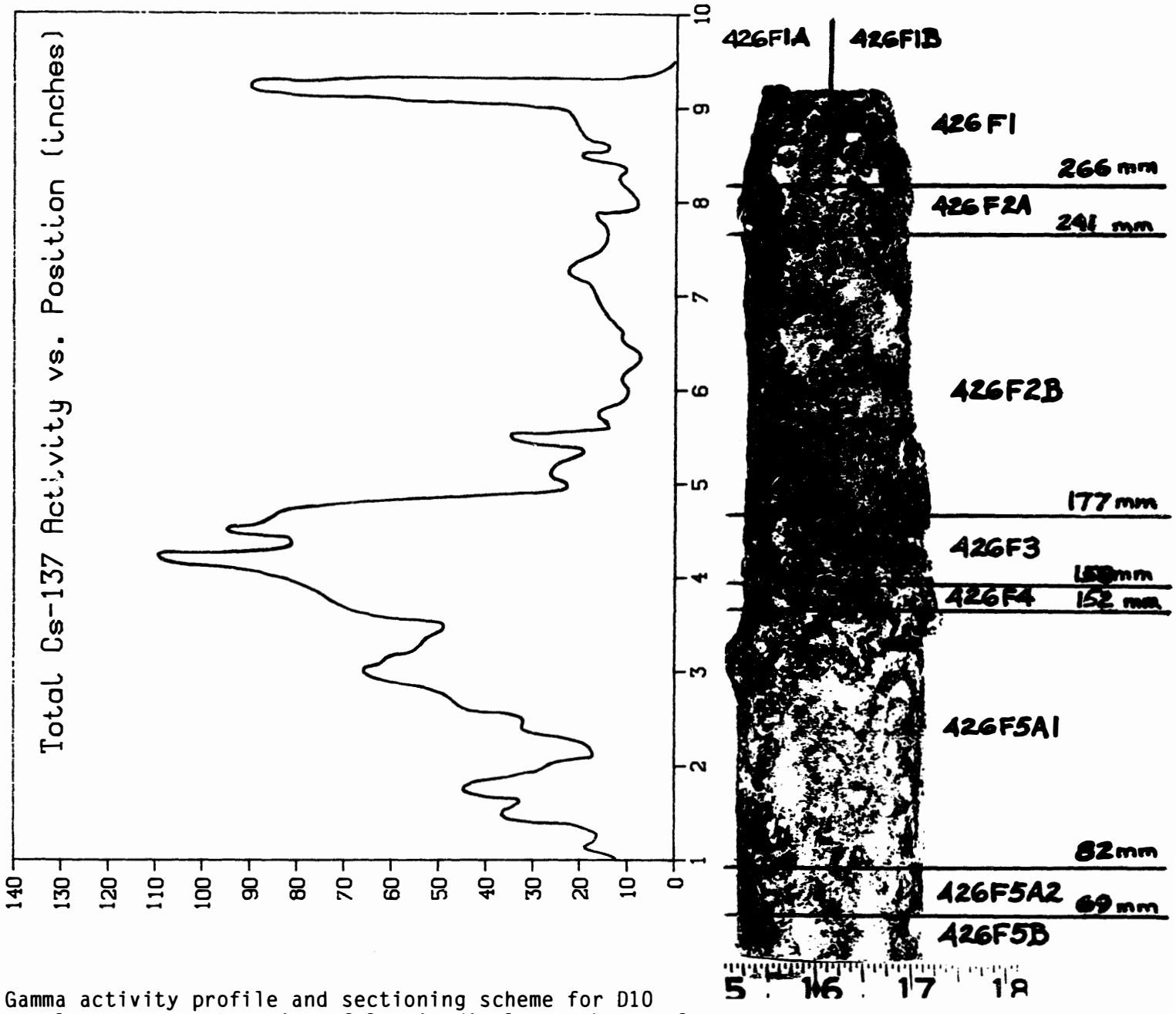

Fig. 42. Gamma activity profile and sectioning scheme for D10 nozzle segment. Location of longitudinal cut shown only to identify specimens, not actual cutting plane.

Fig. 43. Two sides of the longitudinal section through the top of the D10 nozzle. 2X (280650 and 280649)

Fig. 44. Typical area of fuel shards found at top of D10 nozzle.

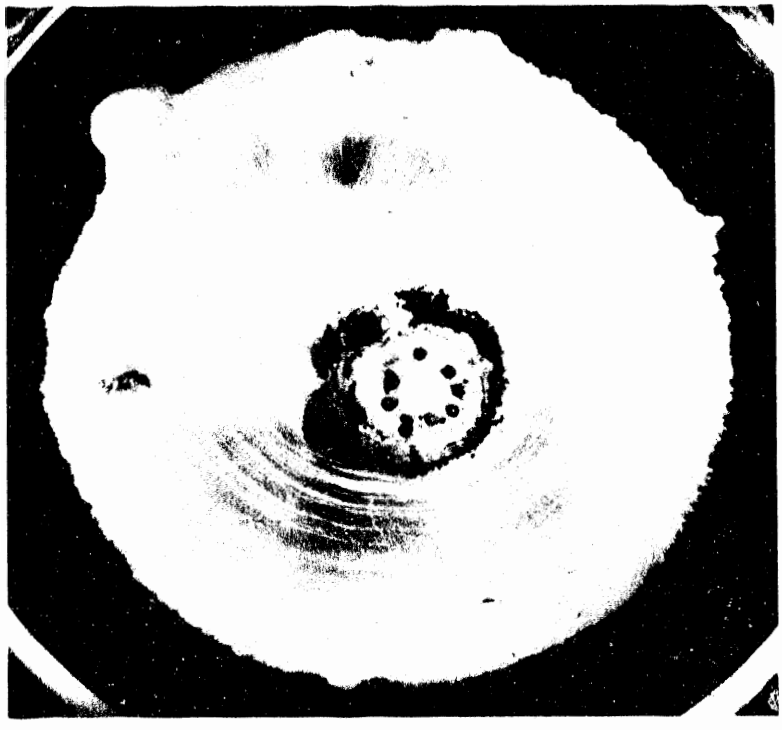

Fig. 45. As-cut transverse section through D10 at the 266-mm elevation, showing metallic and ceramic debris inside. 2X (280641)

Fig. 46. Surface deposits at 266 mm on Nozzle D10.

Fig. 47. As-cut transverse section through D10 at the 177-mm elevation. 2X (280644)

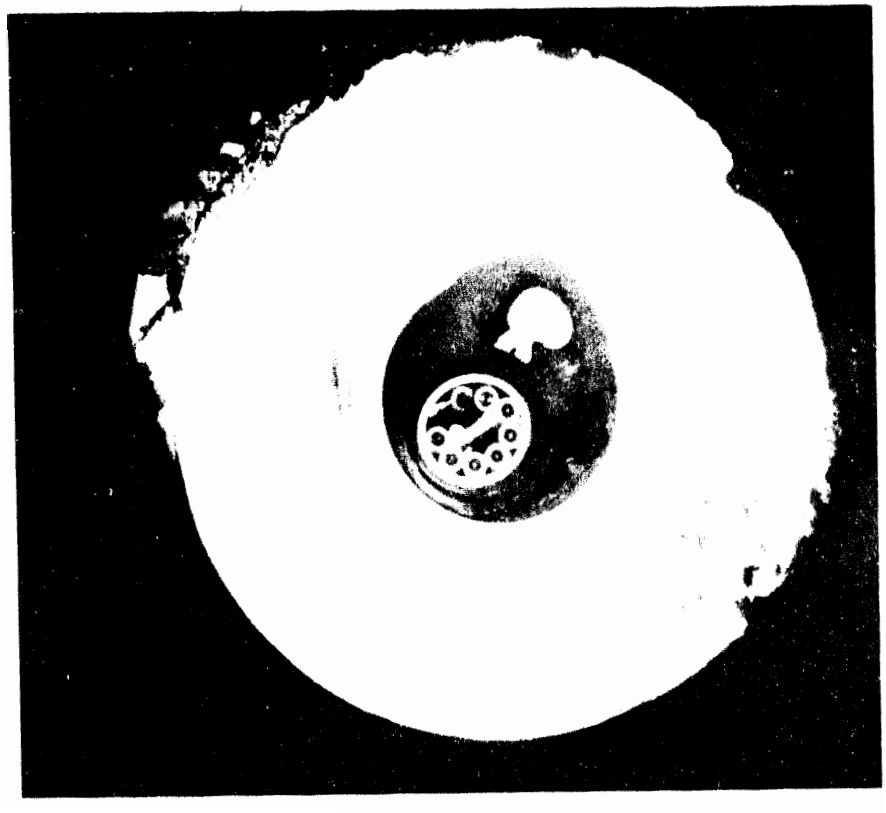

Fig. 48. As-cut transverse section through D10 at the 158-mm elevation. 2X (280646)

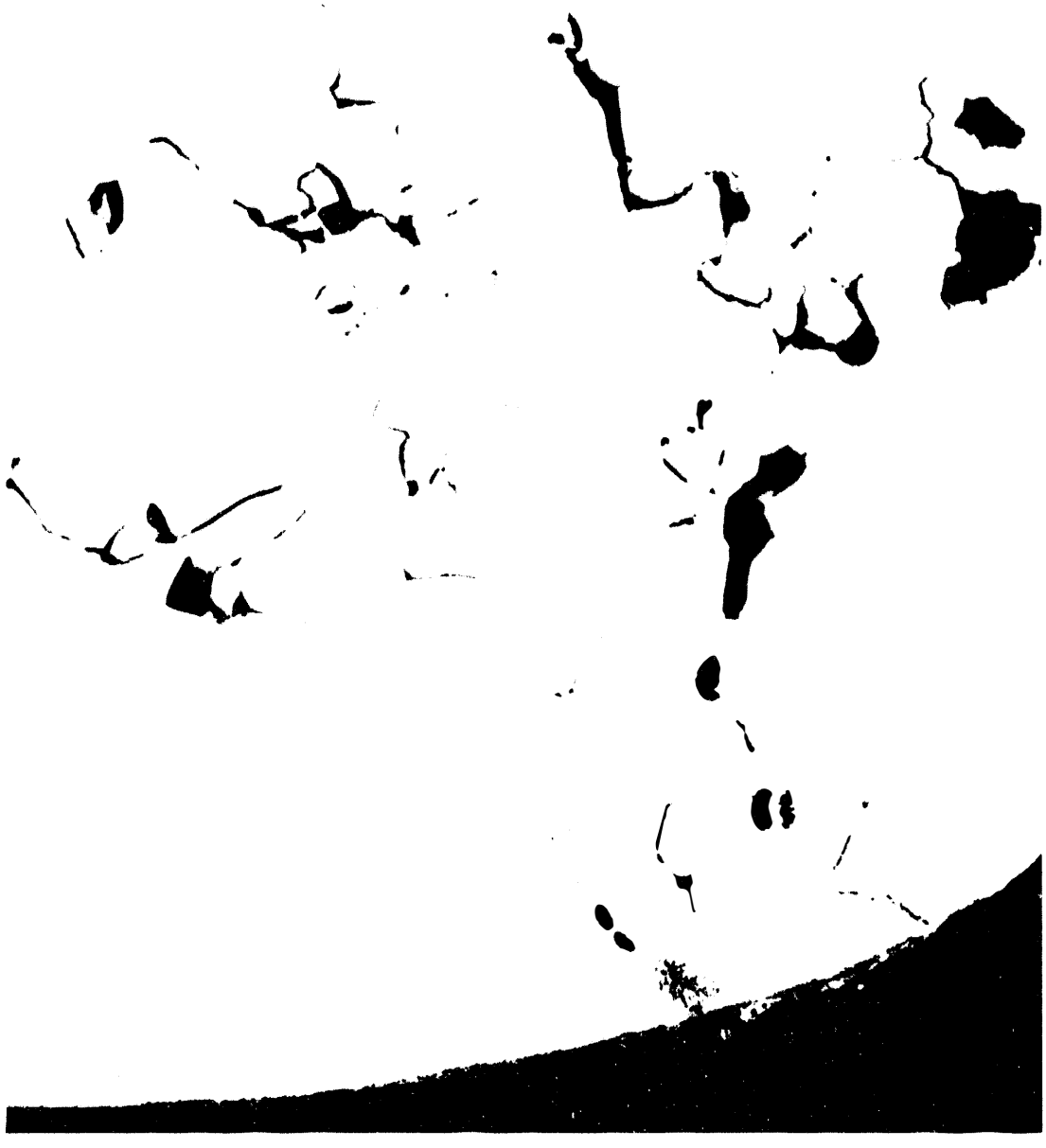

Fig. 49. Area of grain boundary separations in D10 at the 158-mm elevation. (Original at 25X, reduced to 12X, 280688)

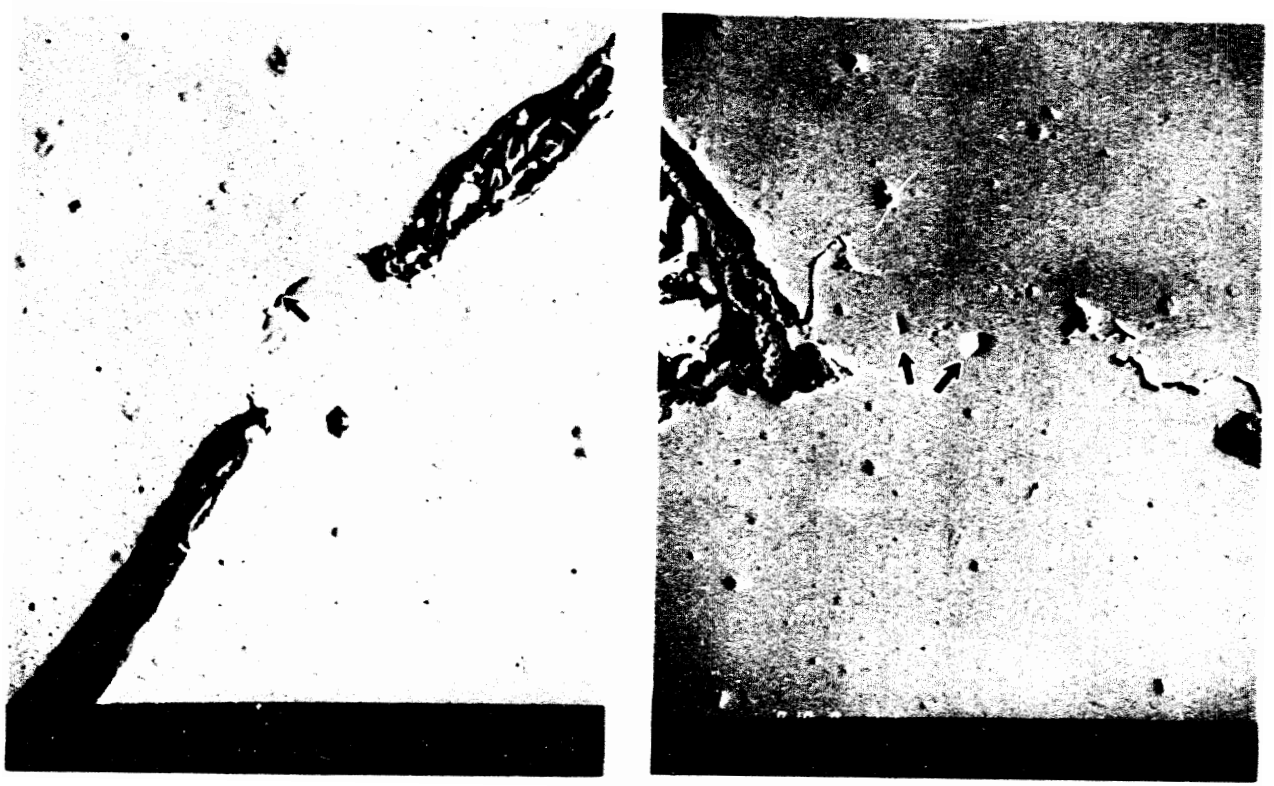

(a) (b)

Fig. 50. Examples of Ag-Cd deposits in D10 at the 158-mm elevation, showing Ag-Cd penetration as (a) stringers and (b) discrete particles.

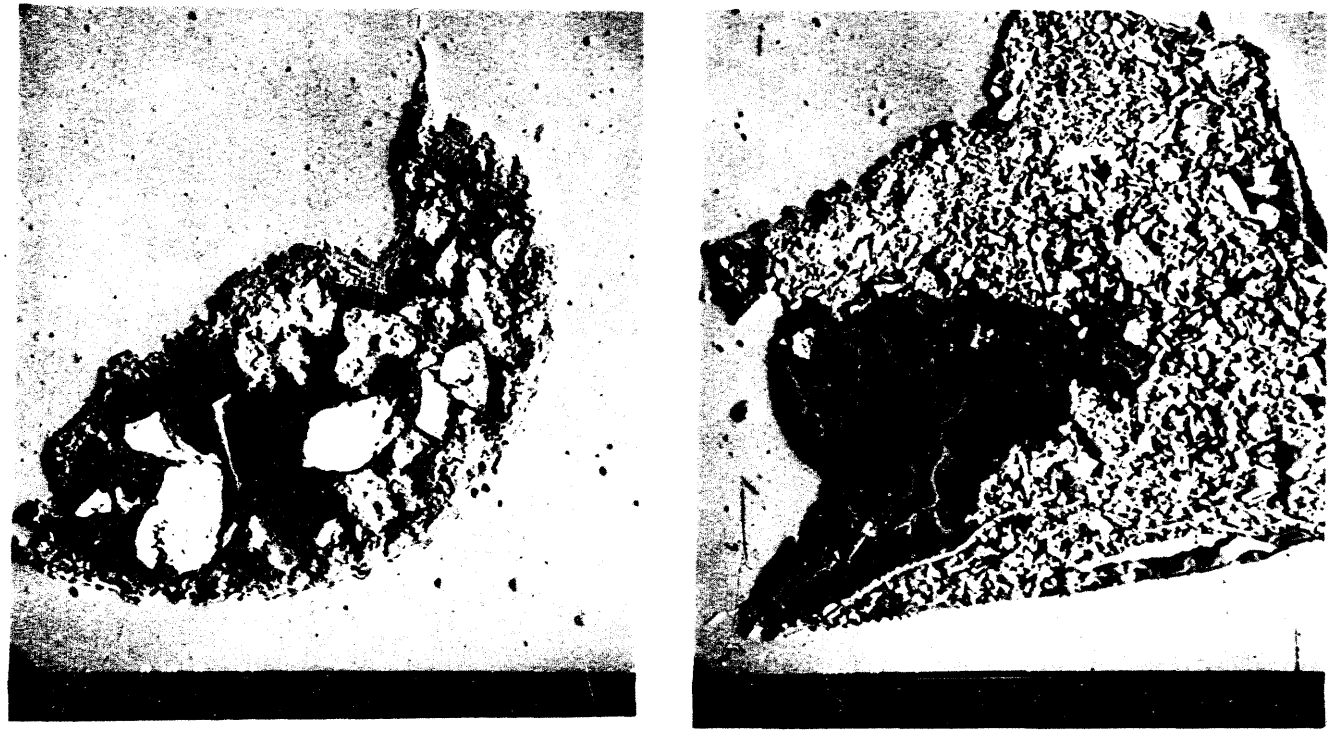

Fig. 51. Examples of particulate fuel debris trapped in grain boundary separations at 158 mm in D10.

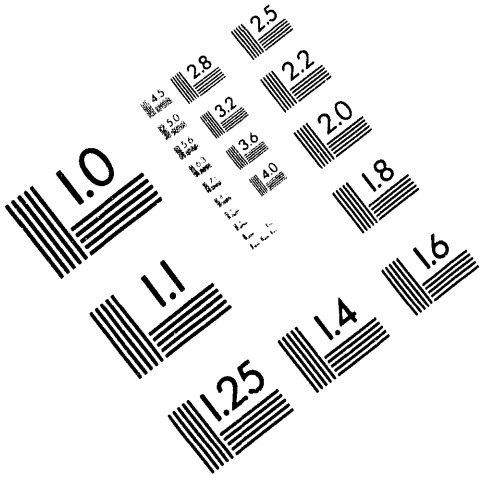

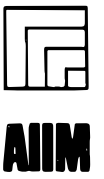

Association for Information and Image Management

1100 Wayne Avenue, Suite 1100
Silver Spring, Maryland 20910

301/587-8202

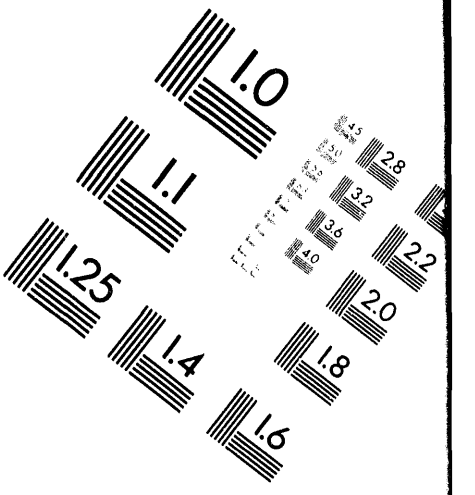

Centimeter

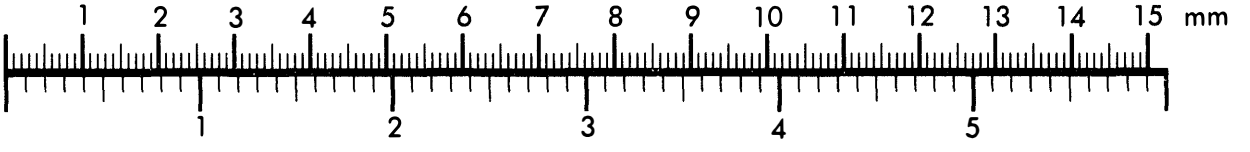

Inches

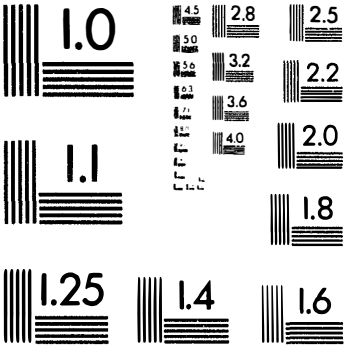

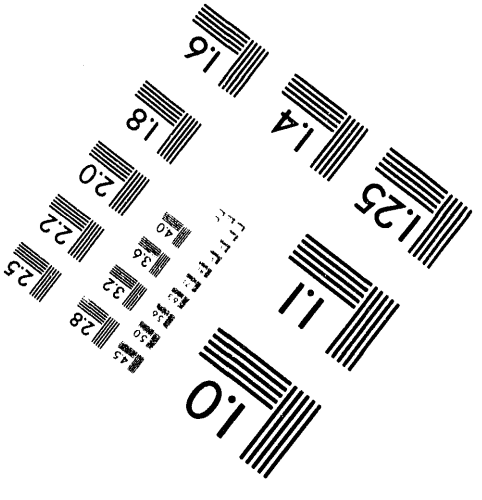

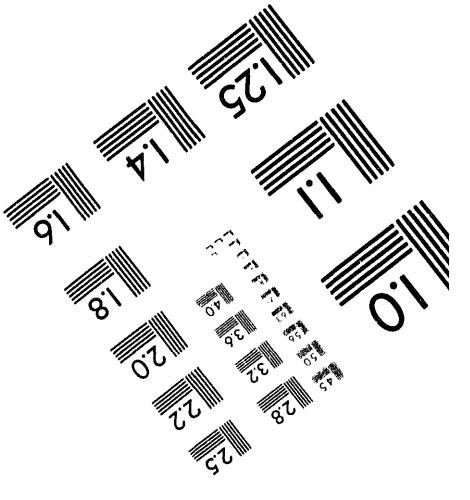

MANUFACTURED TO AIIM STANDARDS
BY APPLIED IMAGE, INC.

2 of 2

Fig. 52. Area of grain boundary separations in D10 at the 158-mm elevation, etched to show possible second phase and internal grain structure. 9X (282558)

Fig. 53. Portion of thick exterior deposit on D10 at the 158-mm elevation. A fuel-containing area is on the left (arrow). (Original at 25X, reduced to 16X, 280694)

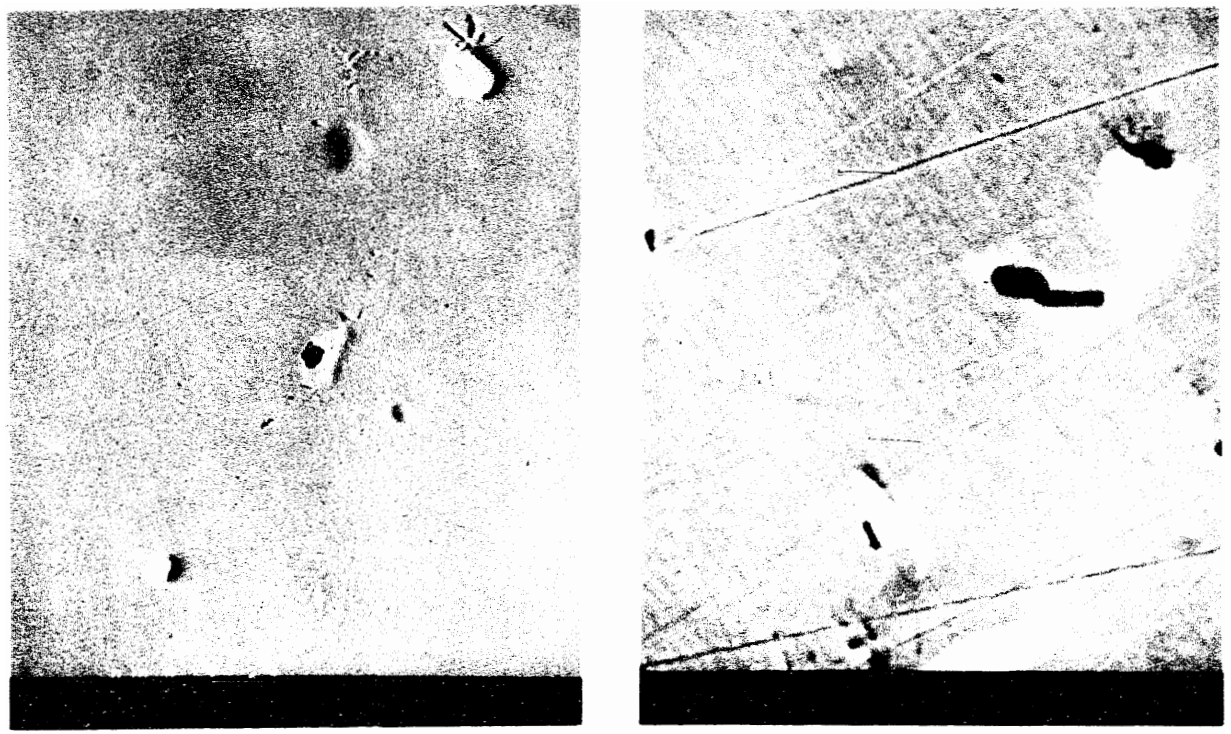

Fig. 54. Examples of Ag-Cd in Inconel at 158 mm in Nozzle D10.

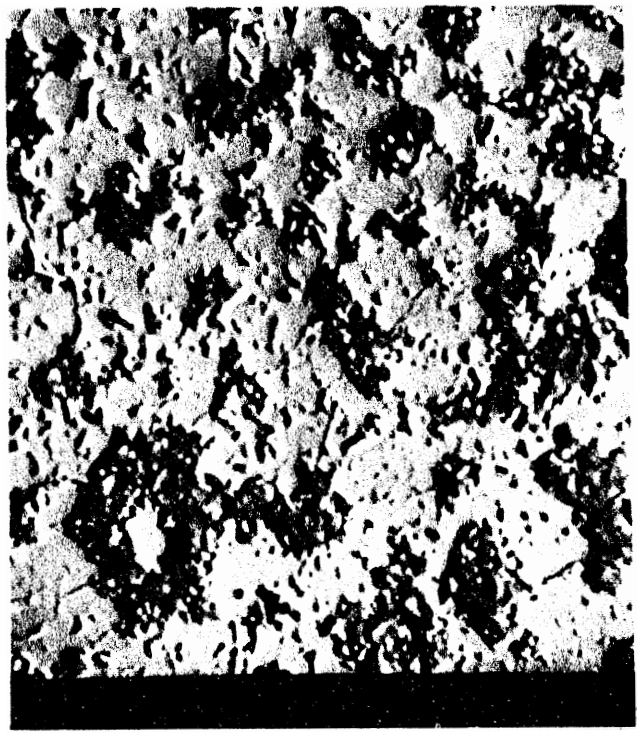

Fig. 55. Segregated U-rich (light) and Zr-rich (dark) phases in fuel particle in a deposit at 158 mm on D10.

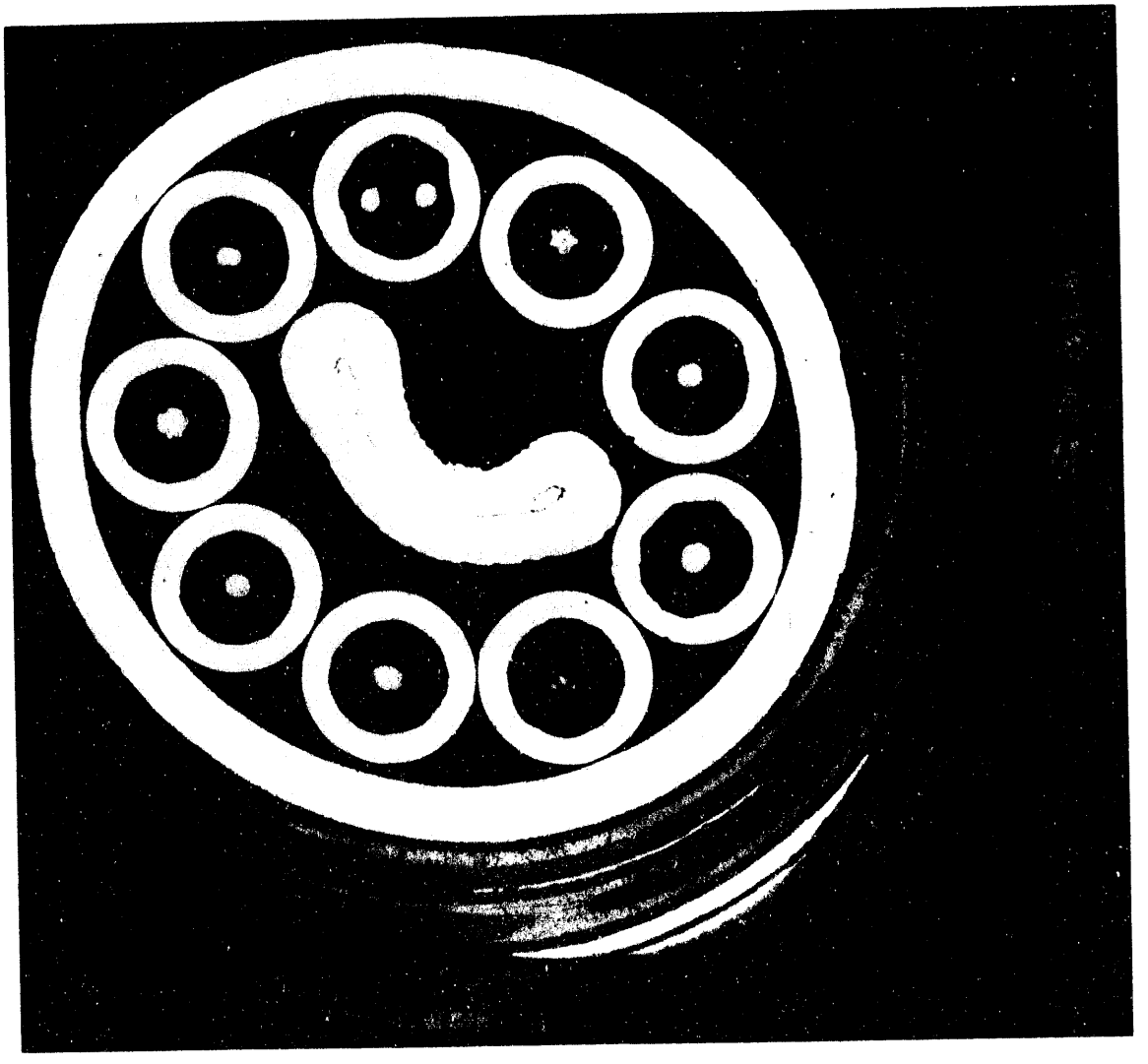

Fig. 56. Instrument string at 158 mm in D10.
(Original at 25X, reduced to 15X (280673)

Fig. 57. Melted Zr lead wire at 158 mm in D10. Phases include Ni, Fe, and Cr back diffused from the locally melted Inconel sheath. 250X (280669)

Fig. 58. Layer of debris on outer surface of D10 at the 82-mm elevation. 250X (281852)

Fig. 59. Elevation view of nozzle segment E11. (282579)

Top (stereo pair)

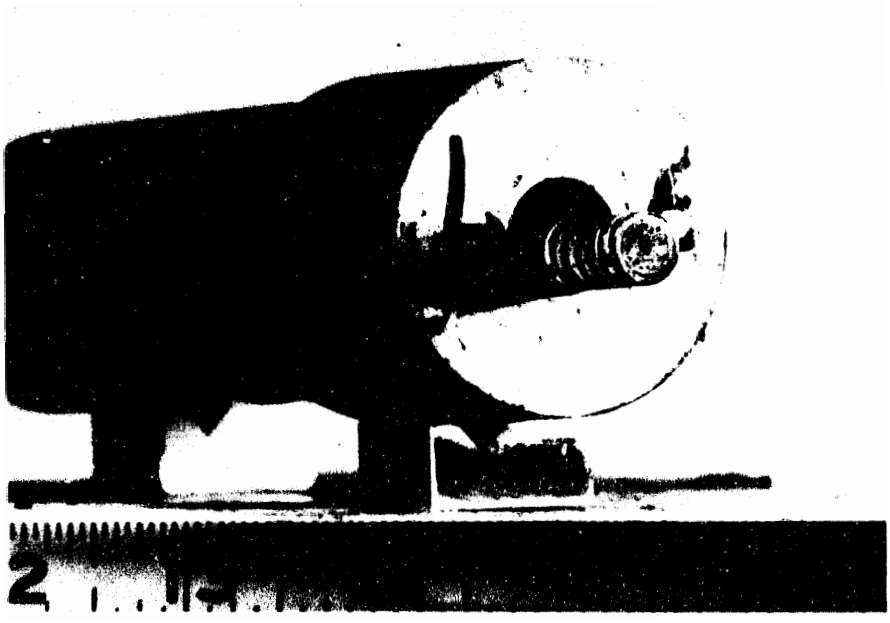

Bottom

Fig. 60. Top and bottom views of nozzle segment E11. (282584)

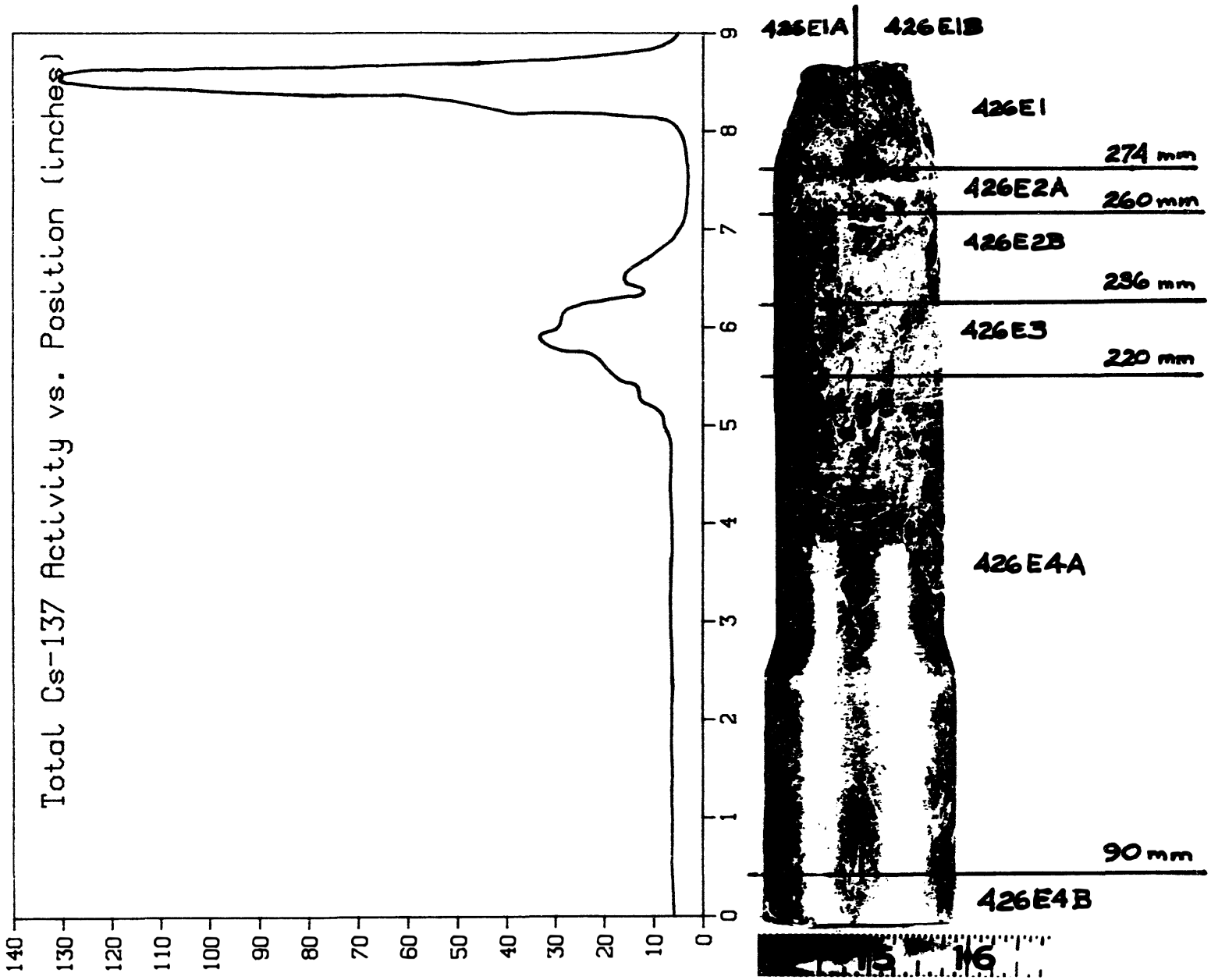

Fig. 61. Gamma activity profile and sectioning scheme for Nozzle E11.

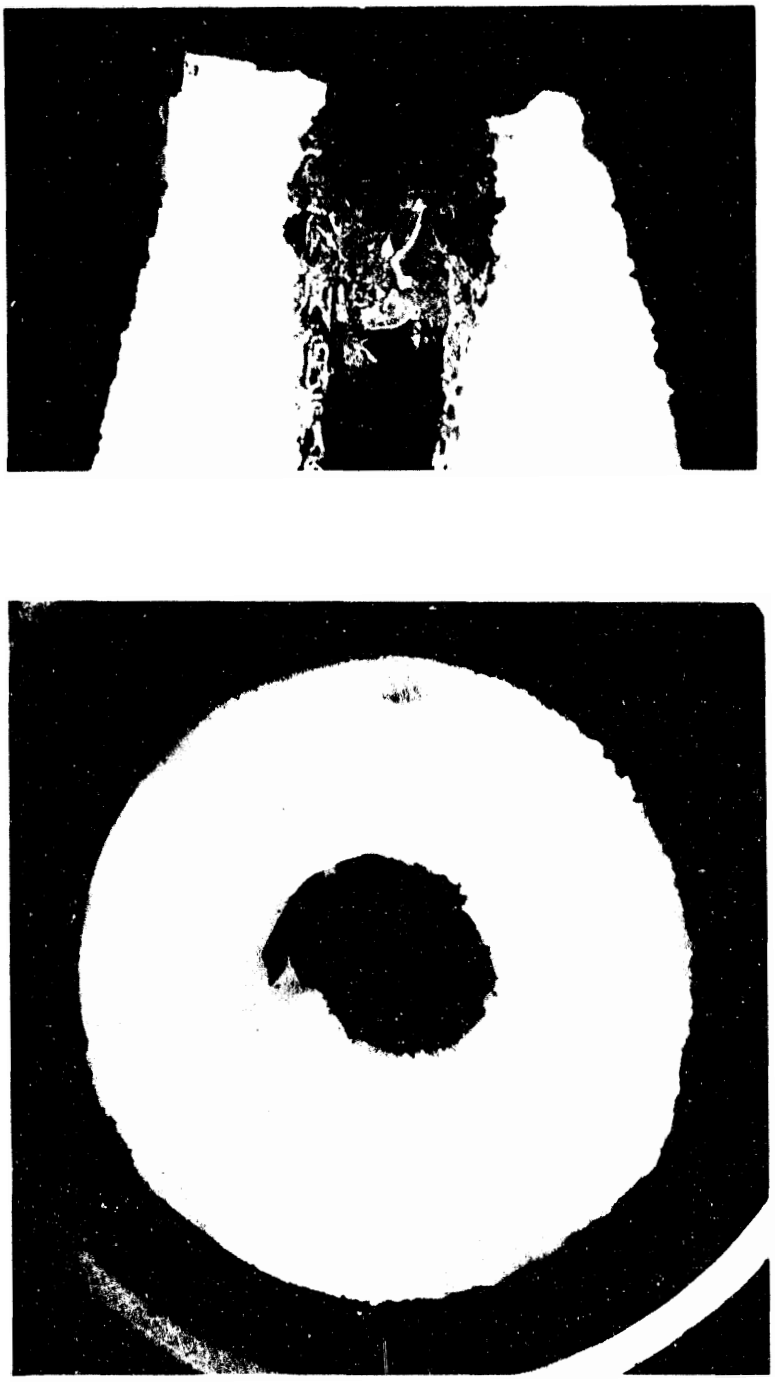

Fig. 62. As-cut transverse section at 274 mm and longitudinal section through top of Nozzle E11. 2X (280522 and 280528)

Fig. 63. Fuel debris in the top of Nozzle E11.
(Original at 25X, reduced to 9X 280636)

Fig. 64. "Micro-folds" with trapped fuel debris in the outer surface at the top of Nozzle E11.

Fig. 65. SEM image of fuel debris attached to the inner surface of E11 at the 274-mm elevation.

Fig. 66. SEM image of surface reaction at 274 mm on E11. Ag-Cd nodules are evident within the nozzle material.

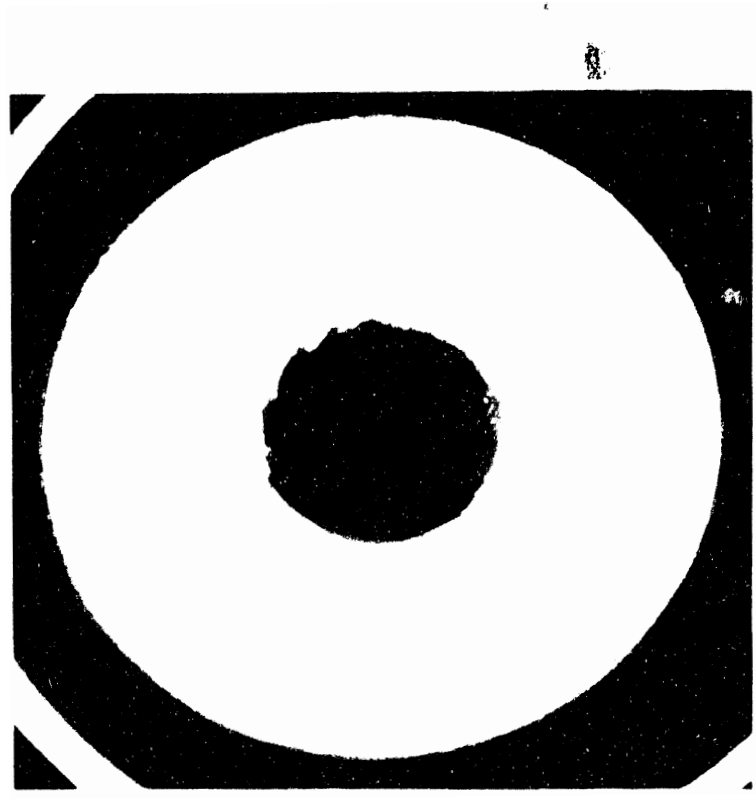

Fig. 67. As-cut transverse section through E11 at 220 mm. Small gray mass at 3 o'clock may contain fuel. 2X (280525)

Fig. 68. Flaking surface debris-bearing scale and surface-adherent scale beneath it at 90-mm elevation on Nozzle E11. 150X (281913)

Fig. 69. SEM-BSE image of scales shown in Fig. 68. White dots along 10-μ inner scale are Ag-Cd particles.

VIII. References

1. D. Akers, S. M. Jensen, and B. K. Schuetz, EGG-OECD-9810, Companion Sample Examinations, April 1992.

2. Phase 4 Status Report, "Removal of Test Specimens from the TMI-2 Reactor Vessel Bottom Head," Project Summary, MPR-1195, MPR Associates, Inc., October 1, 1990.

3. G. Korth, Presentation to the Project Review Group, Idaho Falls, ID, May 12-13, 1992, TMIV(92)EG03.

4. Phase 3 Status Report, "Removal of Test Specimens from the TMI-2 Reactor Vessel Bottom Head," MPR Associates, Inc., April 1, 1990.

5. R. V. Strain, L. A. Neimark, an J. E. Sanecki, "Fuel Relocation Mechanisms Based on Microstructures of Debris," Nucl. Technol. 87, No. 1 (187-190), August 1989.

6. "Video Inspections of Incore Instrument Guide Tubes", TMI-2 Technical Bulletin, TB-89-07, Rev. 0, May 23, 1989.

IX. Appendix

This section includes the descriptive data sheet for each specimen examined by metallography, SEM-EDX, or hardness measurements.

Date of Sheet Preparation: 4/11/92

OECD TMI-2 Vessel Investigation Project
Sample Examination/Test Summary Sheet

Sample Log No.: A/G 426A1B1

Sample Source (check one): ___Vessel steel ___Guide tube X Nozzle ___Companion ___Other (specify)

Performing Organization:	Principal Investigator:	Sample Core Grid Location:
ANL-MCT/IPS	L.A. Neimark	L6

Sample Location Description (attach diagram if necessary):
Sample is from the beveled tip of the nozzle at the 283 mm elevation. Sample covers OD and ID surfaces in a transverse view.

Examination/Test Purpose:
1. Determine nature of any surface deposits on OD and ID surfaces.
2. Determine composition of nozzle material near surface.

Examination/Test Technique and Formatting:
Metallography and SEM-EDX.
Optical photographs, SEM images, and X-ray spectra.

Examination/Test Observation or Results: Hardness is 167±7 DPH. 0.6-1.0 μm thick layer on OD and ID surfaces. No interaction with base metal. Layers are non-uniform in composition, some locations Fe-rich with Cd-Ag and Al particles and others rich in Al. Top-most part contains U-Zr fuel shards. Base metal 50μ in is Inc. 600.

Other Parent Breakoffs (Sample Log Nos.) and Purpose:
426A2A1 (SEM), 426A5A (SEM), 426A5B (hardness), 426A5C (SEM)

Comments:

Add additional sheets if necessary

Date of Sheet Preparation:

OECD TMI-2 Vessel Investigation Project
Sample Examination/Test Summary Sheet

Sample Log No.: A/G426A2A1

Sample Source (check one): ___Vessel steel ✓Nozzle ___Other (specify)
___Guide tube ___Companion

Performing Organization:	Principal Investigator:	Sample Core Grid Location:
ANL-MCT/IPS	L. A. Neimark	L6

Sample Location Description (attach diagram if necessary):
Sample is from center of nozzle at the 283 mm elevation. Contains instrument string and fuel masses.

Examination/Test Purpose: Determine nature of fuel debris, composition of instrument wires, and composition of ceramic insulator material.

Examination/Test Technique and Formatting:
Optical metallography and SEM-EDX.

Examination/Test Observation or Results:
See report text, p.10

Other Parent Breakoffs (Sample Log Nos.) and Purpose: 426A1B1 (SEM and hardness), 426A5A (SEM and hardness), 426A5B (hardness), 426A5C (SEM)

Comments:

Add additional sheets if necessary

Date of Sheet Preparation:

OECD TMI-2 Vessel Investigation Project
Sample Examination/Test Summary Sheet

Sample Log No.: A/G426A5A

Sample Source (check one): ___Vessel steel ✓Nozzle ___Other (specify)
___Guide tube ___Companion

Performing Organization:	Principal Investigator:	Sample Core Grid Location:
ANL-MCT/IPS	L. A. Neimark	L6

Sample Location Description (attach diagram if necessary):
Sample is from outer surface of nozzle at the 77 mm elevation.

Examination/Test Purpose:
Nozzle microstructure, nature of surface deposits, and hardness.

Examination/Test Technique and Formatting:
Metallography, SEM-EDX, and DPH.
Optical photographs, SEM images and EDX spectra, and hardness measurements.

Examination/Test Observation or Results:
For microstructure, see text, p.12.
Hardness is 169 ± 13 DPH, including measurements on 426A5B.
No discernible surface layer > ~10μ; principally Inconel oxidation products plus some Cd (~8%). A single U-Zr fuel particle, 55×140μ, was imbedded in surface.

Other Parent Breakoffs (Sample Log Nos.) and Purpose: 426A1B1 (SEM and hardness), 426A2A1 (SEM), 426A5B (hardness), 426A5C (SEM)

Comments:

Add additional sheets if necessary

Date of Sheet Preparation:

OECD TMI-2 Vessel Investigation Project
Sample Examination/Test Summary Sheet

Sample Log No.: A/G 426A5B

Sample Source (check one): ___Vessel steel ✓Nozzle ___Other (specify)
___Guide tube ___Companion

Performing Organization:	Principal Investigator:	Sample Core Grid Location:
ANL-MCT/IPS	L.A. Neimark	L6

Sample Location Description (attach diagram if necessary):
Sample is from inner surface of nozzle at the 77mm. elevation.

Examination/Test Purpose:
Hardness

Examination/Test Technique and Formatting:
DPH

Examination/Test Observation or Results:
Hardness was 169 ± 13 DPH, including measurements on 426A5A.

Other Parent Breakoffs (Sample Log Nos.) and Purpose: 426A1B1 (SEM and hardness), 426A2A1 (SEM), 426A5A (met, SEM, hardness), 426A5C (SEM)

Comments:

Add additional sheets if necessary

Date of Sheet Preparation:

OECD TMI-2 Vessel Investigation Project
Sample Examination/Test Summary Sheet

Sample Log No.: A/G 426A5C

Sample Source (check one): ___Vessel steel ✓Nozzle ___Other (specify)
___Guide tube ___Companion

Performing Organization:	Principal Investigator:	Sample Core Grid Location:
ANL-MCT/IPS	L.A. Neimark	L6

Sample Location Description (attach diagram if necessary):
Sample is from center of nozzle at the 77 mm elevation. Includes nozzle ID and instrument string.

Examination/Test Purpose:
Determine nature of metallic fragment in annulus, nature of ID surface deposits, and metallurgical condition of instrument lead wires.

Examination/Test Technique and Formatting:
Metallography and SEM-EDX.
Optical photographs, SEM images, and EDX spectra.

Examination/Test Observation or Results:
See text, p. 11.

Other Parent Breakoffs (Sample Log Nos.) and Purpose: 426A1B1 (SEM and hardness), 426A2A1 (SEM), 426A5A (met, SEM, hardness), 426A5B (hardness)

Comments:

Add additional sheets if necessary

Date of Sheet Preparation:

OECD TMI-2 Vessel Investigation Project
Sample Examination/Test Summary Sheet

Sample Log No.: A/G 426B1A1A

Sample Source (check one): ___Vessel steel ✓Nozzle ___Other (specify)
___Guide tube ___Companion

Performing Organization:	Principal Investigator:	Sample Core Grid Location:
ANL-MCT/IPS	L. A. Neimark	M9

Sample Location Description (attach diagram if necessary):
Sample is a transverse section at the 241 mm elevation at the outer surface of the nozzle. Sample captures molten nozzle material and trapped surface debris.

Examination/Test Purpose:
Determine nature of metallic and ceramic phases in the structure. Hardness

Examination/Test Technique and Formatting:
SEM-EDX, metallography.
optical photographs, SEM images, EDX spectra.

Examination/Test Observation or Results: Metal phase contains numerous spherical bubbles. Phase is Cr-depleted Inconel (93 Ni-6.5Fe-0.2Cr). Bubbles contain vapor-deposited structures that contain Ag, Cd, In and Al and Si; Ca and Ti also found. Ceramic phase is a "binder or matrix" of Cr-rich phase (58 Cr-31Fe-11Ni) that contains islands of U-Zr phases, Ag-Cd-In, and "pure" U. Hardness of ~124DPH too low to be Inc. 600.

Other Parent Breakoffs (Sample Log Nos.) and Purpose:
426B1A2A (SEM), 426B2B1 (SEM and hardness)

Comments:

Add additional sheets if necessary

Date of Sheet Preparation:

OECD TMI-2 Vessel Investigation Project
Sample Examination/Test Summary Sheet

Sample Log No. 426B1A2A

Sample Source (check one): ___Vessel steel ✓Nozzle ___Other (specify) ___Guide tube ___Companion

Performing Organization:	Principal Investigator:	Sample Core Grid Location:
ANL-MCT/IPS	L.A. Neimark	M9

Sample Location Description (attach diagram if necessary):
Sample is a longitudinal section through the top of nozzle at the midplane. Sample captures one ID surface, nozzle and core debris in center, and portion of instrument lead. (See Fig. 8 in text.)

Examination/Test Purpose:
Determine nature of metallic and ceramic phases.

Examination/Test Technique and Formatting:
Metallography and SEM-EDX.
25X optical photo and SEM images and EDX spectra.

Examination/Test Observation or Results:
See text, p. 8.

Other Parent Breakoffs (Sample Log Nos.) and Purpose:
426B1A1A (SEM and hardness), 426B2B1 (SEM and hardness).

Comments:

Add additional sheets if necessary

Date of Sheet Preparation:

OECD TMI-2 Vessel Investigation Project
Sample Examination/Test Summary Sheet

Sample Log No. AG426B2B1

Sample Source (check one): ___Vessel steel ✓Nozzle ___Other (specify)
___Guide tube ___Companion

Performing Organization:	Principal Investigator:	Sample Core Grid Location:
ANL-MCT/IPS	L.A. Neimark	M9

Sample Location Description (attach diagram if necessary):
Transverse section at outer surface at the 38 mm elevation.

Examination/Test Purpose:
Determine nature of any surface deposits and nozzle hardness.

Examination/Test Technique and Formatting:
SEM-EDX and DPH hardness.

Examination/Test Observation or Results: Hardness is 202±28 DPH. Thin surface layer; 0.5-1.0 μ, rich in Cr, probably as oxide. Occasional deposits of Al (Al_2O_3?) in layer. Some control rod materials in layer, but not quantified. Base metal is Inc. 600. Occasional grain boundary phases in Inconel, but having only the composition of the base metal; probably nitrides or carbides.

Other Parent Breakoffs (Sample Log Nos.) and Purpose:
426B1A1A (SEM and hardness), 426B1A2A (SEM)

Comments:

Add additional sheets if necessary

Date of Sheet Preparation:

OECD TMI-2 Vessel Investigation Project
Sample Examination/Test Summary Sheet

Sample Log No. ~~AG~~426C1A1

Sample Source (check one): ___Vessel steel ✓Nozzle ___Other (specify)
___Guide tube ___Companion

Performing Organization:	Principal Investigator:	Sample Core Grid Location:
ANL-MCT/IPS	L. A. Neimark	H8

Sample Location Description (attach diagram if necessary):
Longitudinal section through melted tip of nozzle. Captures OD, ID and "top" surfaces.

Examination/Test Purpose:
Determine nature of deposits on the three surfaces and the composition of the base metal.

Examination/Test Technique and Formatting:
SEM-EDX. SEM images and EDX spectra. DPH measurements.

Examination/Test Observation or Results:
See text, p. 15.
DPH was 148±7; base metal was normal Inc. 600.

Other Parent Breakoffs (Sample Log Nos.) and Purpose: 426C1A2 (met.), 426C1A3A(met), 426C1A3B(met), 426C2A (SEM), 426C2C1 (hardness), 426C2D (met. and SEM).

Comments:

Add additional sheets if necessary

Date of Sheet Preparation:

OECD TMI-2 Vessel Investigation Project
Sample Examination/Test Summary Sheet

Sample Log No.: ~~AG~~426 C1A2

Sample Source (check one): ___Vessel steel ✓Nozzle ___Other (specify)
___Guide tube ___Companion

Performing Organization:	Principal Investigator:	Sample Core Grid Location:
ANL-MCT/IPS	L.A. Neimark	H8

Sample Location Description (attach diagram if necessary):
Pseudo transverse section of instrument string and debris at tip of nozzle, ~108 mm elevation.

Examination/Test Purpose:
Originally to determine nature of ceramic debris next to instrument string. However, specimen mounted incorrectly and not further examined beyond 9X macrophoto.

Examination/Test Technique and Formatting:
Metallography. 9X macrophotos of two ground surfaces.

Examination/Test Observation or Results:
Structures appear to be solidified, porous fuel fragments and solidified, cored metal. Some Zr lead wires fractured or reacted.

Other Parent Breakoffs (Sample Log Nos.) and Purpose: 426 C1A1 (SEM and hardness), 426 C1A3A (met), 426 C1A3B (met), 426 C2A (SEM), 426 C2C1 (hardness), 426 C2D (met. and SEM)

Comments:

Add additional sheets if necessary

Date of Sheet Preparation:

OECD TMI-2 Vessel Investigation Project
Sample Examination/Test Summary Sheet

Sample Log No.: A/G 426C1A3A

Sample Source (check one): ___Vessel steel ✓Nozzle ___Other (specify)
___Guide tube ___Companion

Performing Organization:	Principal Investigator:	Sample Core Grid Location:
ANL-MCT/IPS	L. A. Neimark	H8

Sample Location Description (attach diagram if necessary):
Longitudinal section of central instrument string at the ~90 mm elevation. Captures ID surface, string conduit, and solidified debris (mainly metallic) on either side of conduit. Instrument tube and contained instrument leads fell out of conduit during preparation.

Examination/Test Purpose:
Originally to identify "ceramic" material in annulus between nozzle and instrument string. However, sample preparation did not capture desired area.

Examination/Test Technique and Formatting:
Metallography.
Optical photographs to 250X.

Examination/Test Observation or Results:
Structures contain primary dendrites, eutectic fields, and areas of oxidized metal. Similarity of structures to those of 426C2A suggest constituents are solidified Inc. 600 containing U, Zr, and islands of Ag-Cd. (See Fig. 37.)

Other Parent Breakoffs (Sample Log Nos.) and Purpose: 426C1A1 (SEM and hardness), 426C1A2 (met), 426C1A3B (met), 426C2A (SEM), 426C2C1 (hardness), 426C2D (met. and SEM).

Comments:

Add additional sheets if necessary

Date of Sheet Preparation:

OECD TMI-2 Vessel Investigation Project
Sample Examination/Test Summary Sheet

Sample Log No.: A/G 426C1A3B

Sample Source (check one): ___Vessel steel ✓Nozzle ___Other (specify)
___Guide tube ___Companion

Performing Organization:	Principal Investigator:	Sample Core Grid Location:
ANL-MCT/IPS	L. A. Neimark	H8

Sample Location Description (attach diagram if necessary):
Transvere section from the center of nozzle at the ~64 mm elevation. Captured nozzle inner surface with solidified metal against it, and an outer piece of the conduit.

Examination/Test Purpose:
Originally to examine ceramic material in annulus between nozzle and instrument string; however, sample mounted transversely, not longitudinally.

Examination/Test Technique and Formatting:
Metallography.
Optical photographs to 250X.

Examination/Test Observation or Results:
Structures identical to those in 426C2A; possibly mating surfaces. Microstructures also similar to those in 426C1A3A.

Other Parent Breakoffs (Sample Log Nos.) and Purpose: 426C1A1 (SEM and hardness), 426C1A2 (met), 426C1A3A (met), 426C2A (SEM), 426C2C1 (hardness), 426C2D (met and SEM).

Comments:

Add additional sheets if necessary

Date of Sheet Preparation:

OECD TMI-2 Vessel Investigation Project
Sample Examination/Test Summary Sheet

Sample Log No.: A/G 426 C2A

Sample Source (check one): ___Vessel steel ✓Nozzle ___Other (specify)
___Guide tube ___Companion

Performing Organization:	Principal Investigator:	Sample Core Grid Location:
ANL-MCT/IPS	L. A. Neimark	H8

Sample Location Description (attach diagram if necessary):

Transverse section from the center of nozzle at the 64 mm elevation. Captured partial instrument string, metallic debris (solidified) in annulus, and nozzle inner surface. (See Fig. 36 in text.)

Examination/Test Purpose:

Determine nature of metallic debris in the annulus.

Examination/Test Technique and Formatting:

Metallography and SEM-EDX.
Optical photographs to 250X; SEM images; EDX spectra

Examination/Test Observation or Results:

See text pp 15-16.

Other Parent Breakoffs (Sample Log Nos.) and Purpose: 426 C1A1 (SEM and hardness), 426C1A2 (met), 426C1A3A (met), 426 C1A3B (met) 426 C2C1 (hardness), 426 C2D (met and SEM)

Comments:

Add additional sheets if necessary

Date of Sheet Preparation:

OECD TMI-2 Vessel Investigation Project
Sample Examination/Test Summary Sheet

Sample Log No.: A/G 426 C2C1

Sample Source (check one): ___Vessel steel ✓Nozzle ___Other (specify)
___Guide tube ___Companion

Performing Organization:	Principal Investigator:	Sample Core Grid Location:
ANL-MCT/IPS	L.A. Neimark	H8

Sample Location Description (attach diagram if necessary):
Transverse section of outer nozzle surface at the 64 mm elevation. Sample captures ~12 mm of surface and extends ~20 mm into nozzle.

Examination/Test Purpose:
Hardness of nozzle.

Examination/Test Technique and Formatting:
DPH measurements; 8.6x photograph.

Examination/Test Observation or Results:
Average of 6 measurements was 133±4 DPH

Other Parent Breakoffs (Sample Log Nos.) and Purpose: 426C1A1 (SEM and hardness), 426C1A2 (met), 426C1A3A (met), 426 C2A (SEM), 426C1A3B (met), 426C2D (met and SEM).

Comments:

Add additional sheets if necessary

Date of Sheet Preparation:

OECD TMI-2 Vessel Investigation Project
Sample Examination/Test Summary Sheet

Sample Log No.: A/G 426C2D

Sample Source (check one): ___Vessel steel ✓Nozzle ___Other (specify) ___Guide tube ___Companion

Performing Organization:	Principal Investigator:	Sample Core Grid Location:
ANL-MCT/IPS	L. A. Neimark	H8

Sample Location Description (attach diagram if necessary):
Tranverse section of segment of outer nozzle surface at the 64 mm elevation. Surface area is one of severe ablation.

Examination/Test Purpose:
Determine nature of material on nozzle surface and to elucidate mechanism of surface attack.

Examination/Test Technique and Formatting:
Metallography, SEM-EDX analysis. Optical photographs to 500X, SEM images, and EDX spectra.

Examination/Test Observation or Results: (See pg. 16 of text.)
Base metal has nominal composition of Inc. 600. Zr and Ni principal constituents of surface layer that varies from 100 to 600μ in thickness; Fe, Cr and U present in significantly smaller amounts. Zr content in layer is ~24-36 %. Intergranular penetration by Zr into Inc. 600 (~12-20 % Zr, bal Ni with some Fe and Cr). Large inclusion of Ag-Cd in Zr-Ni surface alloy.

Other Parent Breakoffs (Sample Log Nos.) and Purpose: 426C1A1 (SEM and hardness), 426C1A2 (met), 426C1A3A (met), 426C1A3B (met), 426C2A (SEM), 426C2C1 (hardness).

Comments:

Add additional sheets if necessary

Date of Sheet Preparation:

OECD TMI-2 Vessel Investigation Project
Sample Examination/Test Summary Sheet

Sample Log No.: A/G 426D1B1

Sample Source (check one): ___Vessel steel ✓Nozzle ___Other (specify) ___Guide tube ___Companion

Performing Organization:	Principal Investigator:	Sample Core Grid Location:
ANL-MCT/IPS	L.A. Neimark	H5

Sample Location Description (attach diagram if necessary):
Longitudinal section through approximate midplane at the ~135 mm elevation, below top surface. Segment is from "right" side of nozzle and includes outer surface. One of four specimens across top of nozzle.

Examination/Test Purpose:
Determine nature of metallic and ceramic phases.

Examination/Test Technique and Formatting:
Metallography and SEM-EDX. Macrophoto of 25x and micrographs to 250x. SEM images and EDX spectra.

Examination/Test Observation or Results: (See text, p. 13.)
Metallic phase is essentially Cr-doped Inc. 600. Numerous "bubbles" in structure. Needle-like (platelet) structures, associated generally with bubbles, are Cr-rich (oxide?). Bubbles contain vapor-deposited structures, some of which are Ag. "Ceramic" mass is Cr-rich matrix (oxide) containing U-rich/Zr and Zr-rich/U phases. Fuel phases solidified in-situ.

Other Parent Breakoffs (Sample Log Nos.) and Purpose: 426D1B2 (met), 426D1B3 (met), 426D1B4 (met and hardness). All had SEM examination.

Comments:

Add additional sheets if necessary

Date of Sheet Preparation:

OECD TMI-2 Vessel Investigation Project
Sample Examination/Test Summary Sheet

Sample Log No.: A/G 426D1B2

Sample Source (check one): ___Vessel steel ✓Nozzle ___Other (specify)
___Guide tube ___Companion

Performing Organization:	Principal Investigator:	Sample Core Grid Location:
ANL-MCT/IPS	L.A. Neimark	H5

Sample Location Description (attach diagram if necessary):
Longitudinal section through approximate midplane at the ~135 mm elevation, below top surface. Segment is to the "left" of centerline, next to 426D1B4. One of four specimens across top of nozzle.

Examination/Test Purpose:
Determine nature of metallic and ceramic phases.

Examination/Test Technique and Formatting:
Metallography and SEM-EDX.
Macrophoto at 25X and micrographs to 250X.
SEM images and EDX spectra.

Examination/Test Observation or Results: (See text, p.13.)
Metallic phase is essentially Cr-depleted Inc. 600 (but without "bubbles"). Ceramic is Cr-rich (oxide) with intermingled bits of solidified fuel phases and particles of Zr and Cd+Ag+In.

Other Parent Breakoffs (Sample Log Nos.) and Purpose: 426D1B1 (met + SEM), 426D1B3 (met + SEM), 426D1B4 (met, SEM + hardness).

Comments:

Add additional sheets if necessary

Date of Sheet Preparation:

OECD TMI-2 Vessel Investigation Project
Sample Examination/Test Summary Sheet

Sample Log No.: A/G 426D1B3

Sample Source (check one): ___Vessel steel ✓Nozzle ___Other (specify) ___Guide tube ___Companion

Performing Organization:	Principal Investigator:	Sample Core Grid Location:
ANL-MCT/IPS	L.A. Neimark	H5

Sample Location Description (attach diagram if necessary):
Longitudinal section through approximate midplane at the ~135 mm elevation, below the top surface. Segment is to the "right" of centerline, next to 426D1B1. One of four specimens across top of nozzle.

Examination/Test Purpose:
Determine nature of metallic and ceramic phases.

Examination/Test Technique and Formatting:
Metallography and SEM-EDX.
Macrophoto at 25X and micrographs to 250X.
SEM images and EDX spectra.

Examination/Test Observation or Results: (See text, p.13.)
Metallic phases are essentially Cr-depleted Inc. 600, some with bubbles and some not. Cr-rich "platelets" absent. "Ceramic" area is a heterogeneous conglomerate of Cr-rich matrix containing areas of U-rich/Zr, Zr-rich/U, Al- and Ti-rich phases (>70 and 25 %, respectively). Fuel solidified in-situ.

Other Parent Breakoffs (Sample Log Nos.) and Purpose: 426D1B1 (met and SEM), 426D1B2 (met + SEM), 426D1B4 (met, SEM, hardness).

Comments:

Add additional sheets if necessary

Date of Sheet Preparation:

OECD TMI-2 Vessel Investigation Project
Sample Examination/Test Summary Sheet

Sample Log No.: A/9 426D1B4

Sample Source (check one): ___Vessel steel ✓Nozzle ___Other (specify) ___Guide tube ___Companion

Performing Organization:	Principal Investigator:	Sample Core Grid Location:
ANL-MCT/IPS	L.A. Neimark	H5

Sample Location Description (attach diagram if necessary):
Longitudinal section through approximate midplane at the ~135 mm elevation, below top surface. Segment is on the "left" side of nozzle and contains outer surface.

Examination/Test Purpose:
Determine nature of metallic and ceramic phases and hardness of the former.

Examination/Test Technique and Formatting:
Metallography, SEM-EDX, and DPH microhardness. Macrophoto at 25x, microphotos at 250x.

Examination/Test Observation or Results: (See text, p.13) 105±2 DPH
Metallic phase solidified from melt with numerous "spherical" balls having Cr-oxide surfaces. Numerous Cr-rich needles/platelets, some as dendrites; matrix generally devoid of Cr. Large "bubble" lined with Al, Zr, Cd, Ag and Ti. "Ceramic" on outer surface is Cr-based with inclusions of Fe, Cd, Ag. U-rich and Zr-rich fuel in "ceramic".

Other Parent Breakoffs (Sample Log Nos.) and Purpose: 426D1B1 (met + SEM), 426D1B2 (met + SEM), 426D1B3 (met + SEM).

Comments:

Add additional sheets if necessary

Date of Sheet Preparation:

OECD TMI-2 Vessel Investigation Project
Sample Examination/Test Summary Sheet

Sample Log No.: A/G 426 D2B

Sample Source (check one): ___Vessel steel ✓Nozzle ___Other (specify)
___Guide tube ___Companion

Performing Organization:	Principal Investigator:	Sample Core Grid Location:
ANL-MCT/IPS	L.A. Neimark	H5

Sample Location Description (attach diagram if necessary):
Specimen is lowest piece of candling on nozzle outer surface at the ~70 mm elevation.

Examination/Test Purpose:
Determine nature of the candled metal, including its hardness.

Examination/Test Technique and Formatting:
Metallography, SEM-EDX.
Macrophoto at 35x, microphotos to 1000x.
SEM images, EDX spectra.

Examination/Test Observation or Results:
Piece is irregularly shaped and has various "ceramic" deposits on its surfaces. Base metal is 18w% Cr, 10w% Ni, 72w% Fe (i.e. Type 304 SS). Mn found as islands. Hardness is 142±6 DPH. No foreign materials in metal. One area of heavy "oxide" was 25Cr-63Fe-12Ni. Metallography shows finely dispersed, unidentified metal particles in oxide.

Other Parent Breakoffs (Sample Log Nos.) and Purpose:
None on 426 D2

Comments:

Add additional sheets if necessary

Date of Sheet Preparation:

OECD TMI-2 Vessel Investigation Project
Sample Examination/Test Summary Sheet

Sample Log No.: A/G 426D3A

Sample Source (check one): ___Vessel steel ✓Nozzle ___Other (specify)
___Guide tube ___Companion

Performing Organization:	Principal Investigator:	Sample Core Grid Location:
ANL-MCT/IPS	L.A. Neimark	H5

Sample Location Description (attach diagram if necessary):
Transverse section at the 0 mm elevation of the center of nozzle. Captures most of instrument string, segment of nozzle inner surface, large metallic debris ingot in annulus, and some particulate debris between ingot and nozzle body.

Examination/Test Purpose:
Determine nature of metallic ingot, the debris in the annulus, the metallic shards in the instrument string, and the metallurgical state of the instrument wires.

Examination/Test Technique and Formatting:
Metallography and SEM-EDX.
Macrophoto at 25X, microphotos to 250X.
SEM images and EDX spectra.

Examination/Test Observation or Results:
Ingot composition is 72%Ni-9%Fe-16 The debris in the annulus consists of Cr-rich particles with U-Zr impurities. The shards (angular) between instrument leads are Inc. 600 + Mn. Some instrument leads are radially cracked, while others may be transforming $\alpha \rightarrow \beta$; photos not sufficiently definitive of microstructure.

Other Parent Breakoffs (Sample Log Nos.) and Purpose: 426 D3B1 (met + hardness), 426D3C1 (met, SEM and hardness)

Comments:

Add additional sheets if necessary

Date of Sheet Preparation:

OECD TMI-2 Vessel Investigation Project
Sample Examination/Test Summary Sheet

Sample Log No.: A/G 426 D3B1

Sample Source (check one): ___Vessel steel ✓Nozzle ___Other (specify)
___Guide tube ___Companion

Performing Organization:	Principal Investigator:	Sample Core Grid Location:
ANL-MCT/IPS	L. A. Neimark	H5

Sample Location Description (attach diagram if necessary):
Transverse section from the outer surface of the nozzle at the 0 mm elevation. Captures only a ~15 mm segment of the surface.

Examination/Test Purpose:
Examine the grain structure of the nozzle and determine its hardness.

Examination/Test Technique and Formatting:
Metallography and DPH measurements. Macrophotos at 8.6x (unetched and etched), microphoto at 200x. DPH measurements.

Examination/Test Observation or Results:
Microstructure that of weldment. Weld passes and cast structure evident. Hardness is 217±13 DPH.

Other Parent Breakoffs (Sample Log Nos.) and Purpose:
426D3A (met and SEM), 426D3C1 (met, SEM, hardness)

Comments:

Add additional sheets if necessary

Date of Sheet Preparation:

OECD TMI-2 Vessel Investigation Project
Sample Examination/Test Summary Sheet

Sample Log No.: A/G 426D3C1

Sample Source (check one): ___Vessel steel ✓Nozzle ___Other (specify) ___Guide tube ___Companion

Performing Organization:	Principal Investigator:	Sample Core Grid Location:
ANL-MCT/IPS	L. A. Neimark	H5

Sample Location Description (attach diagram if necessary):
Transverse section from the outer surface of the nozzle at the 25 mm elevation. Captures ~25 mm of surface and ~10 mm of depth inward.

Examination/Test Purpose:
Evaluate any surface deposits, examine the Inc. 600 grain structure, and determine the hardness.

Examination/Test Technique and Formatting:
Metallography, SEM-EDX, and DPH measurements. Macrophoto (unetched) at 8.6x; micrographs (etched) at 100 and 150x; hardness measurements in DPH.

Examination/Test Observation or Results: 198±8 DPH (avg. of 5 meas.)
Non-equilibrium grain structure of equiaxed grains up to 0.5 mm in diameter. Some annealing twins present. Apparent precipitation of second phases within grains and at grain boundaries (Ti?). 50μ-thick oxide surface layer; mixture of fine core debris particles atop oxide. Oxide appears to be Fe-based (not analyzed)

Other Parent Breakoffs (Sample Log Nos.) and Purpose:
426D3A (met + SEM), 426D3B1 (met + hardness)

Comments:

Add additional sheets if necessary

Date of Sheet Preparation: 4/11/92

OECD TMI-2 Vessel Investigation Project
Sample Examination/Test Summary Sheet

Sample Log No.: AGA26E1A1

Sample Source (check one): ___Vessel steel ✓Nozzle ___Other (specify) ___Guide tube ___Companion

Performing Organization:	Principal Investigator:	Sample Core Grid Location:
ANL-MCT/IPS	L.A. Neimark	E11

Sample Location Description (attach diagram if necessary):
Longitudinal section through debris in top of nozzle. Captures metallic shards and fuel fragments in a fine particulate matrix, and one side of nozzle inner surface.

Examination/Test Purpose:
Determine nature of debris and fine particulate matrix.

Examination/Test Technique and Formatting:
Metallography and SEM-EDX. Optical photos, SEM images and x-ray spectra.

Examination/Test Observation or Results:
Matrix is very fine (<100μ) fuel particles of varying compositions locally. Fuel shards are various compositions, e.g. 83 w% U-14 w% Zr. Some oxidized pieces of stainless conduit. Fe most plentiful other constituent of matrix besides U and Zr.

Other Parent Breakoffs (Sample Log Nos.) and Purpose:
426E1B2 (met, SEM and hardness)

Comments:

Add additional sheets if necessary

Date of Sheet Preparation: 4/11/92

OECD TMI-2 Vessel Investigation Project
Sample Examination/Test Summary Sheet

Sample Log No.: AG426 E1B2

Sample Source (check one): ___Vessel steel ✓Nozzle ___Other (specify)
___Guide tube ___Companion

Performing Organization:	Principal Investigator:	Sample Core Grid Location:
ANL-MCT/IPS	L. A. Neimark	E11

Sample Location Description (attach diagram if necessary):
Longitudinal section on nozzle tip including both inner and outer surfaces.

Examination/Test Purpose:
Determine nature of nozzle degradation.
Determine hardness.

Examination/Test Technique and Formatting:
Metallography, SEM-EDX, microhardness.
Optical photos, SEM images, x-ray spectra, and DPH values.

Examination/Test Observation or Results:
Al major surface reactant. Outer surface close to or at solidus temperature. Outer surface showed "micro-folds" that trapped particulate matter including fuel particles. Hardness is 208 ± 29 DPH (avg. of 7 measurements)

Other Parent Breakoffs (Sample Log Nos.) and Purpose:
426E1A1 (met and SEM)

Comments:

Add additional sheets if necessary

Date of Sheet Preparation:

OECD TMI-2 Vessel Investigation Project
Sample Examination/Test Summary Sheet

Sample Log No.: A/G 426 E2A1

Sample Source (check one): ___Vessel steel ✓Nozzle ___Other (specify)
___Guide tube ___Companion

Performing Organization:	Principal Investigator:	Sample Core Grid Location:
ANL-MCT/IPS	L.A. Neimark	E11

Sample Location Description (attach diagram if necessary):
Transverse section of nozzle inner surface segment at the 274 mm elevation. Captures metallic rundown on inner surface and some particulate ceramic debris along inner surface.

Examination/Test Purpose:
Determine nature of metallic rundown and the ceramic particles.
Determine nozzle hardness.

Examination/Test Technique and Formatting:
Metallography and SEM-EDX; DPH measurements.
Macrophoto at 8.6x; SEM images and EDX spectra.

Examination/Test Observation or Results:
Metallic rundown contiguous with base metal and concluded to be Inc. 600 (analysis performed but not documented). Ceramic debris a potpourri of fuel shards, fuel particles in an Fe-(oxide) matrix (yielding an agglomerate shard), and extraneous core material constituents, e.g. Ca, Si. "Fuel" had range of U/Zr ratios from 0.02 to 2.2. Some control rod constituents in Fe/Ni matrix. Al and Ti in reaction areas on Inc. surface. Hardness is 137±4 DPH (avg. of 9 measurements with E2A4)

Other Parent Breakoffs (Sample Log Nos.) and Purpose:
426 E2A4 (SEM and hardness)

Comments:

Add additional sheets if necessary

Date of Sheet Preparation:

OECD TMI-2 Vessel Investigation Project
Sample Examination/Test Summary Sheet

Sample Log No.: A/G 426E2A4

Sample Source (check one): ___Vessel steel ✓Nozzle ___Other (specify)
___Guide tube ___Companion

Performing Organization:	Principal Investigator:	Sample Core Grid Location:
ANL-MCT/IPS	L. A. Neimark	E11

Sample Location Description (attach diagram if necessary):

Transverse section of nozzle outer surface segment at the 274 mm elevation. Captures ~20 mm of outer surface.

Examination/Test Purpose:

Determine nature of any surface interactions or deposits.
Determine nozzle hardness.

Examination/Test Technique and Formatting:

Metallography and SEM-EDX; DPH measurements. Macrophoto at 8.6x; SEM images and EDX spectra.

Examination/Test Observation or Results: (See text, p.21.)

Multilayered surface deposit 10-20μ thick. Up to 5 layers found. Inner layers contain principally Cr & Ti from the Inconel. Outer layers are Fe-rich and laden with Al, Zr and Ag-Cd. Reacted region contained Cd, In, Ag, Al, Zr, Si in addition to enhanced Fe and Cr. Reaction intergranular to pervasive. Ag-Cd nodules in nozzles up to 1 mm. Hardness 20 ± 4 DPH (avg of 9 measurements with E2A1.

Other Parent Breakoffs (Sample Log Nos.) and Purpose:

426E2A1 (SEM and hardness)

Comments:

Add additional sheets if necessary

Date of Sheet Preparation:

OECD TMI-2 Vessel Investigation Project
Sample Examination/Test Summary Sheet

Sample Log No.: A/G 426 E4B1

Sample Source (check one): ___Vessel steel ✓Nozzle ___Other (specify) ___Guide tube ___Companion

Performing Organization:	Principal Investigator:	Sample Core Grid Location:
ANL-MCT/IPS	L.A. Neimark	E11

Sample Location Description (attach diagram if necessary):
Transverse section of nozzle outer surface at the 90mm elevation. Captures ~15 mm of surface and ~10mm into nozzle; abuts 426E4B3.

Examination/Test Purpose:
Determine nature of any surface deposits.
Determine nozzle hardness.

Examination/Test Technique and Formatting:
Metallography, SEM-EDX, DPH measurements.
Macrophoto at 8.6x; microphotos at 150 and 500x.
SEM images and EDX spectra.

Examination/Test Observation or Results:
Nonadherent 0.13mm thick scale on surface. Contains potpourri of particulate shards in an Fe-rich matrix. Shards are principally U-Zr fuel. 10μ adherent layer on nozzle; Fe-based. 1-5μ particles atop this layer are Ag-Cd; traces of In.
Hardness is 190±19 DPH (avg. of 8 measurements with E4B3)

Other Parent Breakoffs (Sample Log Nos.) and Purpose:
426E4B3 (hardness)

Comments:

Add additional sheets if necessary

Date of Sheet Preparation:

OECD TMI-2 Vessel Investigation Project
Sample Examination/Test Summary Sheet

Sample Log No.: A/G 426E4B3

Sample Source (check one): ___Vessel steel ✓Nozzle ___Other (specify) ___Guide tube ___Companion

Performing Organization:	Principal Investigator:	Sample Core Grid Location:
ANL-MCT/IPS	L. A. Neimark	E11

Sample Location Description (attach diagram if necessary):

Transverse section of nozzle inner surface at the 90 mm elevation. Captures ~15 mm of surface and ~15 mm into nozzle; abuts 426E4B1.

Examination/Test Purpose:

Determine nature of any surface deposits. Determine nozzle hardness.

Examination/Test Technique and Formatting:

Metallography, SEM-EDX, and DPH hardness. Macrophoto at 8.6x. SEM exam not performed.

Examination/Test Observation or Results:

Hardness is 190±19 DPH (avg. of 8 measurements with E4B1).

Other Parent Breakoffs (Sample Log Nos.) and Purpose:

426E4B1 (SEM and hardness).

Comments:

Add additional sheets if necessary

Date of Sheet Preparation:

OECD TMI-2 Vessel Investigation Project
Sample Examination/Test Summary Sheet

Sample Log No.: A/G 426E5B

Sample Source (check one): ___Vessel steel ✓Nozzle ___Other (specify) ___Guide tube ___Companion

Performing Organization:	Principal Investigator:	Sample Core Grid Location:
ANL-MCT/IPS	L.A. Neimark	E11

Sample Location Description (attach diagram if necessary):
Transverse section of bottom surface (77 mm elevation) of removed instrument string only.

Examination/Test Purpose:
Determine nature of extraneous materials.

Examination/Test Technique and Formatting:
Metallography only; SEM-EDX not performed. Macrophoto at 50X of center tube. Microphotos to 1000X.

Examination/Test Observation or Results:
Metallic shards inside center tube and between it and instrument leads appear to be from brittle fractures, but rounding on some surfaces suggest ductility or short-period high temperatures. Possibly cutting debris from nozzle acquisition.

Other Parent Breakoffs (Sample Log Nos.) and Purpose:
None

Comments:

Add additional sheets if necessary

Date of Sheet Preparation:

OECD TMI-2 Vessel Investigation Project
Sample Examination/Test Summary Sheet

Sample Log No.: A/G 426F1A2

Sample Source (check one): ___Vessel steel ✓Nozzle ___Other (specify) ___Guide tube ___Companion

Performing Organization:	Principal Investigator:	Sample Core Grid Location:
ANL-MCT/IPS	L.A. Neimark	D10

Sample Location Description (attach diagram if necessary):
Longitudinal section of nozzle inner surface at the top (~290 mm elevation). Captures "left" side of inner surface, top of nozzle, instrument conduit (partial), and instrument string remnants.

Examination/Test Purpose:
Determine nature of material (metallic) between nozzle and conduit; nature of "ceramic" materials; and nature of gray, liquid-appearing phase.

Examination/Test Technique and Formatting:
Metallography and SEM-EDX.
Macrophoto at 8.6x, microphotos at 250x. SEM images and EDX spectra.

Examination/Test Observation or Results:
Metallic phase in annulus is essentially Inc. 600 (74 Ni-14Cr-12 Fe). Nozzle next to above phase is also Inc. (74 Ni-15Cr-11 Fe). Some "ceramic" is Cr-oxide on conduit and Inc. surfaces. Al- and Ti-rich phases in Inc. nozzle. 10-100μ-size fuel (U-Zr) shards trapped in folds of solidified metal at top of nozzle. Gray "liquid" phase is Cr(oxide) on folds on stainless steel conduit.

Other Parent Breakoffs (Sample Log Nos.) and Purpose:
426F1A4 (Met, SEM, hardness)

Comments:

Add additional sheets if necessary

Date of Sheet Preparation: 9/24/92

OECD TMI-2 Vessel Investigation Project
Sample Examination/Test Summary Sheet

Sample Log No.: A/G 426 F1A4

Sample Source (check one): ___Vessel steel ___Guide tube X Nozzle ___Companion ___Other (specify)

Performing Organization:	Principal Investigator:	Sample Core Grid Location:
ANL-MCT/IPS	L.A. Neimark	D10

Sample Location Description (attach diagram if necessary):
Longitudinal section, top 13 mm of nozzle showing top and side surfaces. (Substitute for 426F1A1)

Examination/Test Purpose:
Determine nature and extent of surface interaction.

Examination/Test Technique and Formatting:
Metallography, SEM-EDX, microhardness. Optical and SEM photographs; x-ray spectra.

Examination/Test Observation or Results:
Surface oxidation of Cr and Ti; some U-Zr involvement. Al penetration beneath oxide areas; Mg also present. Ag-Cd with U-Zr nodules up to 300μ from surface. Avg. hardness (6) = 140±4DPH

Other Parent Breakoffs (Sample Log Nos.) and Purpose:
426F1A2; metallography and SEM-EDX

Comments:

Add additional sheets if necessary

Date of Sheet Preparation: 9/24/92

OECD TMI-2 Vessel Investigation Project
Sample Examination/Test Summary Sheet

Sample Log No.: A/G426 F2A1

Sample Source (check one): ___Vessel steel ___Guide tube X Nozzle ___Companion ___Other (specify)

Performing Organization:	Principal Investigator:	Sample Core Grid Location:
ANL-MCT/IPS	L.A. Neimark	D10

Sample Location Description (attach diagram if necessary):
Transverse section at nozzle surface at the 266 mm elevation.

Examination/Test Purpose:
Determine nature of surface debris and nozzle degradation.

Examination/Test Technique and Formatting:
Metallography, SEM-EDX, and microhardness, Optical and SEM photographs; x-ray spectra

Examination/Test Observation or Results:
Surface ablation up to 2mm deep, irregularly on surface. Aggressive Al penetration, Cr + Ti surface oxidation overlaid with Fe-oxide. Cd-Ag in inner layers; U-Zr/Ag-Cd particles in outer Fe-rich layer. Average hardness (5) = 136 DPH

Other Parent Breakoffs (Sample Log Nos.) and Purpose:
None

Comments:

Add additional sheets if necessary

Date of Sheet Preparation: 4/11/92

OECD TMI-2 Vessel Investigation Project
Sample Examination/Test Summary Sheet

Sample Log No.: AG426F3A

Sample Source (check one): ___Vessel steel ✓Nozzle ___Other (specify)
___Guide tube ___Companion

Performing Organization:	Principal Investigator:	Sample Core Grid Location:
ANL-MCT/IPS	L.A. Neimark	D10

Sample Location Description (attach diagram if necessary):
Sample is a transverse cross-section of the instrument string at the 158 mm elevation.

Examination/Test Purpose:
Determine the nature of conduit degradation, material inside collapsed tube, and the metallurgy of the Zr lead wires.

Examination/Test Technique and Formatting:
Metallography and SEM-EDX. Optical photographs, SEM images and X-ray spectra.

Examination/Test Observation or Results:
Stainless steel conduit has oxidized; no other reactants found. Material in tube is Cr-depleted Inconel. Zr wires generally have had redox reaction with Al_2O_3 insulation; Zr-Al eutectic found. One wire apparently melted and then reacted with Inconel sheath.

Other Parent Breakoffs (Sample Log Nos.) and Purpose:
None

Comments:

Add additional sheets if necessary

Date of Sheet Preparation: 9/25/92

OECD TMI-2 Vessel Investigation Project
Sample Examination/Test Summary Sheet

Sample Log No.: A/G 426F4A

Sample Source (check one): ___Vessel steel ___Guide tube X Nozzle ___Companion ___Other (specify)

Performing Organization:	Principal Investigator:	Sample Core Grid Location:
ANL-MCT/IPS	L. A. Neimark	D10

Sample Location Description (attach diagram if necessary):
Transverse section at nozzle surface at the 158 mm elevation. Area is of gross "intergranular" cavities in nozzle.

Examination/Test Purpose:
Determine nature and content of cavities and microstructure of nozzle.

Examination/Test Technique and Formatting:
Metallography, SEM-EDX, and microhardness. Optical and SEM photographs; x-ray spectra.

Examination/Test Observation or Results:
Cavities filled with fuel debris in Cr-rich matrix. Inner surfaces have Cr-(oxide) layer; Ag-Cd stringers in grain boundaries and as small nodules in nozzle matrix. Large grain microstructure, shape of grains, annealing twins, and low hardness (124 DPH) indicative of high temperature.

Other Parent Breakoffs (Sample Log Nos.) and Purpose:
426F4B (central Inc. nugget) and F4C (exterior fuel deg)

Comments:

Add additional sheets if necessary

Date of Sheet Preparation: 4/11/92

OECD TMI-2 Vessel Investigation Project
Sample Examination/Test Summary Sheet

Sample Log No.: NG426F4B

Sample Source (check one): ___Vessel steel ✓Nozzle ___Other (specify) ___Guide tube ___Companion

Performing Organization:	Principal Investigator:	Sample Core Grid Location:
ANL-MCT/IPS	L.A. Neimark	D10

Sample Location Description (attach diagram if necessary):
Sample is from center of nozzle at 158 mm elevation. Area shows nozzle ID and metallic ingot trapped in annulus.

Examination/Test Purpose: Determine nature of ingot and seek evidence for reason for material loss on nozzle ID.

Examination/Test Technique and Formatting:
Metallography, SEM-EDX. Optical photographs, SEM images and X-ray spectra.

Examination/Test Observation or Results:
Ingot is Cr-depleted Inconel with Cr-oxide on surface. Ag-Cd nodules in ingots as well as Fe-rich areas, probably oxides. ID of nozzle deficient in Cr, which now is on ID surface as probably an oxide. ID surface contains no significant elements other than Cr, Ti, and Ni.

Other Parent Breakoffs (Sample Log Nos.) and Purpose:
426F4A, 426F4C.

Comments:

Add additional sheets if necessary

Date of Sheet Preparation: 9/30/92

OECD TMI-2 Vessel Investigation Project
Sample Examination/Test Summary Sheet

Sample Log No.: A/G426F4C

Sample Source (check one): ___Vessel steel ___Guide tube X Nozzle ___Companion ___Other (specify)

Performing Organization:	Principal Investigator:	Sample Core Grid Location:
ANL-MCT/IPS	L. A. Neimark	D10

Sample Location Description (attach diagram if necessary):
Sample is from surface of nozzle in an area of significant debris deposition 158 mm above bottom of nozzle.

Examination/Test Purpose:
Determine nature of surface debris, type of interaction with nozzle, and thermal effects in the nozzle

Examination/Test Technique and Formatting:
Metallography, SEM-EDX.
High and low magnification as-polished optical photographs. High and low magnification SEM-SE images and x-ray spectra.

Examination/Test Observation of Results:
Debris is a mixture of Cr and Fe oxides, a few fuel particles, and masses of Cr-depleted Inconel metal. Nozzle "surface" interaction involved Cr oxidation and Al penetration. Ag-Cd particles found in nozzle and in Cr-depleted masses.

Other Parent Breakoffs (Sample Log Nos.) and Purpose:
426F4A, 426F4B; same purpose.

Comments:

Add additional sheets if necessary

Date of Sheet Preparation: 10/6/92

OECD TMI-2 Vessel Investigation Project
Sample Examination/Test Summary Sheet

Sample Log No.: AG426F5A2B1

Sample Source (check one): ___Vessel steel ✓Nozzle ___Other (specify) ___Guide tube ___Companion

Performing Organization:	Principal Investigator:	Sample Core Grid Location:
ANL-MCT/IPS	L. A. Neimark	D10

Sample Location Description (attach diagram if necessary):
Sample is from the nozzle surface at the 82 mm elevation.

Examination/Test Purpose:
Determine nature of layer adhering to surface.

Examination/Test Technique and Formatting:
Metallography, SEM-EDX. Optical photographs, SEM images, and x-ray spectra. Microhardness

Examination/Test Observation or Results:
Fe(ox) matrix contains fuel shards of various compositions. In on and into nozzle surface formed layers with Ni; Ni_3In, likely. Ag and Cd found in Fe(ox) layer.

Other Parent Breakoffs (Sample Log Nos.) and Purpose:
426F5B1; surface interrogation, microhardness

Comments:

Add additional sheets if necessary

Date of Sheet Preparation:

OECD TMI-2 Vessel Investigation Project
Sample Examination/Test Summary Sheet

Sample Log No.: A/G426 F5B1

Sample Source (check one): ___Vessel steel ✓Nozzle ___Other (specify)
___Guide tube ___Companion

Performing Organization:	Principal Investigator:	Sample Core Grid Location:
ANL-MCT/IPS	L. A. Neimark	D10

Sample Location Description (attach diagram if necessary):
Transverse section of outer nozzle surface at the 69 mm elevation. Captures ~15mm of surface and ~7mm into nozzle.

Examination/Test Purpose:
Determine nature of any surface layers.

Examination/Test Technique and Formatting:
Metallography and SEM-EDX. DPH hardness. Macrophoto at 8.6x. SEM images and EDX spectra.

Examination/Test Observation or Results: (See text, p.22)
Thin layer of variable thickness, 1 to 10μ. Layer "banded" in some places; bands of different composition. Elements found were Al, Si, Ag, Cd, In and Sn; outer bands also contained U, Zr, Mo in thickest region of layer.

Other Parent Breakoffs (Sample Log Nos.) and Purpose:
None

Comments:

Add additional sheets if necessary

Distribution for NUREG/CR- 6185 (ANL-94/5)

Internal:

L. A. Neimark (15)
H. Drucker
C. E. Till
R. W. Weeks
R. B. Poeppel
W. J. Shack
D. R. Diercks
T. F. Kassner
B. W. Spencer
TIS File

External:

NRC, for distribution per R1, R3
Manager, Chicago Operations Office, DOE
ANL Libraries
  ANL-E
  ANL-W
Manager, Chicago Field Office, DOE
Energy Technology Division Review Committee:
  H. K. Birnbaum, University of Illinois, Urbana
  R. C. Buchanan, University of Cincinnati, Cincinnati, OH
  M. S. Dresselhaus, Massachusetts Institute of Technology, Cambridge, MA
  B. G. Jones, University of Illinois, Urbana
  C.-Y. Li, Cornell University, Ithaca, NY
  S.-N. Liu, Fremont, CA
  R. E. Smith, SciTech, Inc., Morrisville, NC

D. W. Akers, Idaho National Engineering Laboratory, EG&G Idaho, Inc., Idaho Falls, ID
C. Alexander, Battelle Columbus Laboratory, Columbus, OH
S. F. Armour, USDOE, Idaho Field Office, Idaho Falls, ID
R. J. Barrett, U.S. Nuclear Regulatory Commission, Washington, DC
E. S. Beckjord, U.S. Nuclear Regulatory Commission, Washington, DC
S. A. Chavez, Idaho National Engineering Laboratory, EG&G Idaho, Inc., Idaho Falls, ID
N. Cole, MPR Associates, Washington, DC
A. Drozd, U.S. Nuclear Regulatory Commission, Washington, DC
R. O. Gauntt, Sandia National Laboratory, Albuquerque, NM
S. Hodge, Oak Ridge National Laboratory, Oak Ridge, TN
M. D. Houston, U.S. Nuclear Regulatory Commission, Washington, DC
T. L. King, U.S. Nuclear Regulatory Commission, Washington, DC
G. E. Korth, Idaho National Engineering Laboratory, EG&G Idaho, Inc., Idaho Falls, ID
R. Long, General Republic Utilities Nuclear Corp., Parsippany, NJ

M. Merilo, EPRI, Palo Alto, CA
R. L. Palla, Jr., U.S. Nuclear Regulatory Commission, Washington, DC
M. M. Pilch, Sandia National Laboratory, Albuquerque, NM
J. R. Rashid, Anatech Research Corp., San Diego, CA
K. O. Reil, Sandia National Laboratory, Albuquerque, NM
J. L. Rempe, Idaho National Engineering Laboratory, EG&G Idaho, Inc., Idaho Falls, ID
A. M. Rubin, U.S. Nuclear Regulatory Commission, Washington, DC
R. Schmidt, Sandia National Laboratory, Albuquerque, NM
C. Z. Serpan, U.S. Nuclear Regulatory Commission, Washington, DC
S. P. Snow, Idaho National Engineering Laboratory, EG&G Idaho, Inc., Idaho Falls, ID
T. P. Speis, U.S. Nuclear Regulatory Commission, Washington, DC
L. A. Stickler, Idaho National Engineering Laboratory, EG&G Idaho, Inc., Idaho Falls, ID
J. Sugimoto, JAERI, Tokyo, Japan
G. L. Thinnes, Idaho National Engineering Laboratory, EG&G Idaho, Inc., Idaho Falls, ID
S. Thompson, Sandia National Laboratory, Albuquerque, NM
J. Tulenko, U. of Florida, Gainesville, FL
U. S. NRC, Div. Technical Information & Document Control, Bethesda, MD
K. Washington, Sandia National Laboratory, Albuquerque, NM
R. J. Witt, Dept. of Nuclear Engineering, U. of Wisconsin, Madison, WI
R. W. Wright, U.S. Nuclear Regulatory Commission, Washington, DC
J. R. Wolf, Idaho National Engineering Laboratory, EG&G Idaho, Inc., Idaho Falls, ID

NRC FORM 335 (2-89) NRCM 1102, 3201, 3202

U. S. NUCLEAR REGULATORY COMMISSION

BIBLIOGRAPHIC DATA SHEET

(See instructions on the reverse)

1. REPORT NUMBER *(Assigned by NRC. Add Vol., Supp., Rev., and Addendum Numbers, if any.)*

NUREG/CR-6185
ANL-94/5
TMIV(93)AL01

2. TITLE AND SUBTITLE

TMI-2 Instrument Nozzle Examinations at Argonne National Laboratory

February 1991 – June 1993

3. DATE REPORT PUBLISHED

MONTH	YEAR
March	1994

4. FIN OR GRANT NUMBER

A2220

5. AUTHOR(S)

L. A. Neimark, T. L. Shearer, A. Purohit, and A. G. Hins

6. TYPE OF REPORT

Technical

7. PERIOD COVERED *(Inclusive Dates)*

8. PERFORMING ORGANIZATION – NAME AND ADDRESS *(If NRC, provide Division, Office or Region, U.S. Nuclear Regulatory Commission, and mailing address; if contractor, provide name and mailing address.)*

Argonne National Laboratory
9700 South Cass Avenue
Argonne, IL 60439

9. SPONSORING ORGANIZATION – NAME AND ADDRESS *(If NRC, type "Same as above": if contractor, provide NRC Division, Office or Region, U.S. Nuclear Regulatory Commission, and mailing address.)*

Division of Systems Research
Office of Nuclear Regulatory Research
U.S. Nuclear Regulatory Commission
Washington, DC 20555-0001

10. SUPPLEMENTARY NOTES

11. ABSTRACT (200 words or less)

Six of the 14 instrument-penetration-tube nozzles removed from the lower head of TMI-2 were examined to identify damage mechanisms, provide insight to the fuel relocation scenario, and provide input data to the margin-to-failure analysis. Visual inspection, gamma scanning, metallography, microhardness measurements, and scanning electron microscopy were used to obtain the desired information. The results showed varying degrees of damage to the lower head nozzles, from ≈50% melt-off to no damage at all to near-neighbor nozzles. The elevations of nozzle damage suggested that the lower elevations (near the lower head) were protected from molten fuel, apparently by an insulating layer of fuel debris. The pattern of nozzle damage was consistent with fuel movement toward the hot-spot location identified in the vessel wall. Evidence was found for the existence of a significant quantity of control assembly debris on the lower head before the massive relocation of fuel occurred.

12. KEY WORDS/DESCRIPTORS *(List words or phrases that will assist researchers in locating this report.)*

TMI-2
Instrument nozzle
Fuel debris crusts
Inconel 600
Fuel debris relocation
Molten debris interactions

13. AVAILABILITY STATEMENT

Unlimited

14. SECURITY CLASSIFICATION

(This Page)

Unclassified

(This Report)

Unclassified

15. NUMBER OF PAGES

16. PRICE

NRC FORM 335 (2-89)